THE ARABIDOPSIS TT5 MUTANT ACCUMULATES NARINGENIN CHALCONE AND EXHIBITS ENHANCED RESISTANCE TO FUNGAL PATHOGENS WHEN GROWN UNDER LONG DAY CONDITIONS

A Thesis Submitted to the
College of Graduate and Postdoctoral Studies
In Partial Fulfillment of the Requirements
For the Degree of Doctor of Philosophy
In the Department of Biology
University of Saskatchewan
Saskatoon

By

IGOR DE ALBUQUERQUE

PERMISSION TO USE

In presenting this thesis in partial fulfillment of the requirements for a Postgraduate degree from the University of Saskatchewan, I agree that the Libraries of this University may make it freely available for inspection. I further agree that permission for copying of this thesis in any manner, in whole or in part, for scholarly purposes may be granted by the professor or professors who supervised my thesis work or, in their absence, by the Head of the Department or the Dean of the College in which my thesis work was done. It is understood that any copying or publication or use of this thesis or parts thereof for financial gain shall not be allowed without my written permission. It is also understood that due recognition shall be given to me and to the University of Saskatchewan in any scholarly use which may be made of any material in my thesis.

Requests for permission to copy or to make other uses of materials in this thesis in whole or part should be addressed to:

Head of the Department of Biology
112 Science Place
University of Saskatchewan
Saskatoon, Saskatchewan S7N 5E2 Canada

OR

Dean
College of Graduate and Postdoctoral Studies
University of Saskatchewan
116 Thorvaldson Building, 110 Science Place
Saskatoon, Saskatchewan S7N 5C9 Canada

ABSTRACT

Fungal diseases such as powdery mildew (*Erysiphe cichoracearum*) and anthracnose (*Colletotrichum higginsianum*) cause symptoms leading to death in many crop species. In order to stop the progression of diseases, plant species deploy several metabolites such as flavonoids. In this research, we used the model plant Arabidopsis thaliana to evaluate the effect of the Flavonoid Naringenin Chalcone (NC) against both pathogens. We discovered that when grown under long days, the *tt5* mutant of Arabidopsis (which accumulates NC) exhibits reduced growth but enhanced resistance to the above pathogens. The TT5 gene encodes Chalcone Isomerase, a key enzyme in the flavonoid pathway which converts naringenin chalcone to naringenin. Observing the *tt5* plant phenotype, we found that they exhibited increased cell death, callose deposition and reactive oxygen species (ROS) accumulation in leaves. They also constitutively expressed transcripts encoding the pathogenesis-related (PR) proteins: PR1 and PR5. To isolate the cause of these phenotypes, *tt4* (Chalcone Synthase) and *tt4/tt5* mutants were also examined. Neither exhibited pathogen resistance, cell death, callose deposition, ROS or PR expression phenotypes. When *tt5* plants were grown under short days, they behave like wild type plants with respect to growth patterns, pathogen resistance, cell death, callose deposition, ROS accumulation, and PR expression. These responses correlate with the accumulation of naringenin chalcone, the compound expected to accumulate in *tt5* plants. The same behavior was observed when tt5 plants were crossed with Salicylic acid (SA) insensitive mutants (*sid2, nahG*), except for *tt5/sid2* that presented small traces of NC. Our results suggest a link between naringenin chalcone accumulation and SA signaling cascade during plant defense.

ACKNOWLEDGEMENTS

It is a pleasure to express my gratitude to my supervisors Dr. Kenneth Wilson and Dr. Yangdou Wei for guiding me during my PhD. work. I would not be able to accomplish what I did If it were not for their knowledge and continuous support during these years.

I would also like to thank my research committee, Dr. Chris Todd, Dr. Zitou Zao, Dr..Bill Roesler for their guidance and suggestions. Thank everyone for your time and efforts during my Ph. D program.

I am very grateful to the University of Saskatchewan for supporting my studies through the Dean's scholarship and the Graduate Teaching Fellowship from the Department of Biology.

I thank my friends, lab mates and colleagues for their help and technical support along the way: Dr. Carvalho, Dr. Chris Ambrose, Dr. Guosheng Liu, Dr. Ewa Miskiewicz, Dr. Maryam Nourimand. Finally, I would like to thank the most important thing in my life which is my family, thanks for everything.

TABLE OF CONTENTS

LIST OF TABLES

LIST OF FIGURES

LIST OF ABBREVIATIONS

ABBREVIATION	FULL NAME
ABA	abscisic acid
ANOVA	analysis of variance
Avr	avirulence
cDNA	complementary DNA
CHI	chalcone isomerase
CHR	chalcone reductase
CHS	chalcone synthase
Dpi	days post inoculation
ET	ethylene
ETI	effector-triggered immunity
HL	high light
HPLC	high performance liquid chromatography
HR	hypersensitive response
JA	jasmonic acid
LD	long day
LT	low temperature
NC	naringenin chalcone
PAMP	pathogen-associated molecular patterns
PCD	programmed cell death
PR	pathogenesis-related
PRR	pattern recognition receptors

R-gene	resistance-gene
ROS	reactive oxygen species
RT-PCR	reverse-transcription polymerase chain reaction
SA	salicylic acid
SAR	systemic acquired resistance
SD	short day
Tt	Transparent testa

CHAPTER 1 INTRODUCTION

Higher plants are multicellular organisms. Being predominantly photosynthetic eukaryotes they are able synthesize sugar using light, H_2O and CO_2. Plant metabolism can provide organisms with all 20 amino acids and vitamins, making them the one of the main sources of food for terrestrial heterotrophs on our planet. Plant cells contain several structures and macromolecules including proteins, carbohydrates, and lipids which provide energy and nutrients for consumers. To that end, fungal pathogens attack plants to obtain nutrition. During evolutionary development pathogens acquired the ability to attack plants and live off the substances produced by their hosts. While the cytoplasm of plant cells has many substances that are required to the metabolism of pathogens, to get access to different cell compartiments, pathogens need to surpass both structural plant defenses such as the cell wall and chemical defense compounds. If the fungus can overcome the defense systems, the result is disease, leading to huge agricultural crop losses. In the next sections I will review aspects of plant-pathogen interaction and how plant metabolites affect disease progression.

1.1. Plant abiotic and biotic stress

Plants are exposed to many conditions that lead to abiotic and biotic stresses. Abiotic stress can be defined as unfavorable environmental factors that affect plant development such as extreme temperatures, low water disponibility, ultraviolet radiation exposure, or nutrient limitation (Stewart et al., 1991; Agrios, 2004; Ververidis et al., 2007). Responses to adverse conditions may lead to altered metabolism, growth inhibition, and/or cell death (Mur et al, 2008). Ultimately what happens in the plant depends on the stress being detected by the plant and that detection being signaled to regulate gene expression so that the plant can respond to mitigate the stress condition. The plant response mechanisms vary depending on the genes that are up- or down-regulated in

response to the stress. A well characterized example that is relevant to this work is the up-regulation of the flavonoid biosynthesis pathway in response to light (Dao et al., 2011; Guidi et al., 2016; Idris et al., 2018). I will outline this process in more detail below, but consider that increased light, or UV exposure is detected by photoreceptors in the plant, which in turn signal the increased transcription of a series of genes. The end result is a coordinated set of biosynthetic reactions that produce flavonols and anthocyanins (Shirley, 1996). What can seem like a simple cause and effect process involves many complex biochemical steps between detection and physiological response.

Following the detection of an abiotic or biotic stress, a signaling process begins. Plant cells use hormones and secondary signaling molecules to perform intracellular communication. Common signaling compounds include calcium (Ca^{2+}), nitric oxide (NO), abscisic acid (ABA), jasmonates (JA), salicylic acid (SA), ethylene (ET), and polyamines. Exogenous stress also causes metabolic imbalances in plant cells resulting in oxidative stress through the generation and/or accumulation of reactive oxygen species (ROS), including hydrogen peroxide (H_2O_2), superoxide anion ($O_2^{\cdot -}$), singlet oxygen ($^1O_2$), and hydroxyl radicals ($OH^{\cdot}$). When ROS production is not detoxified, cellular components will be damaged. Specifically, lipid peroxidation and oxidative damage to proteins and nucleic acids affects translation, transcription, and protein stability, possibly leading to programmed cell death (Blokhina et al., 2003). Under prolonged adverse conditions plants acclimate to diminish ROS production and increased ROS detoxification as part of the defense mechanism.

Biotic stress is caused by disease-producing agents, known as pathogens. Plants have developed several strategies to prevent and endure pathogen infections. Similar to their response to abiotic stress, plants first need to detect the presence of pathogens, signal their presence, then

respond in an appropriate fashion through the expression of defense-related genes and biomolecules (Hückelhoven et al., 1999; Slaughter et al., 2012). Pathogen recognition may occur due to a specific pathogen-related molecule or through metabolic compounds it releases. Plants have developed membrane localized receptors (PRRs) that are able to recognize pathogen-associated molecular patterns (PAMPs) and activate PAMP-triggered immunity (PTI) (Boyd et al., 2013). A wide range of chemical structures can activate plant defense mechanisms, including pathogen produced oligosaccharides, peptides, proteins, glycoproteins, and lipids, these substances are called elicitors (Shigenaga and Argueso, 2016). A well-known example is the flagellin protein, a bacterial compound that triggers defense responses in Arabidopsis (Mysore and Ryu, 2004).

Pathogens can be classified in two groups based on plant susceptibility. Host Pathogens are a small group of pathogens that can pass through a plant's defenses to cause disease symptoms (Mysore and Ryu, 2004). On the other hand, Non-Host Pathogens are agents that fail to pass through a plant's passive/active defenses and thus do not cause disease symptoms. Plant-Pathogen defense mechanisms are divided into passive and active (Inducible) (Ferreira et al., 2006). Passive mechanisms are the first line of defense against infection. Passive defenses are physical or biochemical barriers that prevent pathogen penetration and colonization. Inducible mechanisms include substances that are capable of inhibiting growth of the pathogen and/or generating adverse conditions for survival of the pathogen in plant tissues. Inducible mechanisms may trigger plants hypersensitive response (HR), which leads to programmed cell death as a way to avoid pathogen infection (Ferreira et al., 2006). In penetration resistance, substances can be constitutively present in high concentrations or can be produced in response to a penetration attempt (Lipka et al., 2008). For instance, Arabidopsis plants synthesize camalexin, a secondary metabolite (phythoalexin) that provides nonhost resistance against the fungus *Plectosphaerella cucumerina* (Sanchez-Vallet et

al., 2010). The plant cytoskeleton can also work as a physical barrier against plant pathogens. Moreover, plant actin microfilaments also play a role in defense against fungal penetration (Mysore and Ryu, 2004; Yang et al., 2014).

On the other hand, substances derived from induced mechanisms are absent or present at low levels before the infection and are only synthesized in response to pathogen presence (Barber and Mitchell, 1997; Hyun et al., 2011). In this kind of response, host plant disease resistance (R) genes mediate the recognition of the products of pathogen avirulence (avr) genes (Figure 1.1).

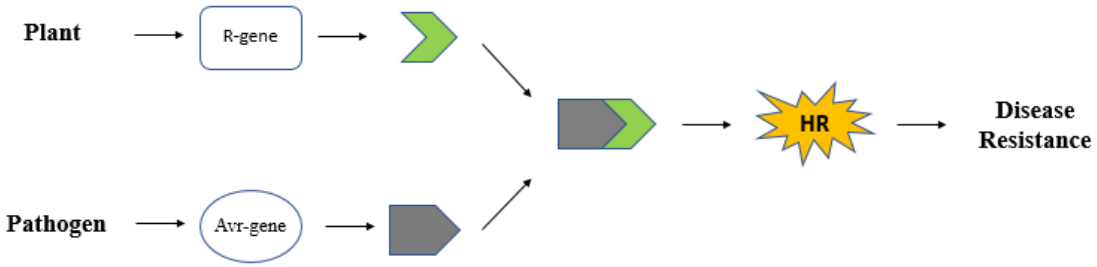

Figure 1.1: Disease resistance process through resistance and avirulence genes (Gururani et al., 2012).

When complementary pairs of R and avr genes are present, the interaction between the host and the pathogen is said to be incompatible. This triggers host-cell defense mechanisms and results in resistance to disease by inducing a hypersensitive response (Stangarlin et al., 2011). However, other proteins mediate the disease process leading to the guard hypothesis. In this hypothesis, the R proteins need an intermediate protein (guardee protein) to activate resistance. When the R protein detects an interaction with its guardee the resistance process is initiated. Resistance can also be activated if the R protein recognizes the product of the pathogen attack (Gill et al., 2015). In such a case the plant does not depend on the interaction between the R and Avr proteins (Bent and Mackey, 2007). For instance, *Arabidopsis thaliana*-bacterial R-Avr interaction, presents RIN4 (RPM1- interacting protein 4) identified as a cellular protein that is required for resistance to

Pseudomonas syringae pv. *tomato* mediated by RPM1 and RPS2 (Mackey et al., 2003). In addition, the activation of RPS5 mediated resistance in Arabidopsis is caused by the cleavage of PBS1 (guardee) by the cysteine protease AvrPphB from *P. syringae* pv. *Tomato* (Katagiri, et al., 2002).

One of the most studied classes of defense metabolites are phenolic compounds. These compounds are characterized by an aromatic ring linked to a hydroxyl group substituent (Xiao et al., 2014). Based on the complexity of the carbon structure, substitution, modification degree, and linkage with other molecules, phenolic compounds can be classified into several groups such as flavonoids and lignin (Takshak and Agrawal, 2014). Those without a direct relationship to the bioenergetic pathways of plant cell metabolism are known as secondary metabolites. Among the secondary metabolites are important defensive compounds such as flavonoids and lignin. Flavonoids are C6-C3-C6 compounds that, depending on their chemical structure, can act in plant defense systems (Mierziak et al. 2014). Lignin is part of the secondary cell wall, and one of the most common phenolic polymers. Lignin biosynthesis comprises: the biosynthesis of monolignols, followed by the translocation to the cell wall, and polymerization of monolignols (Heldt et al., 2011). Lignified cell walls are crucial in repelling attacks of pests by acting as a physical barrier to suppress invasion of microorganisms and blocking the diffusion of toxins (Barber and Mitchell, 1997). Several studies report lignin deposition during pathogen penetration attempts. Lignin and flavonoid accumulation are detected during the early stages of infection pointing to the synergy of these two groups of compounds in preventing initial disease symptoms (Vogt, 2010).

In Arabidopsis, flavonoid biosynthesis genes (e.g. *CHS*) are transcriptionally upregulated by different forms of stress including UV, wounding, herbivory, and pathogens resulting in the production of anti-microbial compounds, antioxidant activity, and absorbance of UV light (Lei et

al., 2018). The upregulation *PAL-1* transcription is also a common response to a variety of environmental stimuli, including pathogen infection, wounding, nutrient depletion, UV irradiation, and extreme temperatures (Dixon and Paiva, 1995). In sunflower, thiourea-mediated heat stress tolerance was attributed to *PAL1* up-regulation (Waqas et al., 2019). PAL is also an important player in pathogen resistance. For example, transgenic tobacco plants overexpressing a phenylalanine ammonia-lyase cDNA exhibited enhanced resistance against fungal pathogens *Phytophthora parasitica* pv. Nicotianae and *Cercospora nicotianae* (Way et al., 2002).

1.2. Plant hormones in the interactions plant-pathogen

Although the hormones Cytokinin, Auxin, Gibberellic Acid, Brassinosteroids, and ABA are involved in plant responses to pathogens, the relationship between the SA/JA, and ET pathways orchestrate the most important regulation of the hormonal control of the plant defense system (Shigenaga and Argueso, 2016). The balance between SA/JA and ET can be regulated in response to other hormones, which may be considered auxiliary hormones in plant immunity (Robert-Seilaniantz et al, 2011). In general, necrotrophic pathogens, that must feed on dead tissue content, and herbivorous insects are affected by JA/ET-mediated defense, while biotrophic pathogens that require a living host are usually more sensitive to SA-mediated defense responses.

1.2.1. Salicylic Acid

Salicylic acid (SA) is a phenolic compound derived from the primary metabolite chorismic acid (a precursor to the amino acid phenylalanine), it is formed through two general pathways (Figure 1.2), one derived from isochorismic acid, and another dependent on phenylalanine (Martínez et al., 2004). The isochorismate pathway involves the enzymes isochorismate synthase (ICS) and isochorismate pyruvate lyase (IPL) (Shigenaga and Argueso, 2016). The ICS enzyme converts chorismate to isochorismate, and IPL catalyzes the conversion of isochorismate into SA

(Strawn et al., 2007). The SA biosynthesis derived from phenylalanine starts with the formation of *trans*-cinnamic acid, catalyzed by PAL (phenylalanine ammonia lyase - also the first step of the flavonoid biosynthetic pathway). Subsequently, *trans*-cinnamic acid is converted into SA via the *ortho*-coumaric acid or benzoic acid routes (Figure 1.2).

Salicylic acid and JA-mediated plant defenses against pathogens and herbivores have been studied in several host species. The JA-mediated defense trigger the production of defensins (PDF1.2) and is generally linked to responses against necrotrophic pathogens and insects (Yan and Xie, 2015). In response to insect herbivory JA regulates the production of some classes of secondary metabolites (e.g. Alkaloids) that block insect digestion, and acts to increase production of plant volatiles, such as terpenoids, that can repel herbivores and even attract another insects that can control the pest species (Howe and Jander, 2008). The SA-mediated pathway is typically activated in response to pathogens and mediates the initiation of a hypersensitive response and the production of secondary metabolites (e.g. flavonoids and other phytoalexins) and pathogenesis-related (PR) proteins that confer systemic acquired resistance (SAR). Biotrophic and hemibiotrophic pathogens are usually more sensitive to SA-mediated defense responses. For instance, *Hyaloperonospora arabidopsidis* and *P. syringae* infections are controlled by SA-mediated responses. SA also regulates systemic acquired resistance (Glazebrook, 2005). Pathogen infection causes local accumulation of SA and may trigger SA production in uninfected leaves, developing a long-term and broad-spectrum resistance, also known as a SAR state (Kumar, 2014). SA accumulation is often related to the increased expression of PR genes, programmed cell death, ROS burst, and development of SAR (Ton et al., 2009). Exogenous application of SA and its analogs including Aspirin, 2,6-dichloroisonicotinic acid (INA), and benzothiadiazole S-methyl ester (BTH), activates expression of PR genes and results in resistance against a plethora of

pathogens such as viruses, bacteria, oomycetes, and fungi in a variety of dicotyledonous and monocotyledonous plants (Ishikawa et al., 2006; Kohler et al, 2002). On the other hand, Arabidopsis mutants that diminish or block SA accumulation through SA pathway blockage or expression of a bacterial salicylate hydroxylase (eg. *sid2*, *nahG*) exhibit compromised HR and abolish SAR (Delaney et al., 1994).

Loss-of-function mutations in SA regulators may lead to enhanced susceptibility or resistance to pathogens. For example, the Arabidopsis *eds1* mutation leads to enhanced disease susceptibility. EDS1 acts up-stream of SA signaling and physically interacts with two other positive regulators, PAD4 and SAG101 (Feys et al. 2005). Exogenous application of SA can rescue defense gene induction in *eds1* and *pad4* mutants and induce expression of EDS1 and PAD4 in WT, pointing that the presence of SA positively regulates transcription of both genes (Zhou et al. 1998; Falk et al. 1999; Feys et al. 2001). The non-expressor of pathogenesis-related genes 1 (NPR1) is an important regulator of SA-mediated defense responses. NPR1 is localized in the cytoplasm, while NPR3 and NPR4 are SA receptors (Robert-Seilaniantz et al., 2011). The presence of SA leads to the dissociation of the NPR complex and its migration into the nucleus (An and Mou, 2011; Fu and Dong, 2013). There, the NPR1 protein activates the transcription of defensive genes, such as PR (pathogenesis-related protein) (Spoel et al., 2003). SA affects NPR1 activity in two stages: by activating NPR1 expression, and by stimulating the translocation of NPR1 into the nucleus. Overexpression of Arabidopsis NPR1 or its homologs confers broad resistance against diverse pathogens in multiple plant species (Parkhi et al., 2010)

Interestingly, growth vs defense tradeoffs are very expensive for plant metabolism, depending on endogenous or exogenous stimulus, plants tend to prioritize either growth or defense (Xu et al., 2008). For example, lesion mimic mutants (LMM) which constitutively show HR- cell

death lesions were able to restore WT phenotype and fitness after the introduction the SA-degrading enzyme NahG, pointing the side effects of SA overexpression mutants (Mosher et al., 2010). In agriculture, these tradeoffs have profound implications on amplifying or mitigating crop losses. For example, NPR1 homologue (NH1) over-expressing rice plants display retarded growth in comparison to the control (Chern et al., 2005).

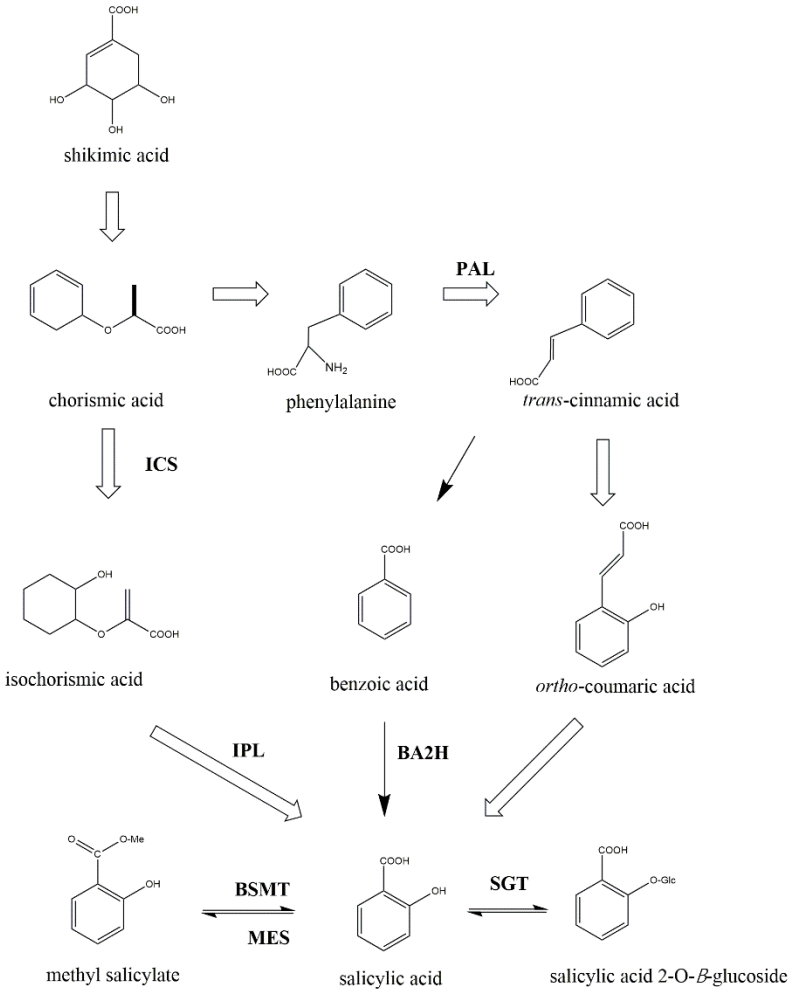

Figure 1.2: The salicylic acid biosynthetic pathway. The isochorismate pathway starts with the conversion of chorismic acid to isochorismic acid catalyzed by isochorismate synthase (ICS). Subsequently, isochorismic acid is converted to salicylic acid by isochorismate pyruvate lyase (IPL). The phenylalanine pathway starts with the conversion of phenylalanine to *trans*-cinnamic acid by action of phenylalanine amonia-lyase (PAL). *Trans*-cinnamic acid is converted to salicylic acid via benzoic acid, involving benzoic acid-2-hydroxylase (BA2H), or via *ortho*-coumaric acid. Salicylic acid can be converted to inactive compounds such as methyl salicylate or salicylic acid

2-*O*-β-glucoside. BSMT, benzoic acid/salicylic acid carboxyl methyltransferase; MES, methyl salicylate esterase; SGT, salicylic acid glucosyl transferase.

1.3. Phenylpropanoid pathway

Plant secondary metabolites are low-molecular weight substances which are not components of the fundamental bioenergetic processes nor the necessary building blocks of cells. However, they are often extremely helpful to plants and have evolved as part of their interactions with the world around them (Izbiańska et al., 2014). Secondary metabolites are derived from building blocks produced by the reactions of photosynthesis and cellular respiration. These compounds are often species specific and frequently used as a defense mechanism. Many drugs used by human and animal medicine are derived from plant secondary metabolites, for example Aspirin (acetyl salicylic acid) or morphine. Similarly, some plant secondary metabolites are amongst the most dangerous poisons, such as ricin. Some of these molecules can be synthesized by all plant tissues, while other compounds are produced in a particular tissue or in response to a specific stimulus (Dixon et al., 2002; Yu et al., 2000). Secondary metabolites can be divided into three main groups according to their biosynthetic origin: terpenoids (carotenoids), nitrogen-containing compounds (alkaloids), and phenylpropanoids (which includes the flavonoids) also known as phenolic compounds (Ribera and Zuñiga, 2012).

The shikimate pathway provides plants many primary metabolic compounds such as aromatic amino acids (Phenylalanine, Tryptophan, Tyrosine), vitamin K , and ubiquinone (Mir et al., 2015). It is also the main entry to the biosynthesis of phenylpropanoids. This pathway is found in bacteria, fungi, plants, and some protists, but not in animals (Stout and Chapple, 2004; Zhang and Björn, 2009). In plants, the shikimate pathway starts with the reaction between Phosphoenol pyruvate (Glycolysis) and Erythrose 4-phosphate (Pentose phosphate pathway), which is catalyzed by DAHP synthase (Tzin and Galili, 2010). After this, reactions involving 6 distinct enzymes

occur. The final product is chorismate, the substrate to many other primary and secondary metabolites.

In the phenylpropanoid pathway, chorismate generated in the shikimate pathway is used to synthesize the amino acid phenylalanine. The phenylpropanoid pathway provides precursors for several important plant metabolites including flavonoids, lignin, and a variety of phenolic esters (Mir et al., 2015). Fist, Phenylalanine is catalyzed by phenylalanine ammonia-lyase (PAL) into cinnamate , which is catalysed by cinnamic acid 4-hydroxylase into 4-coumarate, followed by 4-hydroxycinnamoyl CoA ligase to synthesize 4-coumaroyl CoA (Ververidis et al., 2007). After that, 4-coumaroyl CoA can enter the flavonoid or lignin pathway. The flavonoid pathway starts when 4-coumaroyl CoA is used by chalcone synthase (CHS) to form naringenin chalcone (Ververidis et al., 2007). In the lignin pathway 4-coumaroyl CoA is catalyzed by hydroxycinnamoyl-CoA shikimate/quinate hydroxycinnamoyl transferase (HCT) or cinnamoyl CoA reductase forming 4-coumaroyl shikimate/quinate or 4-coumaraldehyde, respectively (Fraser and Chapple, 2011).

1.4. Flavonoid Pathway

The term flavonoid refers to a large group of compounds including flavonol, flavone, flavanone, flavan-3-ol, isoflavone, and anthocyanidin according to its chemical structure (Pourcel et al., 2007). The metabolites derived from the flavonoid pathway can have different roles in plant biochemistry. For instance, anthocyanins have an important role in pollination processes, acting as visual attractors of insects to facilitate pollination (Uleberg et al., 2012), and affecting the transport of auxin (Peer and Murphy, 2007). Moreover, certain isoflavonones influence symbiosis between legume plants and bacteria (Zhang et al., 2009), by attracting the bacteria. Flavonoids are also important constituents of root secretions where they interact with symbiotic microorganisms (Jones et al., 2019), and even as important molecules in the phototropic response (Silva-Navas et

al., 2016). Foliar flavonoids protect photosynthetic components of the plant from damage caused by UV radiation, and absorb light as part of a high-light photoprotective process, especially in plants grown at low temperatures. For the eaters of plants, flavonoids are thought to provide beneficial health properties and protect against many chronic diseases when taken up in the diet (Wang, et al., 2009).

Luteolin is a flavonoid that acts as an anti-microbial agent in legume-plants. In the susceptible sorghum cultivar BTx623 the absence of luteolin leads to germination of *Colletotrichum sublineolum* (Du et al., 2010). In Malus apples, cultivars that were more resistant to Cedar-apple rust (*Gymnosporangium yamadai* Miyabe) presented high accumulation of anthocyanins and catechins followed by up-regulation of flavonoid related genes including *CHS, DFR, ANS, FLS,* and *MYB10.* In addition, Arabidopsis plants exhibited up-regulation of the CHS gene when challenged by *Verticillium dahlia,* while CHS-silenced cotton plants showed more wilting phenotypes and lower protective ROS production after verticillium infection.Sorghum plants produce a complex mixture of flavonoids in response to fungal infection (Snyder and Nicholson, 1990). For example, the accumulation of 3-deoxyanthocyanidins is toxic to *Colletotrichum graminicola* (Snyder and Nicholson, 1990).

The anti-microbial action of flavonoids has also been reported in Arabidopsis. When sprayed with quercetin, Arabidopsis plants presented higher resistance against *Pseudomonas syringae* pv. *tomato* DC3000. According to Jia et al. (2010), quercetin confers resistance against this pathogen through the SA signaling pathway and resulting H_2O_2 burst. In *Ligustrum vulgare* and *Phillyrea latifolia*, quercetin glycoside content inversely correlated with increased SOD and CAT activities resulting from high light exposure (Tattini et al., 2005). Due to this response, it is thought that flavonoids may act as secondary ROS scavenging mechanism in plants under high

light conditions (Izbiańska et al., 2014). In addition, the biosynthesis of the antioxidant dihydroxy B-ring flavone derivatives are triggered under high-light stress following up-regulation of *PAL* (phenylalanine ammonia lyase, the entry point in the phenylpropanoid metabolism) and *CHS* (the first committed step in the flavonoid biosynthetic pathway) in plants overexpressing alternative oxidase (AOX) (Fiorani et al., 2005)

Following the production of NC by CHS, it is isomerized by chalcone isomerise (CHI/TT5) to form Naringenin, as shown in Figure 1.3 (Tanaka et al., 1998; Holton and Cornisch, 1995). Like *pal*, *chs* is activated by a wide range of environmental and developmental stimuli such as, pathogen attack (Pourcel et al., 2007), wounding (Heldt and Piechulla, 2011), light stress (Guidi et al., 2016; Idris et al., 2018; Shirley et al., 1995), enhancing flavonoid biosynthesis (e.g. flavonones, flavonols, anthocyanins, or isoflavones) (Dao et al., 2011a). Treutter (2005) reported the accumulation of flavonols such as quercetin, luteolin, kaempferol, and apigenin glycosides in plants exposed to high levels of UV-B or excessive light exposure. Consequently, day length also affects the flux of the flavonoid pathway due to the amount of light energy reaching the plant and the interaction between photoreceptors. For example, *Vaccinium myrtillus* L. showed higher levels of anthocyanins compared to when it was grown under 12 hour of light (Inostroza-Blancheteau et al., 2014). Similarly, *Ipomoea batatas* L leaves showed lower flavonoid when grown under short photoperiods (Carvalho et al., 2010). In Arabidopsis mature leaves, CHS gene expression is regulated by interactions among phytochrome, cryptochrome and UV-B photo-transduction network. Cryptochromes *cry1* and *cry2* are involved in UV-a/blue light induction CHS but not seem to participate in the UV-B response. Also, Phytochromes can act as positive or negative regulators of CRY1 in UV-B light. Finally, flavonoids are very important components in plant disease resistance. Flavonoid molecules act at the beginning of the infection being translocated to

the infection site and contributing to cell death induction. Flavonoids were also found to be incorporated into the cell walls, and modulating auxin (IAA) activity. Mierziak et al., (2014) report the effect of flavonoid /auxin crosstalk on tissue differentiation, promotion of callus formation and closure of the vascular system to repel pathogens entrance.

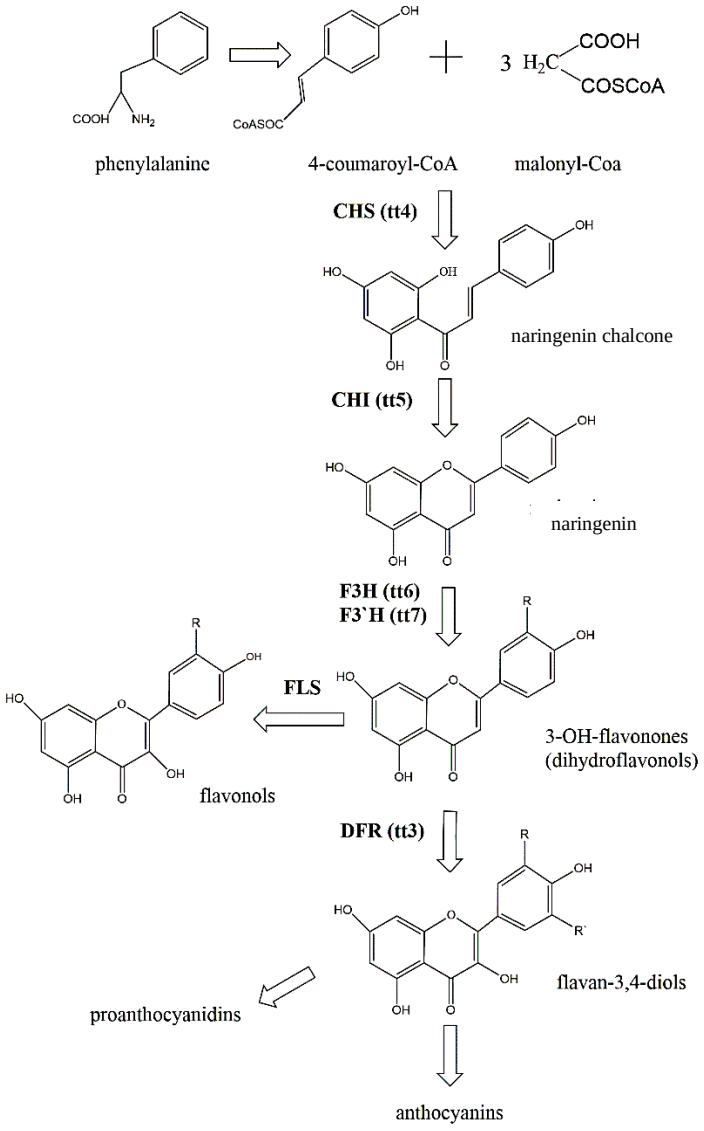

Figure 1.3: Flavonoid pathway in Arabidopsis. Arabidopsis mutants and enzymes are in bold (Burbulis and Winkel-Shirley, 1999)

1.5. Hypothesis and objectives

In Arabidopsis plants, mutants that do not synthesize specific enzymes of the flavonoid pathway are called *transparent testa (tt)*. The *tt* mutant phenotype is characterized by the absence of pigments in the seed coat, which allows the yellow carotenoids present in the underlying cotyledons visible (Bashandy et al., 2009). The flavonoid pathway in Arabidopsis begins with the reaction catalysed by chalcone synthase (Figure 1.3). The enzyme CHS/TT4 catalyzes the condensation of malonyl-CoA with p-coumaroyl-CoA to form NC. Several studies using artificial ultraviolet radiation (UV-B and UV-C light) indicate that mutant plants (*tt4*, deficient in chalcone synthase, and *tt5*, deficient in chalcone isomerase) that are unable to accumulate flavonoids are more sensitive to that stress (Li et al., 1993).

Studies examining disease progression in Arabidopsis *tt4* (no CHS, eliminates all flavonoids) and *tt5* (no CHI, accumulates narigenin chalcone) mutants found that a Col/Ler-*tt4* mutant expressed high susceptibility to infection by host pathogen *Colletotrichum* sp while a Col/Ler-*tt5* mutant demonstrated increased resistance to infection (Wei Y, unpublished data). Also, the *tt5* mutation reduces leaf size (Wei Y, unpublished data). When crossed with *tt4* (chalcone synthase deficient), a double mutant *tt4/tt5* assumed a WT appearance, suggesting that naringenin chalcone could have an important role in *tt5* mutant growth process (Wei Y, unpublished data). However, the disease resistance and leaf size phenotype of *tt5* plants were only observed when the plants were grown under LD conditions (16h per day of light).

Although there is no report mentioning that NC is involved with plant resistance, it is most probably that NC is involved to *tt5* phenotype. Recently, a chalcone derivative ,trans-chalcone, has been suggested to activate plants immune system (Díaz-Tielas et al., 2012). This type of compounds is classified as activators or priming agents. They will activate cellular defense

responses in plants, including ROS burst, transport changes at the plasma membrane, callose deposition, secretion of phytoalexins, and the upregulation of pathogenesis-related (*PR*) genes (Yi et al., 2014). Many compounds such as salicylic acid (SA), 2,6-dichloroisonicotinic acid, benzo (1,2,3) thiadiazole-7-carbothioic acid, chitin, rutin and quercetin have been linked to plant immune system activation (Yang et al., 2016). We hypothesize that the accumulation of NC is the starting point that causes *tt5* LD phenotype. We believe that the retention of NC would redirect the metabolic flux into the SA pathway through the upregulation of defense-related genes such as PAL1 and ICS1.

This research project aimed to accomplish the following objectives:

- To evaluate resistance of the Arabidopsis *tt5* mutant against *Colletotrichum higginsianum* and *Erysiphe cichorancearum* under long- and short-day growth conditions.
- To analyze the physiological and molecular aspects of the *tt5* mutant that relate to its increased pathogen resistance and growth phenotype under LD conditions.
- To determine the accumulation of naringenin chalcone in plants gown under SD and LD.

CHAPTER 2 MATERIAL AND METHODS

2.1. Plant materials and growing conditions

Plants were grown in an environmental growth chamber under four different conditions: Long Day (LD) 22˚C, 16hr light/8 hr dark photoperiod and a light intensity at 200 µmol $m^{-2}s^{-1}$; Short Day (SD) 22˚C, 8 hr light/16 hr dark photoperiod and a light intensity at 200 µmol $m^{-2}s^{-1}$; Long Day, Low Temperature (LD+LT) 4˚C, 16 hr light/8 hr dark photoperiod and a light intensity at 200 µmol $m^{-2}s^{-1}$; Short Day, High Light (SD+HL) 22˚C, 8 hr light/16 hr dark photoperiod and a light intensity at 400 µmol $m^{-2}s^{-1}$. The growth chambers were set to start the lights at the same time in each morning. The seeds were initially sown out in pots containing Sunshine® Mix 1 professional growing mix for bulk growth. When plants reached the 4-6 leaf stage, seedlings were transferred to square pots (3.5-inch by 3.5-inch; Kord Product, Toronto, CA) at a density of 4 plants per pot for all subsequent experiments.

Table 2.1: Arabidopsis Lines used in the experiments.

Mutant Name	Locus	Type of mutation	Gene description	Source Reference
tt4-T1	At5g13930	T-DNA	Encodes chalcone synthase (CHS), a key enzyme involved in the biosynthesis of flavonoids. Required for the accumulation of purple anthocyanins in leaves and stems.	GK_304D03 from NASC
tt5-T1	At3g55120	T-DNA	Encodes chalcone isomerase (CHI). Catalyzes the conversion of chalcones into flavanones. Required for the accumulation of purple anthocyanins in leaves and stems.	SALK_034145 from ABRC
tt6-T1	At3g51240	T-DNA	Encodes flavanone 3-hydroxylase that is coordinately expressed with chalcone	SALK_113321 from ABRC

			synthase and chalcone isomerases. Regulates flavonoid biosynthesis.	
cpr1-1	At4g12560	SNS	Encodes CPR1 (Constitutive Expresser of PR Genes 1, also known as CPR30), a F-Box protein that functions as a negative regulator of defense response and targets resistance proteins	
NahGox	n/a	TP	TP express Pseudomonas gene *NahG*; Inhibit the production SA by degrading it	Lawton et al., 1995
sid2-1	At1g74710	SNS	Encodes a protein with isochorismate synthase activity. It impacts the production of salicylic acid.	Wildermuth et al., 2001
Double Mutants				
tt4/tt5		*tt5/nahG*		*tt5/sid2*

Mutant alleles were created in Arabidopsis ecotype Col-0. SNS: single nucleotide substitution; SND: single nucleotide deletion; T-DNA: T-DNA insertion; TP: transgenic plant.

2.2. Pathogenic fungal materials, cultivation, and inoculation protocol.

Anthracnose disease assay*: Colletotrichum higginsianum* (IMI349061) was obtained from CABI Bioscience (Egham, UK) and maintained in the Wei Lab. *C. higginsianum* was cultured on potato dextrose agar (PDA) plates. PDA medium was pr epared by mixing 39 g of Difco® PDA (Becton Dickinson and Company; Sparks, US) in 1 L of distilled water. To prepare PDA plates, the medium was autoclaved at 121˚C for 20 min and once cool enough to handle was poured into 100 mm×15 mm polystyrene petri dishes (Fisher Scientific; Ottawa, CA). Subsequently, an inoculation loop was used to collect conidia from a stock plate and distribute them on fresh media. After inoculation, the PDA plate was incubated at room temperature until the generation of mature conidia (usually 10 to 14 days after transferring the spores). The conidia were later collected by an inoculation loop and suspended in sterile water. The suspension was centrifuged for 1 minute and the conidia were resuspended in 1 mL of sterile water. The number of conidia per mL was

determined using a hemocytometer and the final solution adjusted to provide 2×10^6 conidia per mL. The prepared inoculum solution was sprayed on 4-5 week old Arabidopsis plants at a rate of forty mL of conidia suspension on 12 pots of Arabidopsis with 4 plants per pot. The trays containing inoculated plants were covered by a transparent plastic lid to retain humidity and provide optimal conditions for pathogen growth (Yang et al., 2014). Images of plants from anthracnose experiments were taken 5 days post inoculation (dpi). Microscopy imaging was performed at 1 dpi and 3 dpi. The penetration frequency of *C. higginsianum* was determined by counting the number of primary hyphae formed per 100 germinated appressorium (Figure 2.1). The leaf was divided in two equal parts and the average between these areas was used to represent the penetration frequency of the sample. The value of 1 leaf was considered 1 replicate and 3 replicates were obtained for each plant line. The experiment was repeated 3 times.

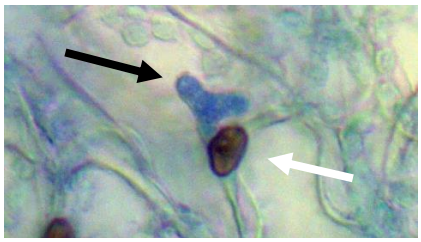

Figure 2.1: Penetration frequency evaluation.

Arabidopsis plant inoculated with *Colletotrichum higginsianum* by spraying with a conidiaspore suspension. The black arrow indicates the primary hypha and the white arrow indicates the melanized appressoria. The penetration frequency of *C. higginsianum* was determined by counting the number of primary hyphae formed per 100 germinated appressorium.

Powdery mildew disease assay: *Erysiphe cichoracearum* was previously isolated from a field in Saskatoon and maintained in the Wei Lab in the Department of Biology at the University of Saskatchewan. *Erysiphe cichoracearum* was cultured on cucumber leaves "National Pickling" (Early's Farm and Garden Center; Saskatoon, CA). Inoculation was performed by shaking heavily infected cucumber leaves over a box containing Arabidopsis plants (Yang et al., 2014). The

inoculated Arabidopsis plants were then transferred to their original growth environment and the samples were collected at specific time points for each experiment described. The total hyphae length of *E. cichoracearum* colonies were measured using ImageJ software (http://rsbweb.nih.gov/ij/) on the digital images photographed after staining with aniline blue. Thirty colonies were randomly chosen from collected leaves of each plant line in each replicate of experiment. The value of 1 leaf was considered 1 replicate and 3 replicates were obtained for each plant line. The experiment was repeated 3 times.

2.3. RT-PCR

Total RNA was extracted from leaves employing the Plant RNA Easy kit (Qiagen) following the manufacturer's instructions. Quality and quantity of extracted RNA were detected and confirmed by 1% agarose gel electrophoresis and a NanoDrop 2000 Spectrophotometer (Thermo Scientific). Subsequently, cDNA was synthesized from 50 ng/µL of total RNA using the QuantiTect Reverse Transcriptase Kit (Qiagen) according to the manufacturer's instructions. The resulting cDNA was used as a template for the analysis of transcript abundance by employing specific primers. The PCR was performed using PCR standard kit Taq DNA Polymerase (NEB) according to the manufacture's instructions. Then, 1% agarose gel electrophoresis containing ethidium bromide was used to separate the PCR products and they were imaged using trans illuminated UV light to determine the relative amount of transcript present in the original plant samples, and thus the relative level of gene expression (Table 2). Actin7 (At5g09810) was used as control (Czechowski et al., 2005).

Table 2.2: Primers used for RT-PCR analyses.

Gene	Sequence

PR1 (At2g14610)	F: CCACAAGATTATCTAAGGGGTC
	R: TTCCACTGCATGGGACCTA
PR5 (At1g75040)	F: AACGGCGGCGGAGTTC
	R: GCCGCCATCGCCTACTAGA
PAL1 (At2g37040)	F: ACTTATTAGATTCCTTAACGCCGG
	R: GTTACCACCGTGAATCGCCTTGTT
ICS1 (At1g74710)	F: TGTCTGCAGTGAAGCTTTGG
	R: TAGATCAATGCCCCAAGACC
PDF1.2 (At5g44420)	F: ACACAACACATACATCTATACATTGAAA
	R: AACAACAACGGGAAAATAAAC
ACT7 (At5g09810)	F: CAGTGTCTGTTCACCGACTTATAG
	R: GAGACTTCATAGGTTAGCTTGTAC

2.4. Histochemical staining

The inoculated and non-inoculated leaves were collected and placed in a fixation solution (methanol :chloroform: acetic acid = 6: 3: 1 v/v/v) until the original green color was completely faded. The fixation solution was then replaced by ethanol and the samples were incubated overnight. Samples were rehydrated by the gradual replacement of ethanol with water starting from 95%, 80%, 70%, 50% to 25% ethanol (Liu et al., 2010).

Erysiphe cichoracearum hyphae staining: the residual ethanol was replaced by adding acidic water (pH 2.0; adjusted with hydrochloric acid) overnight. The samples were then stained in acidic water containing 0.05% aniline blue for 5 min. After staining, the samples were rinsed with acidic water to remove excessive stain. The samples were mounted on glass slides in acidic water (pH 2.0) to view the fungal hypha, and photographed using bright field microscopy (Carl Zeiss Canada, Toronto, CA) (L. Yang et al., 2014b).

Colletotrichum higginsianum hyphae staining: the residual ethanol was replaced with pure water and incubated overnight. Subsequently, samples were stained with 0.05% trypan blue (Hartman-Leddon; Philadelphia, US) dissolved in pure water overnight. Stained samples were rinsed and mounted on glass slides in pure water for observation and photography using bright field microscopy (Carl Zeiss Canada, Toronto, CA) (L. Yang et al., 2014b).

Cell death staining: Non-inoculated leaves were stained with lactophenol trypan blue (Hartman-Leddon; Philadelphia, US) following the protocol described by Fernández-Bautista et al. (2016). Samples were incubated in Latophenol trypan blue (10 mL lactic acid + 10 mL phenol + 10 mL glycerol + 10 mL of distilled water + 40 mg of trypan blue) for 1 hour and transferred to the Fixation Buffer to remove the pigments. Samples were photographed using a bright field microscope (Carl Zeiss Canada, Toronto, CA).

Superoxide staining: The Superoxide evaluation was performed according to the protocol described by (Nourimand and Todd, 2016) . For the O^{-2} assay, leaf samples were immersed in 1 ml of Nitro Blue Tetrazolium (NBT) (Bioshop, Ontario, CA) solution (4.3 mM NBT, 10 mM potassium phosphate pH 7.5, 1 mM NaN_3) and infiltrated under vacuum for 90 min. Samples were placed in the Fixation Buffer and rehydrated. Subsequently, samples were mounted in water and photographed using a bright field microscope (Carl Zeiss Canada, Toronto, CA).

Hydrogen peroxide staining: The in situ histochemical detection of H_2O_2 was examined using 3,3'- diaminobenzidine (DAB; Sigma-Aldrich; Oakville, CA) uptake described by Liu et al. (2010). DAB uptake was carried out by incubating fresh leaves in 1 mg/mL DAB solution for 24 hrs. Subsequently, samples were incubated in the Fixation Buffer to remove pigments and photographed using a bright field microscope (Carl Zeiss Canada, Toronto, CA).

Callose staining: After fixing the leaf samples, they were incubated in a solution containing aniline blue (0.05%) (Fisher Scientific; Ottawa, CA) and 150 mM K_2HPO_4 overnight followed by pure water (pH 9.5) overnight. The samples were mounted in 30% glycerol and photographed using an Axioplan epifluorescence microscope (excitation filter 390 nm) (Carl Zeiss Canada, Toronto, CA) with UV actinic light (Schenk and Schikora, 2015).

Color intensity analysis: The color intensity obtained through the images of the cell death, super oxide, callose and hydrogen peroxide experiments was quantified following the methodology described by McCloy et al. (2014). From each image, area, mean intensity, and background readings were extracted. The corrected intensity (U) = integrated density – (area of selected cell × mean intensity of background readings), was calculated using image J. Each image was considered 1 replicate and 3 replicates were obtained for each plant line. The experiment was repeated 3 times.

2.5. HPLC

Naringenin chalcone (NC) content was quantified using reverse-phase HPLC. An Agilent Technologies 1200-series system equipped with an C18 Column (Agilent Eclipse XDB-C18) was used to control the process and separate the extracted leaf compounds. The HPLC analyses were performed in a manner similar to that described previously (Wilson et al., 1998). For each sample, 100 mg of fresh leaf tissue was ground in 1000 µl of methanol:water (4:1 vol/vol) and centrifuged at maximum speed for 5 min at room temperature. 100 µL supernatant was passed through a 13 mm syringe filter of 0.2 µm pore size made of PTFE (VWR International) and the NC concentration was detected using the absorbance at 265 nm. Two buffers were used in the HPLC analyses: acetonitrile and water (pH 3.0 with phosphoric acid) at a flow rate of 0.6mL/min. The amount of acetonitrile in the mobile phase under the starting conditions was 8% and was increased

from 8% to 10% during the first 3 min, to 11 5% during the next 5 min, to 14% during the next 9 min, to 17% during the next 2 min, to 20% during the next 9 min and to 100% during the next 2 min. The mobile phase was maintained at 100% acetonitrile for an additional 10 min to clean the column. 50 uL samples of leaf extract were injected into the system. The amount of NC found in the samples was calculated by the comparison of the peak area with the standard curve generated using the pure NC (AvaChem Scientific, San Antonio, TX.). To build the standard curve different concentrations of NC (0mM, 5mM, 10mM,25mM, 50mM) were analyzed by HPLC to generate a linear equation (y=3.5975x; R^2=0.9659). This equation was used to analyze the peak areas generated by leaf samples and calculate the amount of NC in the leaf tissue.

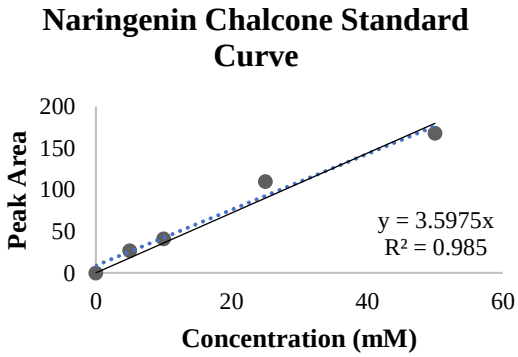

Figure 2.2: Naringenin Chalcone Standard curve

Standard curve for determination of aglycone naringenin chalcone (2',4,4',6'-Tetrahydroxychalcone) content in Arabidopsis plants.

2.6. Chlorophyll analysis

Chlorophylls were extracted and analysed from inoculated (5dpi) and non-inoculated samples following the methodology described by Sumanta et al. (2014). Leaf samples (100mg/sample) were ground in 0.5 mL of 80% acetone and centrifuge (10,000 rpm) for 15 min at 4°C. The supernatant (0.1 mL) was mixed with 0.9 mL of 80% acetone. Subsequently, the

samples were analyzed in spectrophotometer. The equation used for the quantification of Chlorophyll a (Chla) and Chlorophyll b (Chlb) were: $Chla=12.25A^{(663nm)}– 279A^{(645nm)}$ and $Chlb=21.5A^{(645nm)} – 5.1A^{(663nm)}$ (Sumanta et al., 2014). Total Chlorophyll was obtained by the sum (Chla + Chlb).

2.7. Data collection and statistical analysis

Statistical analysis was performed on all data to compare the significant differences between mutant lines and wild type Col-0. All experiments described this thesis were repeated at least three times using independent plants grown at different times. The statistical scheme was the "Completely Random" design. The data was summarized, and the mean values and standard deviations were calculated in Excel of Microsoft Office software (Microsoft Company; Mississauga, CA). Analysis of variance (ANOVA) test ($P < 0.05$) was performed according to each experiment. One-way or two-way (factorial) tests were followed by average comparisons using Tukey's HSD test (0.05).

CHAPTER 3 RESULTS

3.1. Knockout of *tt5* results in enhanced resistance to fungal pathogens when grown under LD conditions

Based on initial observations in the lab of Dr. Wei, Arabidopsis plants exhibiting a defect in the TT5 gene encoding CHI, were more resistant to biotrophic fungal pathogens when grown under long-day (LD) conditions. In this section we evaluated the disease symptoms, penetration, and post-invasion resistance of *transparent testa* (*tt*) lines to *C. higginsianum* (anthracnose disease) and *E. cichoracearum* (powdery mildew disease) grown under LD and SD conditions (Figure 3.1 – 3.3).

Penetration resistance is an important aspect of plant disease resistance (Lee et al., 2017). Its main function is to block pathogen access to the cytoplasm and avoid the infection of the inner structures. To estimate the penetration resistance, the frequency of penetration of *C. higginsianum* was measured on plants grown under LD and SD. Penetration frequency, represented by the ratio between primary hyphae per appressorium, was analyzed in the *tt* plants infected with *C. higginsianum* at 1 dpi. *tt5* plants showed reduced penetration frequency in LD compared to the other plants including the double mutant *tt4/tt5* (Figure 3.1 and 3.2). The double *tt4/tt5* mutant did not show a statistical difference in LD and SD.

In addition to penetration resistance, plant cells also possess post-invasion resistance mechanisms to protect against the successful entry of fungi. Post-invasion resistance is regulated by SA, JA and ET signaling pathways (Andersen et al., 2018). Therefore, subsequent research was performed to investigate if the *tt5* mutation provided enhanced post-invasion resistance using the powdery mildew pathogen (*E. cichoracearum*). In LD grown plants, *tt5* showed reduced hyphae

progression at 5dpi and 7dpi (not statistically different at 7dpi) compared to the other lines including WT (Figure 3.3). *tt5* Plants grown under SD were not statistically different from WT. The data collected points that *tt5* shows enhanced penetration resistance and post-invasion resistance when grown under LD. *tt5* enhanced resistance was compromised when crossed with *tt4* (*tt4/tt5).*

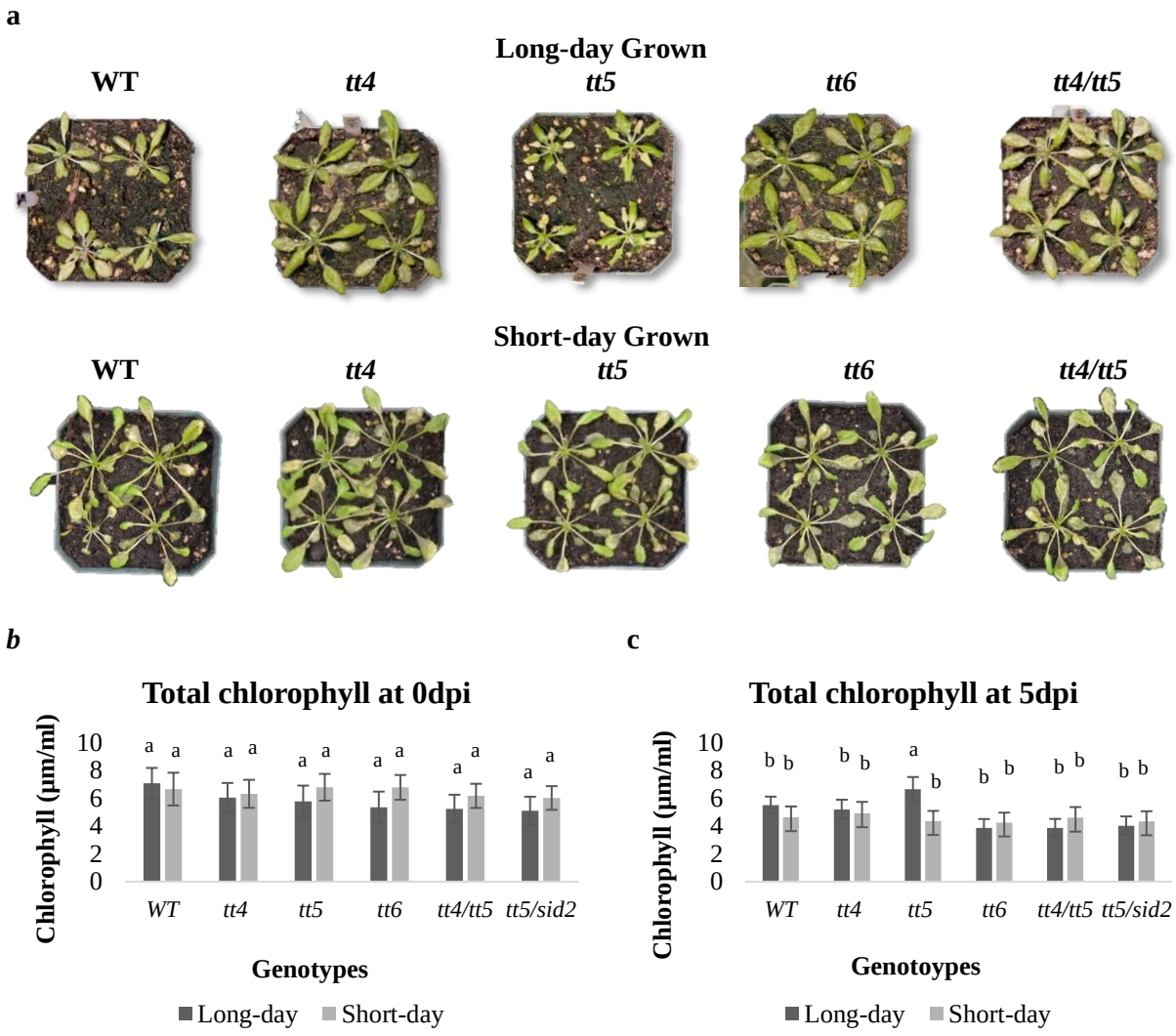

Figure 3.1: Anthracnose (*Colletotrichum higginsianum*) disease symptoms on *transparent testa* lines grown under long and short-days at 5 (dpi).

a) The genotypes in the image were inoculated with *C. higginsianum* by spraying a conidia suspension at density of 1×10^6 spore/ml. Total chlorophyll was measured before (b) and after (c) inoculation with *C. higginsianum.* Images are representative of 3 independent experiments and 3 observations of each independent experiment. Different letters denoted significant differences of the means as determined by a two-way ANOVA with Tukey`s HSD ($P < 0.05$).

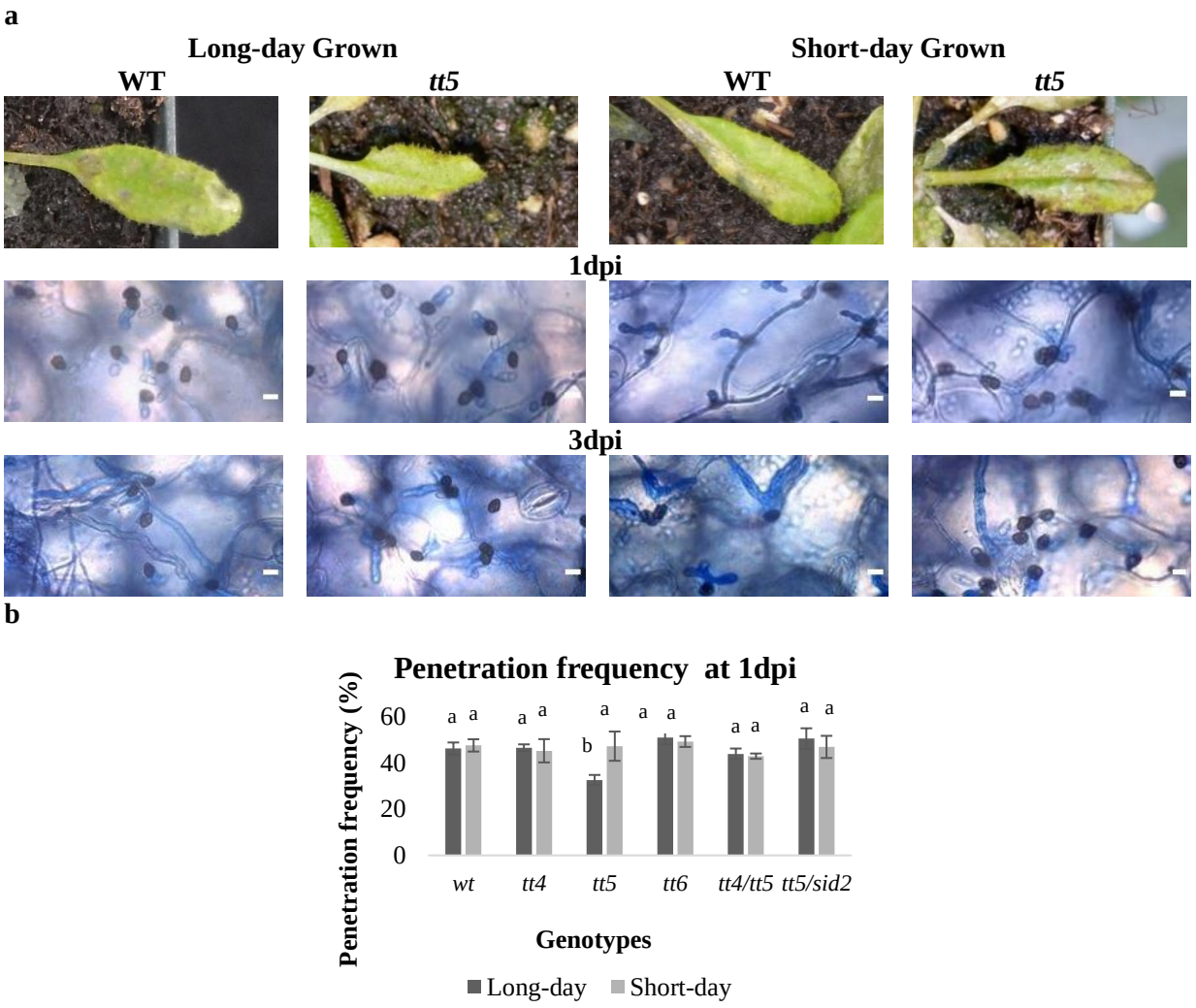

Figure 3.2: Disease symptoms on WT and tt5 leaves at 3 days post inoculation (dpi) with *Colletotrichum higginsianum*.

(a) Leaves were collected at 1 and 3 dpi to observe the hyphae progression. (b) The penetration frequency was measured by the ratio primary hyphae/appressoria at 1 dpi. Images are representative of 3 independent experiments and 3 observations of each independent experiment. Scale bars: 15µm. Different letters denoted significant differences of the means as determined by a two-way ANOVA with Tukey`s HSD ($P < 0.05$).

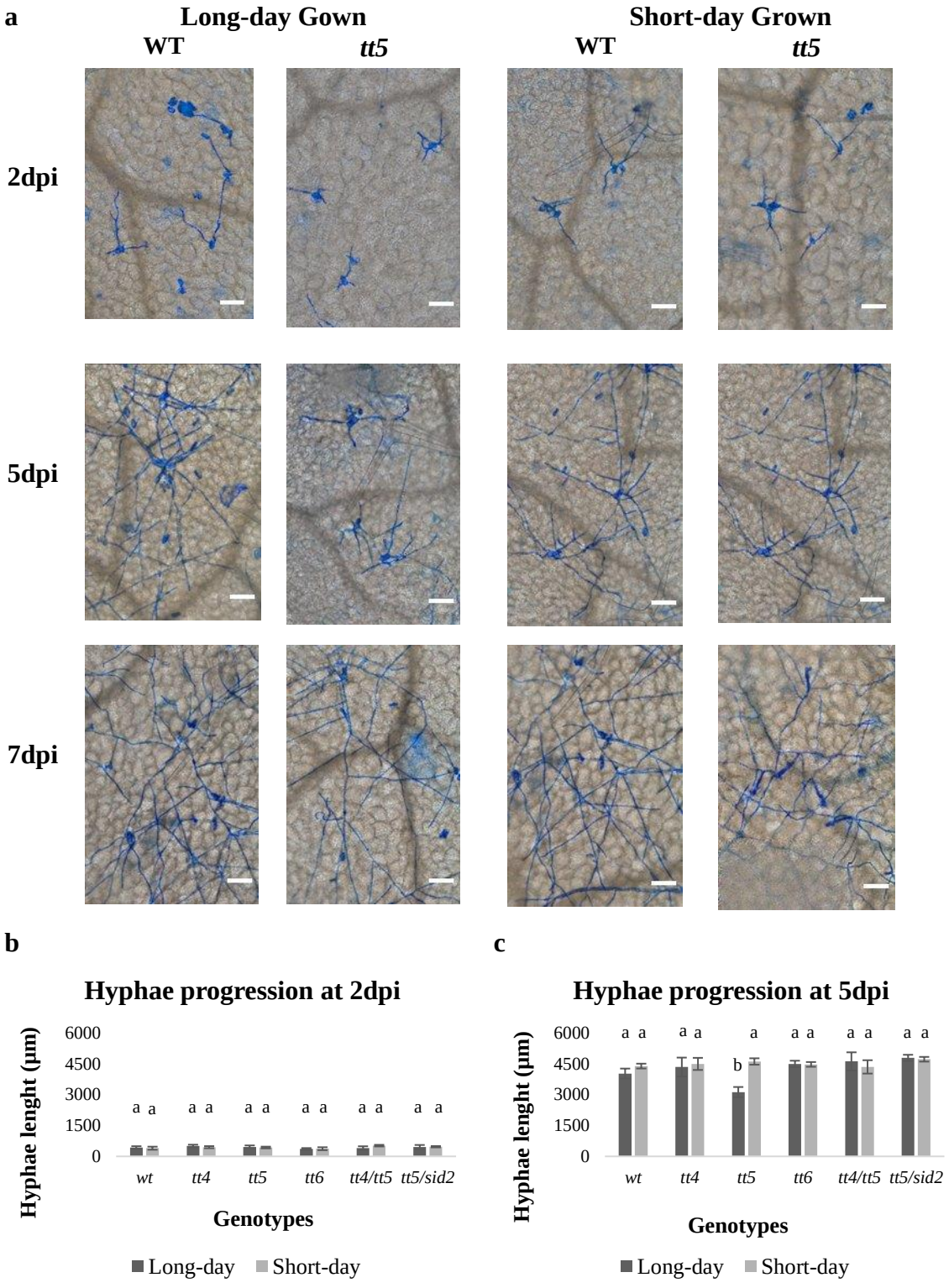
a
Long-day Gown
Short-day Grown
WT
tt5
WT
tt5
2dpi
5dpi
7dpi
b
Hyphae progression at 2dpi
Hyphae lenght (µm)
6000
4500
3000
1500
0
a a a a a a a a a a a a
wt
tt4
tt5
tt6
tt4/tt5
tt5/sid2
Genotypes
Long-day
Short-day
c
Hyphae progression at 5dpi
Hyphae lenght (µm)
6000
4500
3000
1500
0
a a a a a b a a a a a a
wt
tt4
tt5
tt6
tt4/tt5
tt5/sid2
Genotypes
Long-day
Short-day

Figure 3.3: Histochemical analysis of typical *Erysiphe cichoracearum* hyphae development on WT and *tt5* leaves.

a) Powdery mildew (*Erysiphe cichoracearum*) hyphae progression at 2, 5 and 7dpi on WT and *tt5* gown under LD or SD conditions. Total hyphae length per colony of *E. cichoracearum* at 2 dpi (b) and 5 dpi (c). Images are representative of 3 independent experiments and 3 observations of each independent experiment. Scale bars: 100µm Different letters denoted significant differences of the means as determined by a two-way ANOVA with Tukey`s HSD ($P < 0.05$).

3.2. *tt5* plants present different growth patterns in Long days (LD) and Short days (SD)

In this section, the pattern of plant growth and development was evaluated. When grown under LD conditions, *tt5* plants showed reduced growth compared to WT and other flavonoid mutants. However, when grown under SD conditions, all *tt* plants presented similar development to WT (Figure 3.4). Interestingly, the double mutant *tt4/tt5* did not exhibit the typical *tt5* LD phenotype, which exhibits a reduction in plant size and narrowed leaf edges.

To determine the cause of the smaller leaves of LD-grown *tt5* plants, fully expanded leaves were removed and stained for cell death using Lactophenol tryphan blue. When grown under LD conditions, *tt5* plants show HR-like cell death (Figure 3.5), even though there is no pathogen infection. The wild type nor any of the other mutant plants exhibited cell death under LD growth conditions. Thus, there seemed to be increased cell death triggered in LD-grown *tt5*, but no other plants tested. When examining plants grown under SD growth conditions there was no cell-death evident in any of the genotypes (Figure 3.5).

Based on immunity triggered cell death mechanism, cell death is often related to increased reactive oxygen species (ROS) production (Gill and Tuteja, 2010). To investigate if this occurred in LD-grown *tt5* plants, hydrogen peroxide (H_2O_2) and super oxide accumulation (O_2^-) was estimated. Plant leaves were removed and incubated in 3,3'-Diaminobenzidine (DAB) solution as described in the Methods (section 2.4). Leaves from *tt5* plants show higher accumulation of the DAB stain than leaves from the other mutants grown under LD conditions (Figure 3.6). When grown under SD conditions, leaves from all plants exhibited a similar response. The accumulation of superoxide was measured using Nitro Blue Tetrazolium (NBT). Again, *tt5* plants show higher O_2^- intensity (U) when grown under LD conditions (Figure 3.7). The other plants responded similarly to WT in both conditions including *tt4/tt5* under LD and SD.

Callose (β-1,3-glucan) synthesis is often associated with biotic and abiotic stress. For example, it is produced by the plant to reduce pathogen invasion. To evaluate the accumulation of callose, leaf samples were treated with aniline blue (as per section 2.4). *tt5* plants show enhanced deposition when grown under LD conditions (Figure 3.8). *tt5* plants showed a similar response to the other lines when grown in SD conditions including the double mutant *tt4/tt5*. Taken all together, *tt5* plants appear to be responding to a stress when grown under LD conditions. *tt5* stress phenotype was lost when crossed with *tt4* (CHS knock out), and was not observed in *tt6* plants, pointing that *tt5* response is exclusive to plants defective in CHI and grown under LD conditions. SD growth conditions had no effects on the variables tested when compared across the genotypes used in this study.

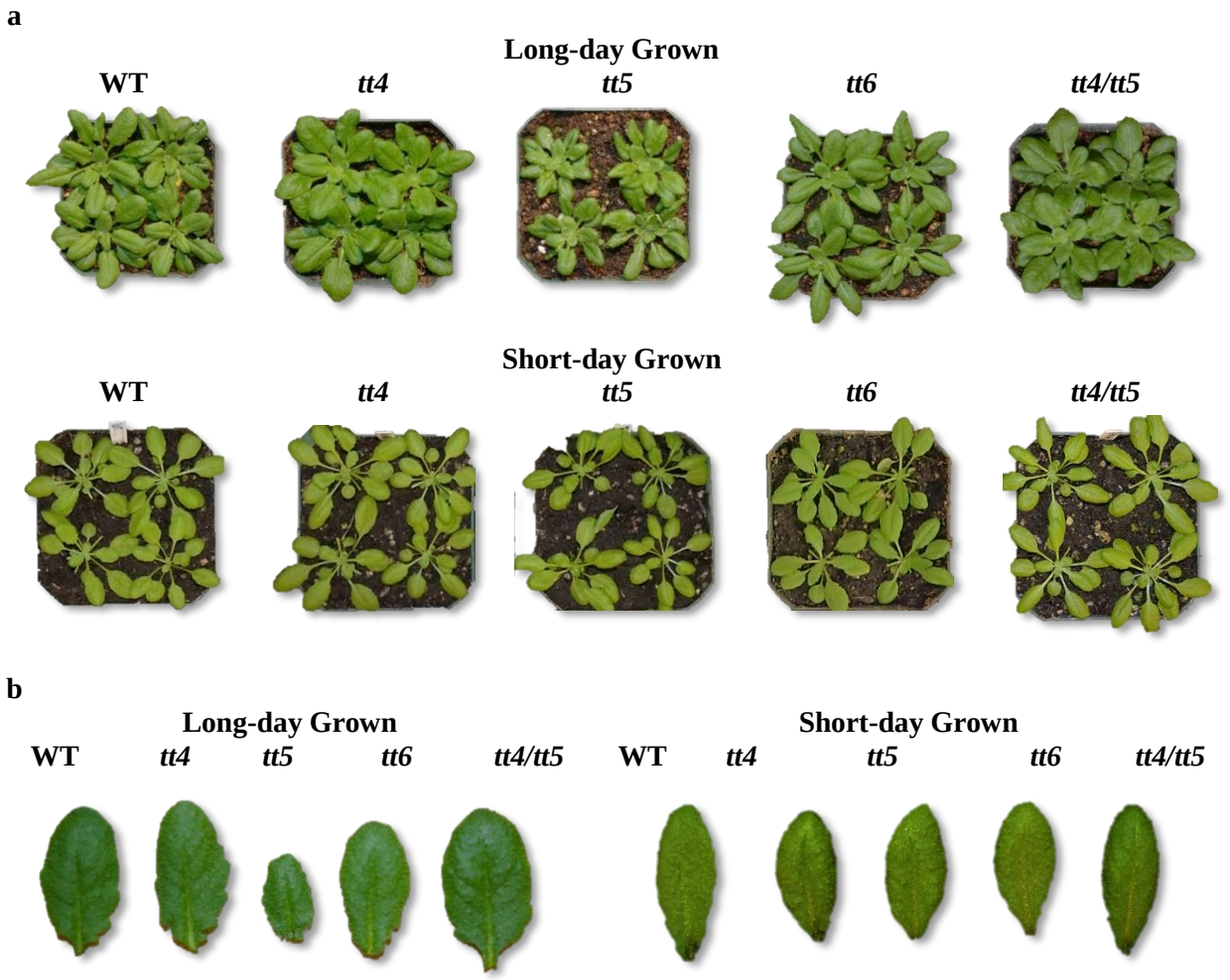

Figure 3.4: Arabidopsis *transparent testa* lines plants grown under Long and Short-day conditions.

Plants were grown in an environmental growth chamber under two different conditions: Long Day (LD) 22˚C, 16hr light/8 hr dark photoperiod and a light intensity at 200 µmol $m^{-2}s^{-1}$; Short Day (SD) 22˚C, 8 hr light/16 hr dark photoperiod and a light intensity at 200 µmol $m^{-2}s^{-1}$. The seeds were initially sown out in pots containing Sunshine® Mix 1 professional growing mix for bulk growth and then transferred to new pots when the 4-6 leaf stage was reached. a) Growth patterns of Arabidopsis lines under long-days and short-days. b) Leaves collected from 4-5 weeks-old plants. Images are representative of 3 independent experiments and 3 observations of each independent experiment.

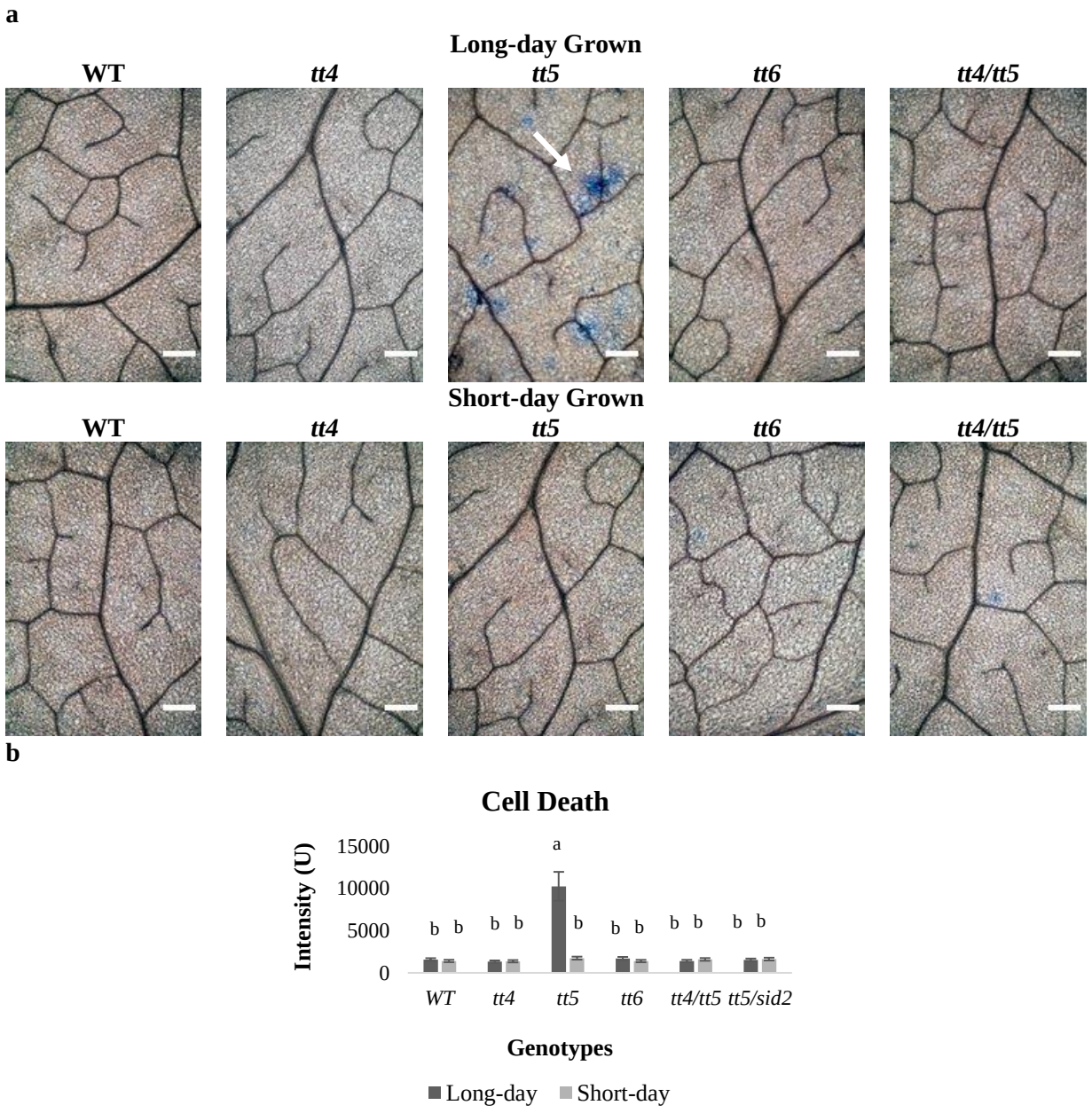

Figure 3.5: HR-like cell death lesions in plants grown under Long and Short-day conditions.

Non-inoculated leaves were incubated in Latophenol trypan blue (10 mL lactic acid + 10 mL phenol + 10 mL glycerol + 10 mL of distilled water + 40 mg of trypan blue) for 1 hour and transferred to the Fixation Buffer to remove the pigments. a) Programmed cell death is indicated by the blue spots (arrow) in different genotypes of Arabidopsis grown under LD and SD conditions before pathogen inoculation. b) The intensity of staining for cell death was measured in each sample using ImageJ. Scale bars: 200µm. Images are representative of 3 independent experiments and 3 observations of each independent experiment. Scale bars: 200µm. Different letters denoted significant differences of the means as determined by a two-way ANOVA with Tukey`s HSD ($P < 0.05$).

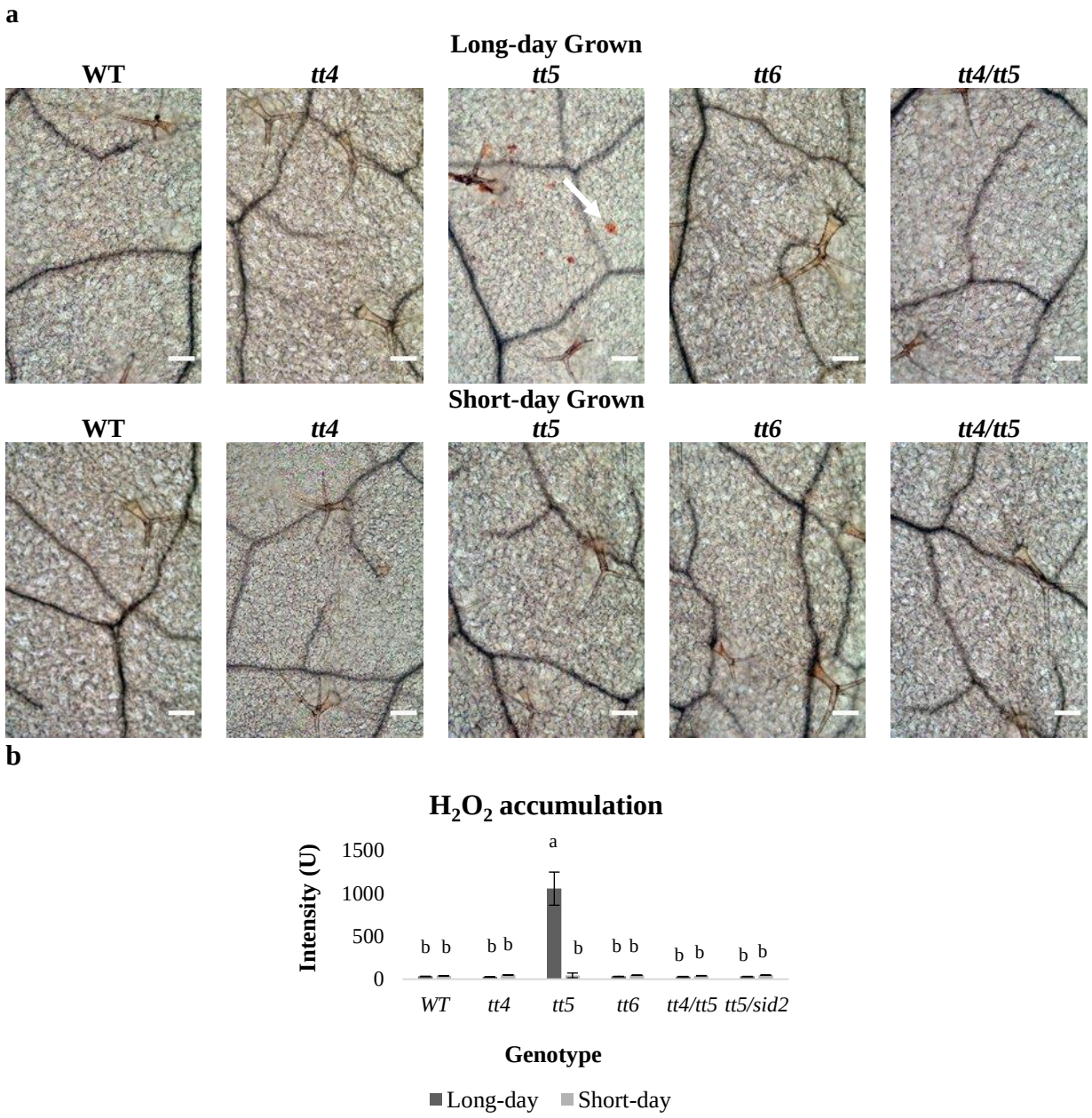

Figure 3.6: Hydrogen peroxide (H_2O_2) accumulation in plants grown under Long and Short-day conditions.

Non-Inoculated leaves were incubated in 3,3'-Diaminobenzidine (DAB) solution for 24 hrs. Subsequently, the samples were fixed for microscopy analysis. The brownish spots (arrow) indicate the accumulation of hydrogen peroxide. a) H_2O_2 accumulation in different genotypes of Arabidopsis grown under long and short-days before pathogen inoculation. b) The intensity of staining for H_2O_2 accumulation was measured in each sample using imageJ. Images are representative of 3 independent experiments and 3 observations of each independent experiment. Scale bars: 100µm. Different letters denoted significant differences of the means as determined by a two-way ANOVA with Tukey`s HSD ($P < 0.05$).

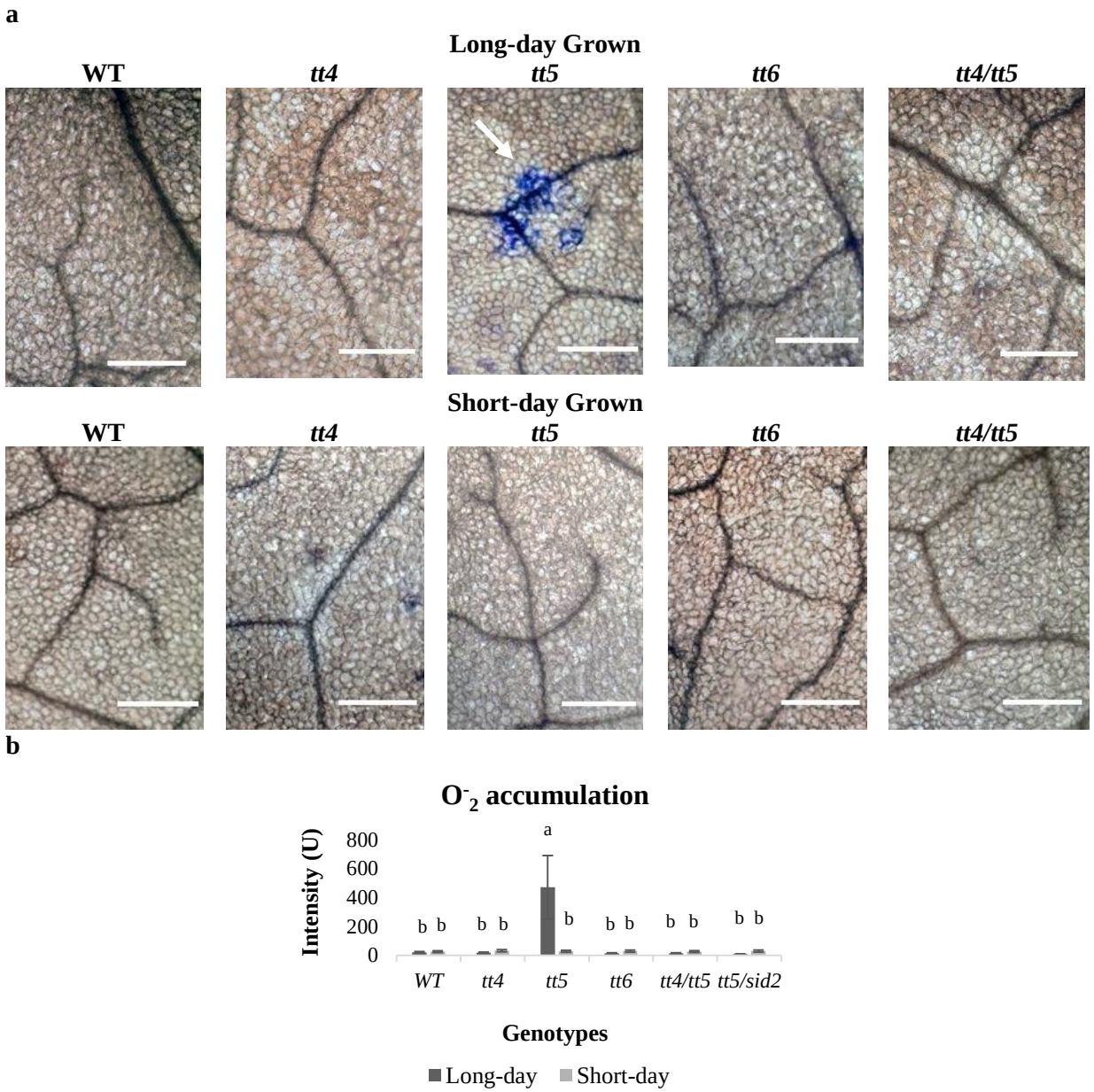

Figure 3.7: Super oxide (O^{-}_{2}) accumulation in plants grown under Long and Short day conditions.

Leaves were immersed in 1 ml of Nitro Blue Tetrazolium (NBT) (solution (4.3 mM NBT, 10 mM potassium phosphate pH 7.5, 1 mM NaN_3) and infiltrated under vacuum for 90 min. Subsequently, the leaves were fixed for microscopy analysis. a) Superoxide radical (O^{-}_{2}) accumulation are identified by blue staining (arrow). b) The intensity of staining for O^{-}_{2} was measured in each sample using imageJ. Images are representative of 3 independent experiments and 3 observations of each independent experiment. Scale bars: 100µm. Different letters denoted significant differences of the means as determined by a two-way ANOVA with Tukey`s HSD ($P < 0.05$).

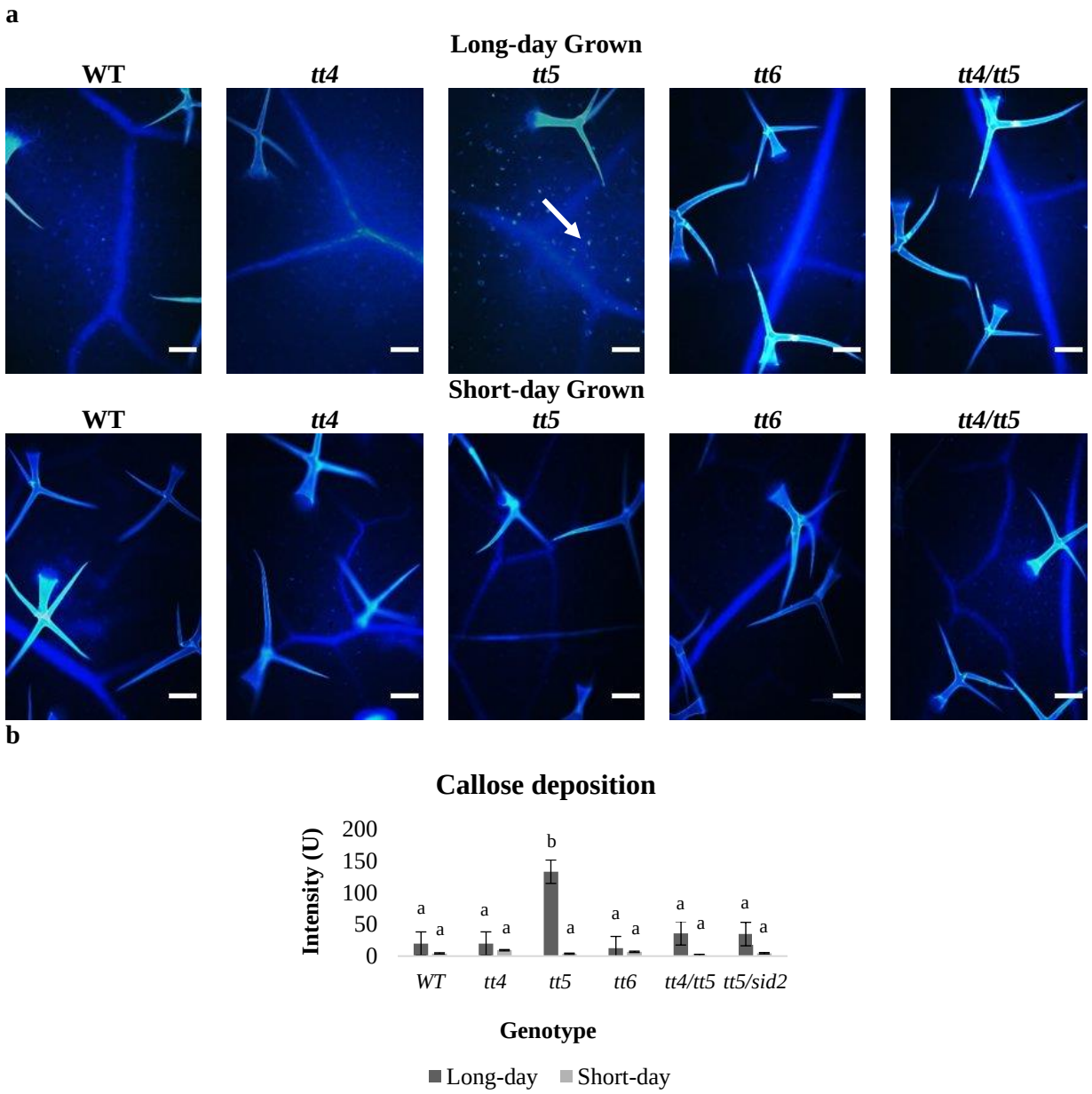

Figure 3.8: Callose deposition in plants grown under Long and Short-day conditions.

Leaves of non-inoculated plants were fixed and incubated in a solution containing aniline blue (0.05%) and 150 mM K_2HPO_4 overnight. Subsequently, samples incubated in water (pH 9.5) overnight. The samples were mounted in 30% glycerol and photographed under an Axioplan epifluorescence microscope with UV actinic light. a) Callose deposition (blue spots) in different genotypes of Arabidopsis grown under long and short-days before pathogen inoculation. b) The intensity of staining for callose was measured in each sample using imageJ. Images are representative of 3 independent experiments and 3 observations of each independent experiment Different letters denoted significant differences of the means as determined by a two-way ANOVA with Tukey`s HSD ($P < 0.05$).

3.3. Growth of *tt5* plants under LD conditions leads to expression of SA related genes

Traits observed in the LD grown plants suggest an active SA response. As mentioned earlier post-invasion resistance relies on SA, JA, and ET pathways. To determine if the SA response traits observed in the LD grown tt5 plants is consistent with an SA disease response, the expression of key enzymes of the salicylic acid biosynthesis pathway (ICS1, PAL1) and SA-induced defense markers (PR1, PR5, PDF.2) of were tested by RT-PCR. The ICS1, PAL1, PR1 and PR5 genes were upregulated in *tt5* LD despite no exposure to a pathogen (Figure 3.9). Although the double mutant (*tt4/tt5*) exhibits minor increases in ICS1 and PAL1 expression, it did not show PR1 upregulation. When grown under SD conditions, *tt5* plants did not show upregulation of the evaluated genes. These results suggest that the SA signaling pathway was affected by the *tt5* mutation in LD grown plants.

Arabidopsis plants with the *cpr-1* mutation display constitutive expression of SA-inducible defenses including: elevated PR-1 expression, programmed cell death, callose deposition and ROS accumulation (Kohler et al., 2002). When *cpr-1* plants were grown under LD and SD they exhibited a similar phenotype to *tt5* plants grown under LD (Figure 3.10). However, unlike *tt5* plants, day length did not impact the expression of SA-inducible defenses in *cpr-1* plants.

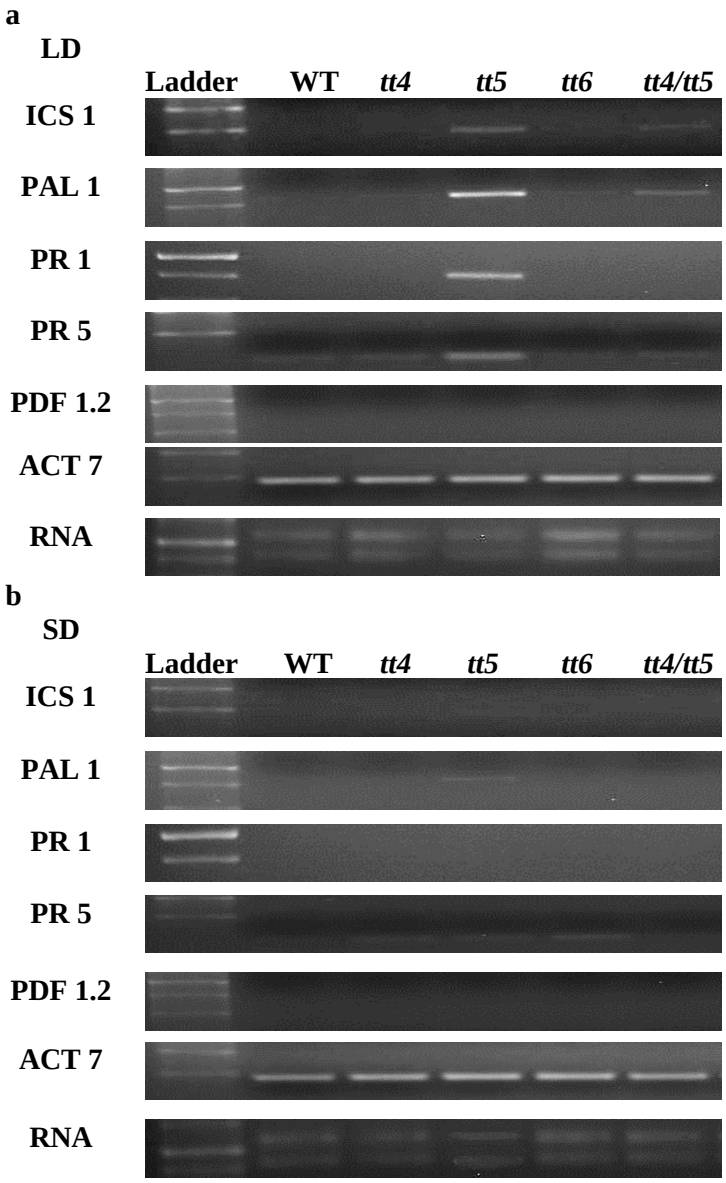

Figure 3.9: Expression of Salicylic Acid related genes in plants grown under Long and Shortday conditions

Leaf tissue from each of the plant lines grown under LD (a) and SD (b) were collected for RNA isolation. Expression level of each gene was estimated by RT-PCR. Gene abbreviations: ICS1 – isochorismate synthase; PAL1 - phenylalanine ammonia lyase 1; PR-1, Pathogenesis Related Gene-1; PR-5 - Pathogenesis Related Gene; PDF1.2, Plant defensing 1.2; ACT7 - actin 7. Images are representative of 2 independent experiments.

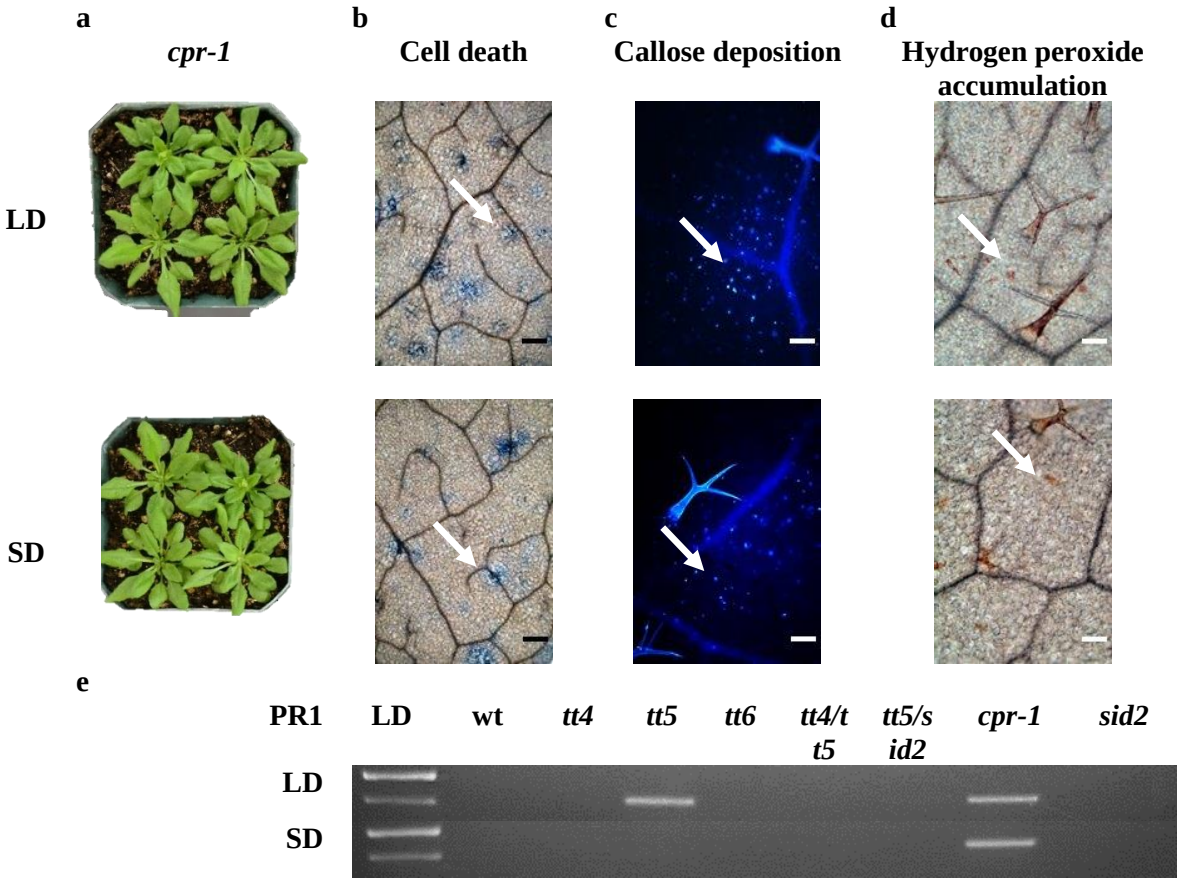

Figure 3.10: Analysis of the *cpr-1* mutant.

a) *cpr-1* phenotype grown under short (SD) and long days (LD). b) leaves were stained with lactophenol toluidine blue to identify programmed cell death (arrows). c) samples were stained with aniline blue to show callose deposition (arrows). d) leaves were stained with DAB to show H_2O_2 accumulation (arrows). Black scale bars: 200µm; white Scale bars: 100µm. PR1 expression in *cpr-1* mutant grown under long and short-days. Images are representative of 3 independent experiments and 3 observations of each independent experiment (except the RT-PCR analysis).

The knockout *tt5* provides enhanced resistance to powdery mildew (*Erysiphe cichoracearum*) and anthracnose (*Colletotrichum higginsianum*) infection, biotrophic and hemibiotrophic pathogens, respectively. Histological and molecular analyses suggest the *tt5* plants exhibit elevated gene expression of components of the SA biosynthetic pathway before the pathogen infection when grown under LD conditions. To confirm that the *tt5* LD phenotype is SA-dependent, *tt5* plants were crossed with SA-insensitive lines (*sid2* and *nahG*). The SID2 gene encodes isochorismate synthase, which is necessary for SA biosynthesis via the non-PAL pathway (Figure 3.11) (Brodersen and Malinovsky, 2005). The NAHG gene encodes a bacterial salicylate hydroxylase, which degrades SA as it is produced in the plant cell (Heck et al, 2003). Subsequent experiments examined the phenotype and disease resistance of *tt5/sid2* and *tt5/nahG*. The double mutants *tt5/sid2* and *tt5/nahG* lost the *tt5* LD phenotype and did not exhibit HR-like cell death, callose deposition, or hydrogen peroxide accumulation when grown under LD conditions (Figure 3.11). The *tt5/sid2* plants also lost enhanced resistance to *E. cichoracearum* and *C. higginsianum.* Similarly, non-inoculated *tt5/sid2* plants fail to express PR1 when grown under LD conditions. Taken together, these results reinforce the suggestion that the *tt5* LD phenotype and the enhanced disease resistance *tt5* plants exhibit is SA-dependant.

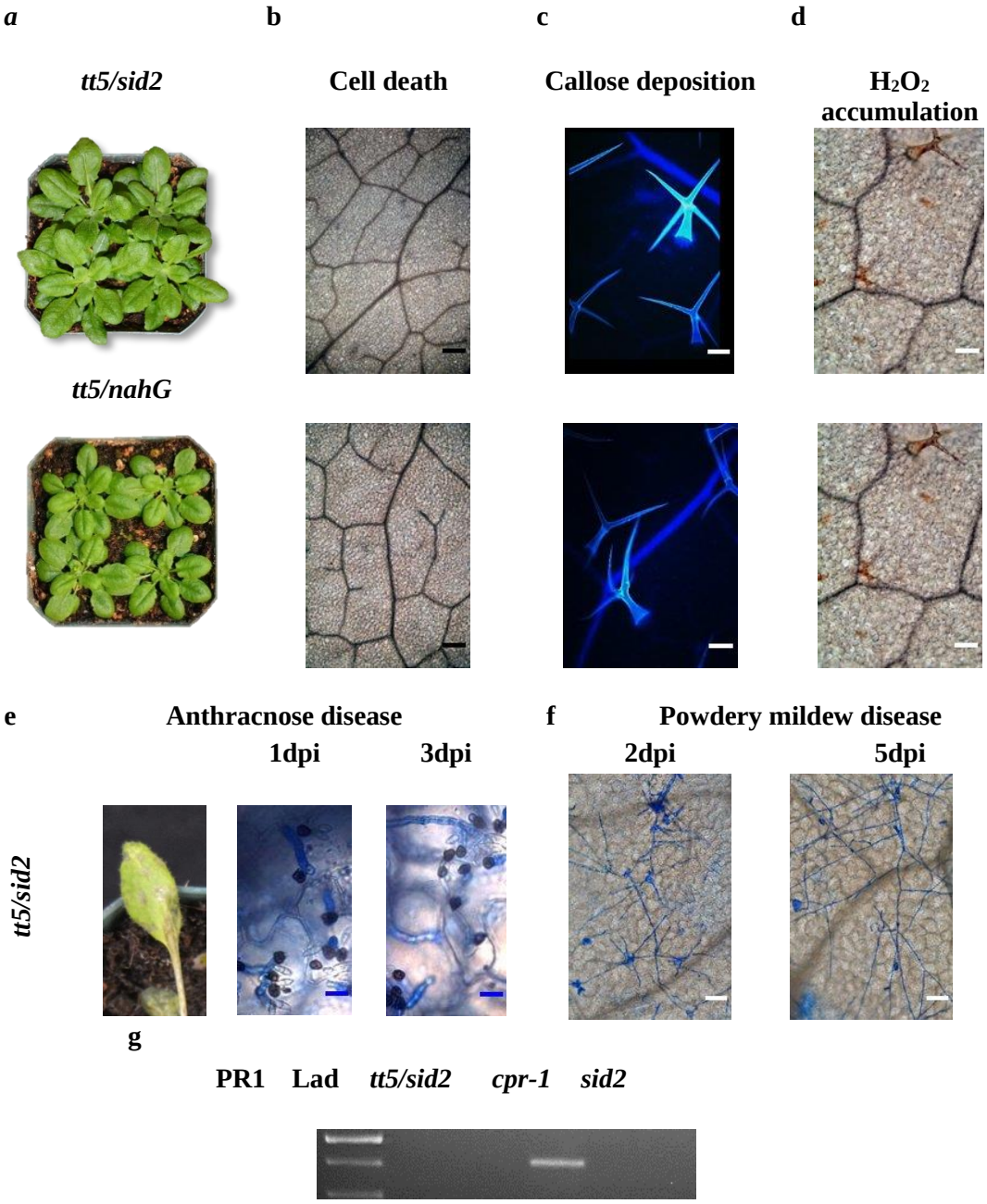

Figure 3.11: Growth patterns and disease symptoms on *tt5sid/2 and tt5/nahG* grown under Long day conditions.

a) Double mutants grown under LD. b) Non-inoculated leaves were stained with Lactophenol tryphan blue to identify programmed cell death. c) samples were stained with 0.05% aniline blue to show callose deposition. d) leaves were stained with DAB to show H_2O_2 accumulation. e) Symptoms on *tt5/sid2* inoculated with *Colletotrichum higginsianum* g) Colletotrichum hyphae progression on *tt5/sid2*. f) *Erysiphe cichoracearum* hyphae progression on *tt5/sid2*. g) PR1 expression in *tt5/sid2* mutant. The graphs for *C. higginsianum* penetration frequency and *E. cichoracearum* hyphae progression are illustrated on figures 3.1 and 3.3, respectively. Images are representative of 3 independent experiments and 3 observations of each independent experiment. Black scale bars: 200µm; white scale bars: 100µm; blue scale bars: 15µm.

3.4. Naringenin Chalcone is only accumulated in *tt5* plants grown under LD conditions.

Flavonoids are secondary metabolites that have several functions in plants, from attracting pollinators to defense compounds. To better understand the metabolic flux of naringenin chalcone (NC) in the flavonoid mutants NC was quantified in leaves using HPLC. The leaves of *tt5* plants accumulate a greater amount of NC compared to other mutants (Figure 3.12). *tt4* and *tt4/tt5* were not able to accumulate NC due to the lack of chalcone synthase. Surprisingly, WT and *tt6* did not show detectable traces of NC. The double mutant *tt5/sid2* showed small traces of NC. Plants grown under SD showed no detectable traces of NC (Fig 3.13).

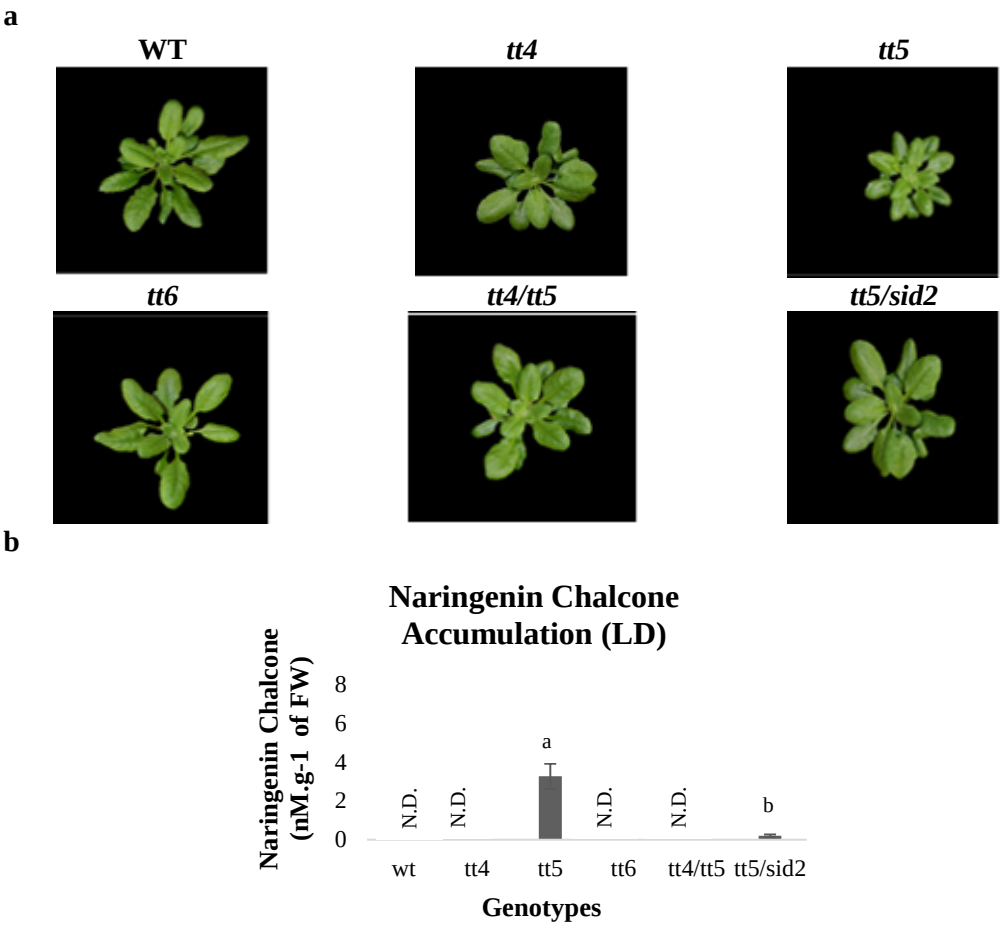

Figure 3.12: Naringenin Chalcone (NC) accumulation in Arabidopsis lines grown under LD.

a) Arabidopsis lines grown under LD b) NC accumulation (nM g^{-1} of FW). N.D.: Non detected. N.D. Images are representative of 3 independent experiments and 3 observations of each independent experiment. Different letters denoted significant differences of the means as determined by a one-way ANOVA with Tukey`s HSD ($P < 0.05$).

a

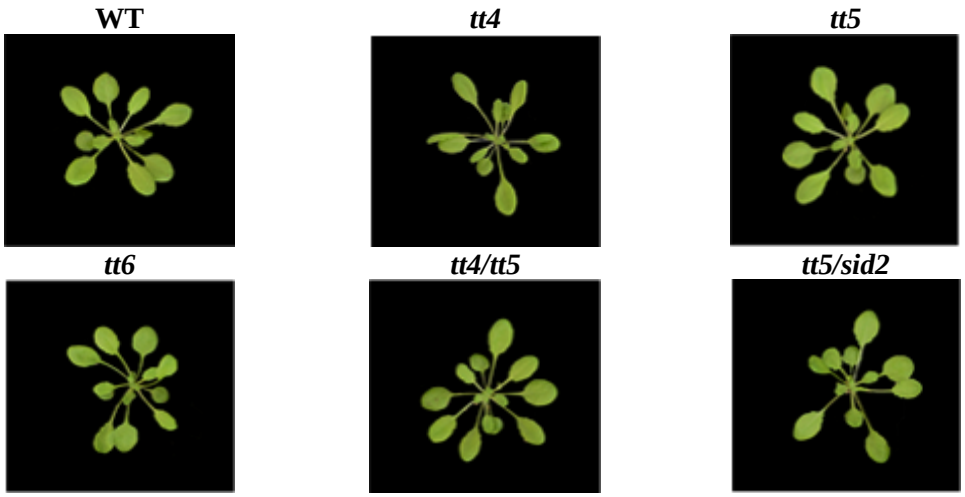

b

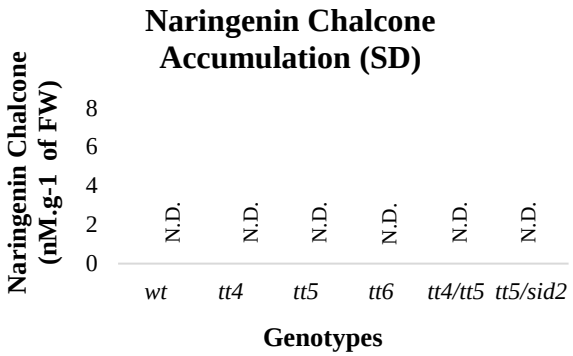

Figure 3.13: Naringenin Chalcone (NC) accumulation in *transparent testa* lines grown under Short-day conditions.

a) Arabidopsis lines grown under short- day conditions. b) NC accumulation ($nM.g^{-1}$ of FW). N.D.: Non detected. N.D. Images are representative of 3 independent experiments and 3 observations of each independent experiment. Different letters denoted significant differences of the means as determined by a one-way ANOVA with Tukey`s HSD ($P < 0.05$).

3.5. Stress conditions trigger Naringenin Chalcone accumulation.

Because the CHI protein encoded by the TT5 gene blocks further metabolism of NC, we evaluated the accumulation of NC in plants grown under biotic and abiotic stress conditions (Figures 3.14 to 3.16). The leaves of plants infected with Powdery mildew (*E. cichoracearum)* and anthracnose (*C. higginsianum)* were evaluated 3dpi and 5dpi, respectively. Plants infected with powdery mildew accumulated NC except for *tt4* and *tt4/tt5* plants (Figure 3.3). In this case, WT accumulated more NC than *tt5*, *tt6*, and *tt5/sid2* although they were not statistically different. All plants infected with anthracnose were able to accumulate NC except for *tt4* and *tt4/tt5* due to the lack of chalcone synthase. *tt5* plants accumulated more NC than WT and *tt6* although they were not statistically different. *tt5/sid2* accumulate NC but in smaller amounts. Long Day + Low Temperature (LD+LT) and Short Day + High Light (SD+HL) conditions promoted the accumulation of NC in WT and *tt5*. Arabidopsis lines grown under LD+LT showed higher average of NC retention than lines grown under SD+HL.

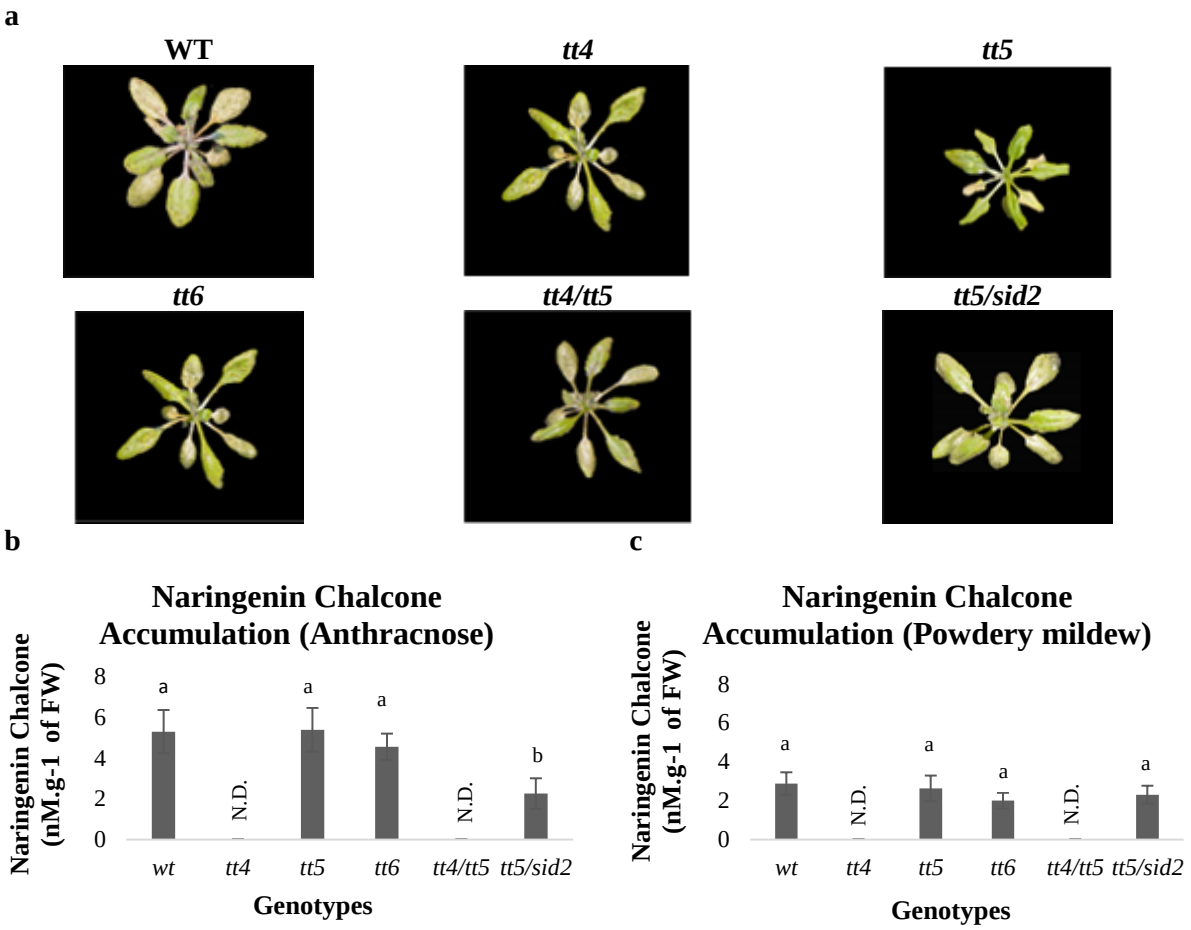

Figure 3.14: Naringenin chalcone (NC) accumulation in infected plants grown under Long-day conditions.

a) Arabidopsis mutants inoculated with *Colletorichum higginsianum* 5 days post inoculation (dpi). b) NC accumulation in plants inoculated with *C. higginsianum* 3dpi. c) NC accumulation in plants inoculated with *Erysiphe cichoracearum* 5dpi ($nM.g^{-1}$ of FW). N.D.: Non detected Images are representative of 3 independent experiments and 3 observations of each independent experiment. Different letters denoted significant differences of the means as determined by a one-way ANOVA with Tukey`s HSD ($P < 0.05$).

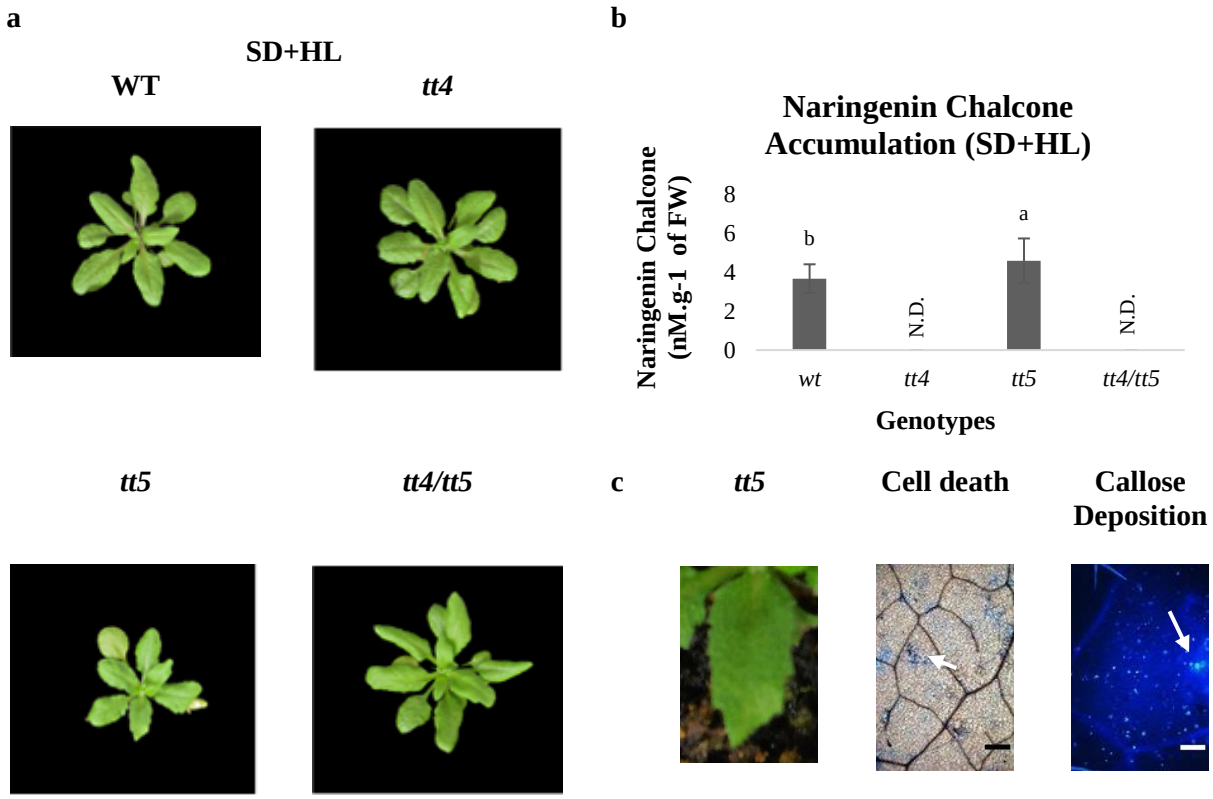

Figure 3.15: Naringenin chalcone (NC) accumulation of plants grown under Short day + High light conditions.

a) WT, *tt4*, *tt5* and *tt4/tt5* were grown under SD+HL. b) NC accumulation in Arabidopsis mutants (nM.g^{-1} of FW). N.D.: Non detected. c) Representative leaf of *tt5* mutant stained with lactophenol tryphan blue to identify programmed cell death (black arrow) and aniline blue to identify callose deposition (red arrow), respectively. Images are representative of 3 independent experiments and 3 observations of each independent experiment. Black scale bars: 200µm; white scale bars: 100µm. Different letters denoted significant differences of the means as determined by a one-way ANOVA with Tukey`s HSD ($P < 0.05$).

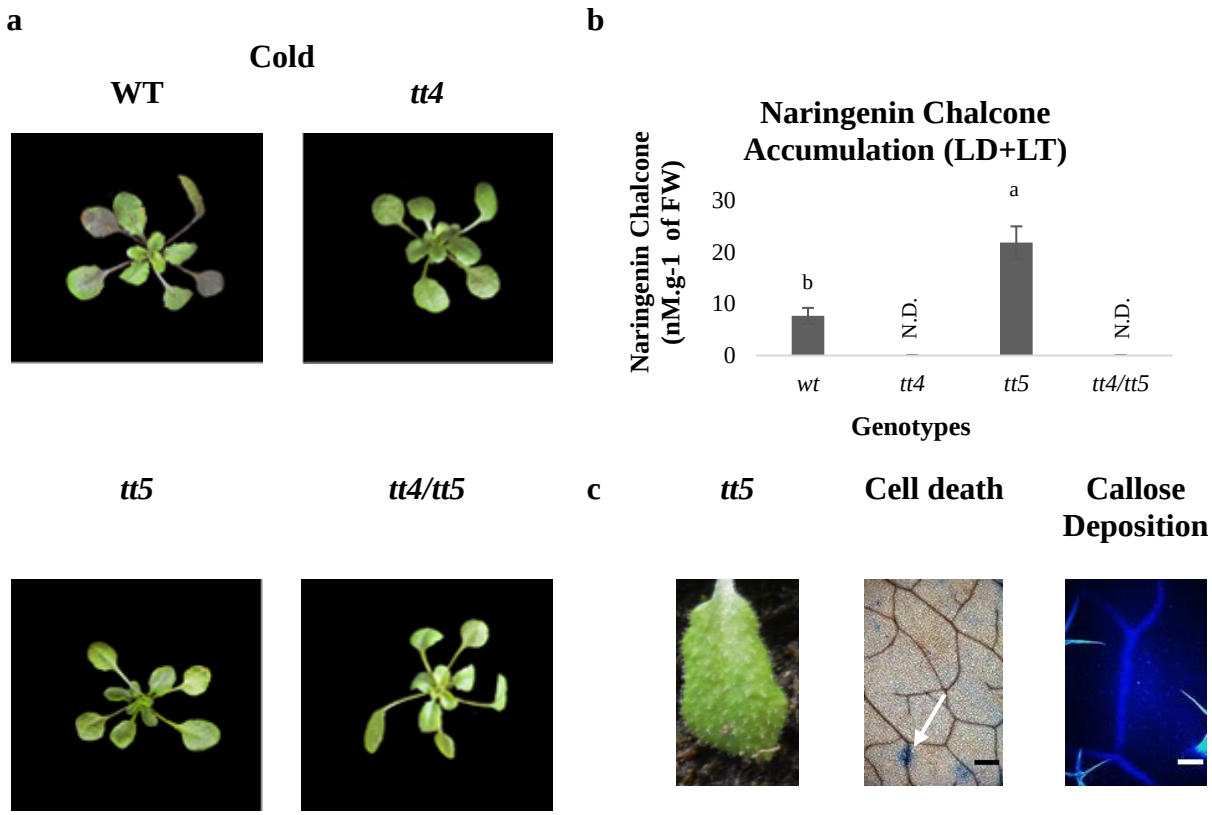

Figure 3.16: Naringenin chalcone accumulation and phenotype of plants grown under Long day + Low temperature conditions.

a) WT, *tt4*, *tt5* and *tt4/tt5* grown under long-day + cold conditions b) NC accumulation in Arabidopsis lines (nM.g-1 of FW). c) Representative leaf of *tt5* mutant stained with lactophenol tryphan blue to identify HR-like cell-death (arrow) and aniline blue to identify callose deposition, respectively. N.D.: Non detected. Images are representative of 3 independent experiments and 3 observations of each independent experiment. Black scale bars: 200µm; white scale bars: 100µm. Different letters denoted significant differences of the means as determined by ANOVA with Tukey`s HSD ($P < 0.05$).

3.6. Naringenin Chalcone as Stress Factor

During my project I observed that *tt5* plants grown under long days would show a unique phenotype and enhanced disease resistance. *tt5* plants grown in these conditions would exhibit many stress signals before pathogen challenge such as callose deposition, callose accumulation HR-like cell death. I found that *tt5* would only accumulate NC under long days and it would be followed by the expression of SA markers. Interestingly, SA-insensitive lines do not accumulate NC. I hypothesized that NC is the primary reason behind *tt5*-LD response. If this is true, all the other genotypes should exhibit *tt5*-LD phenotype or at least *tt4/tt5* due to the lack of CHI. To confirm the role of NC in *tt5* phenotype and disease resistance, I sprayed a 200 µg/mL of NC solution on plants grown under LD and SD conditions (Figure 4.3). My first results showed the toxic effect of NC in plants grown under LD. WT and the other *tt* mutants showed a similar aspect to the *tt5* mutant. Plants grown under short days showed no morphological changes. However, I did not get the same results when I repeated the experiment. One possible reason for the discrepancy in my results is the age of the NC solution. NC can be naturally converted into naringenin and is generally unstable in solution. I confirmed the conversion of NC to Naringenin in the solution by HPLC. Therefore, the second experiment may have been compromised due to a much lower concentration of NC. This needs to be repeated with a fresh batch of NC.

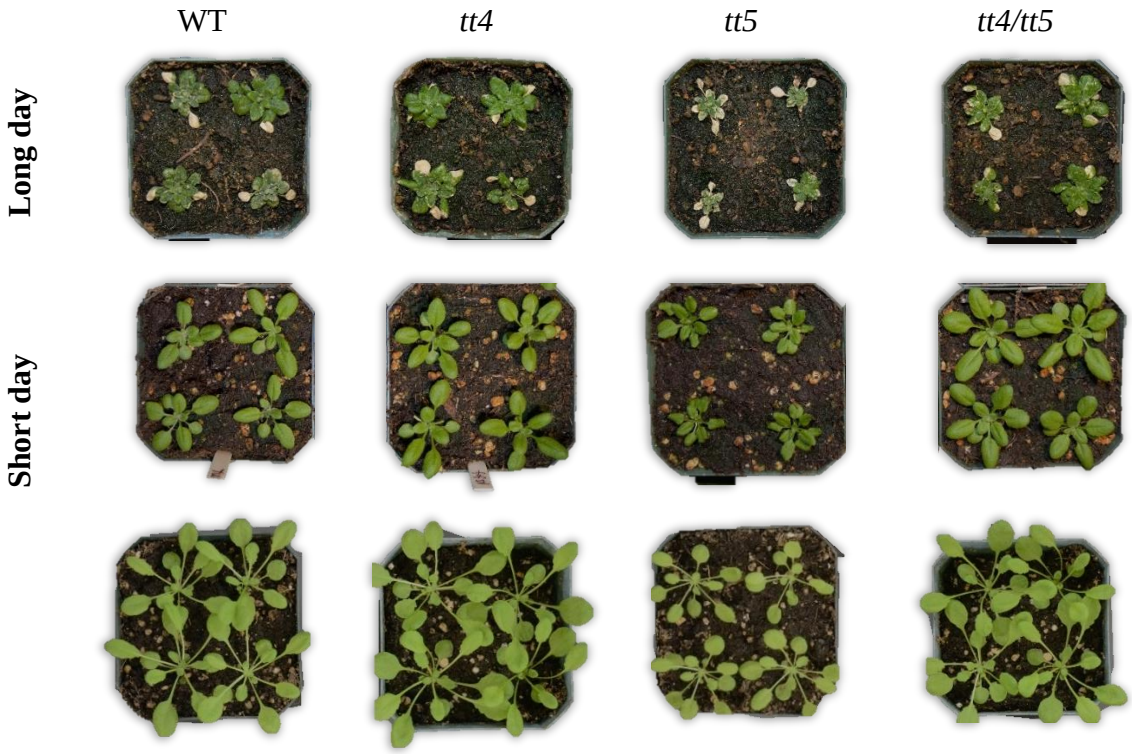

Figure 3.17: Plants sprayed with NC (2',4,4',6'-Tetrahydroxychalcone) solution.

Plants were grown in an environmental growth chamber under two different conditions: Long Day (LD) 22˚C, 16hr light/8 hr dark photoperiod and a light intensity at 200 µmol $m^{-2}s^{-1}$; Short Day (SD) 22˚C, 8 hr light/16 hr dark photoperiod and a light intensity at 200 µmol $m^{-2}s^{-1}$. Plants were sprayed with NC solution (200 µg/mL) and kept under control conditions. Control samples are in the appendix section (7).

CHAPTER 4 DISCUSSION AND FUTURE PERSPECTIVES

4. Discussion

Plants have developed multiple layers of sophisticated surveillance mechanisms that recognize potentially dangerous pathogens and rapidly respond before those organisms have a chance to cause serious damage. Among these mechanisms secondary metabolites, and hormones play an important role in plant-pathogen interactions. This PhD study is based on initial observations by Dr. Song Tao and Dr. Yangdou Wei where they found that the Arabidopsis flavonoid mutant *tt5* presented enhanced resistance to *Colletotrichum higginsianum* and *Erysiphe cichoracearum*. The phenylpropanoids are classified into three main groups: phytoalexins, phytoanticipins, and signal molecules (these roles can overlap). For example, lignins are important in the formation of the cell wall and the papillae after pathogen interaction (Kubitzki, 1987; Heldt et al., 2011). Flavonoids act as regulators of auxin transport (Pourcel et al., 2007), and SA as a regulator of both local and systemic pathogen-induced defense gene activation, the oxidative burst, and pathogen-induced cell death (Vlot et al., 2009). The flavonoid branch starts with the conversion of p-coumaroyl-CoA to naringenin chalcone (NC) by CHS (*tt4*), followed by the conversion to naringenin by CHI (*tt5*) and converted to dihydrokaempferol by F3H (*tt6)* the precursors of other flavonoids (Figure 1.3). Differently from *tt4* and *tt6*, the *tt5* mutation presents a unique phenotype and enhanced resistance against fungal diseases when grown under long days. Although authors report the beneficial role of Naringenin as an antifungal agent, there is no evidence of the antifungal role of NC so far (Bido et al., 2010; Wasson et al., 2006).

4.1. *tt5* long day growth phenotype and enhanced disease resistance are SA-Dependent

Plants have several mechanisms to counteract pathogen infection. To avoid pathogens access to cell nutrients, plants rely on several mechanisms such as callose appositions, ROS burst, known

as penetration resistance. After penetration, plants switch their metabolism employing many signal molecules to block pathogen colonization, known as post-invasion resistance. The induction of post-invasion resistance is often related to the expression of defense genes such as Pathogenesis Related Gene-1 for the salicylic acid (SA) pathway and Plant Defensin 1.2 for the jasmonic acid/ethylene (JA/ET) signaling pathway. We evaluated *tt5* performance and resistance mechanisms against *C. higginsianum* and *E. cichoracearum.* We observed that *tt5* plants exhibited unique behavior when grown under long days and exhibited resistance against anthracnose and powdery mildew disease. The penetration resistance of the *tt5*-LD mutant was compared to WT and other *tt* lines grown under SD and LD. Consistently, the *tt5* mutant allowed significantly less penetration frequencies of *C. higginsianum*. We attribute this resistance to *tt5*-LD high ROS accumulation and callose deposition previous the pathogen infection. Its been extensively suggested that early callose deposition and H_2O_2 play an important role against fungal pathogens, such as *Alternaria brassicicola* and *Plectosphaerella cucumerina* (Ton and Mauch-Mani, 2004). However, it was not clear if impaired penetration resistance in the *tt5* mutant was the only reason causing the enhanced susceptibility against host pathogen. When inoculated with *C. higginsianum* and *E. cichoracearum*, the *tt5*-LD showed less severe disease symptoms than WT and the others *tt* lines. These results point that plants carrying the *tt5* mutation are "activated" under LD and the tt5-LD phenotype affects both penetration and post-invasion resistance. Interestingly, *tt5*-LD post invasion resistance is strongly linked to the presence of hypersensitive response (HR)-like cell death. HR-like cell death is a form of programed cell death often induced by exogenous stress and is related with an increase of SA levels.

Plants often respond to adverse conditions with an increase in the endogenous SA level (Martínez et al., 2004). SA does not only induce direct protective mechanisms, but it may also

cause oxidative stress in plants through the generation of ROS, thus participating in the development of stress symptoms (Gill and Tuteja, 2010; Khalil et al., 2018). The exogenous application of SA has multiple effects on secondary metabolism, including flavonoid biosynthesis. The pathogen susceptibility investigation was tested using knockouts of several genes in Arabidopsis Columbia background impacting the flavonoid biosynthesis pathway and the accumulation of specific compounds. Further experiments revealed that *tt5* disease resistance was SA-mediated. Plants grown under long days exhibited upregulation of PAL-1, ICS-1, and PR-1 key genes involved in SA metabolism. While I did not measure SA accumulation directly in these plants, the coordinated upregulation of multiple SA-responsive genes is very strong evidence that SA accumulation correlates with the disease resistance observed in long-day grown *tt5* plants.

Careful examination of the *tt5* LD grown plants exposed other SA-related changes to the plants. We saw that the plant size was diminished (Figure 3.4). Other observations observed only in the LD grown *tt5* plants are callose deposition, ROS production, and cell death (Figure 3.5 to 3.8). These are physiological and biochemical changes normally observed in Arabidopsis plants exposed to pathogens that activate the SA defense system. However, in this case it is observed simply due to LLD growth conditions.

I also used a genetics approach to demonstrate the role of SA in the *tt5* growth and disease resistance phenotype. I crossed *tt5* plants with plants missing the ICS gene (*sid2*) and with plants overexpressing a bacterial gene that degrades SA (*nahG*). The results in each case fit the hypothesis that the *tt5* phenotype was SA dependent. The *tt5/sid2* plants and the *tt5/nahG* both had a normal, wild type phenotype when grown under long days. They did not express *PR1*, nor did they produce callose and ROS, or exhibit cell death (Figure 3.11). Thus, I am quite confident that the phenotype of the *tt5* plants is due to SA production. A question remains: why?

Both SA and flavonoids are synthesized from phenylalanine via cinnamic acid (Figure 4.1). It has been extensively demonstrated that exogenous application of flavonoids can trigger SA production and SA can alter flavonoid metabolism (Jia et al., 2010; Li et al., 2019; Su et al., 2013; Williams et al., 2004). However, in this situation, only *tt5* plants exhibit SA response, which points to the accumulation of NC being directly involved in this phenomenon especially considering that *tt6* could not only accumulate naringenin but kaempferol, quercetin, and naringenin chalcone (cotyledonary node) (W. A. Peer et al., 2001).

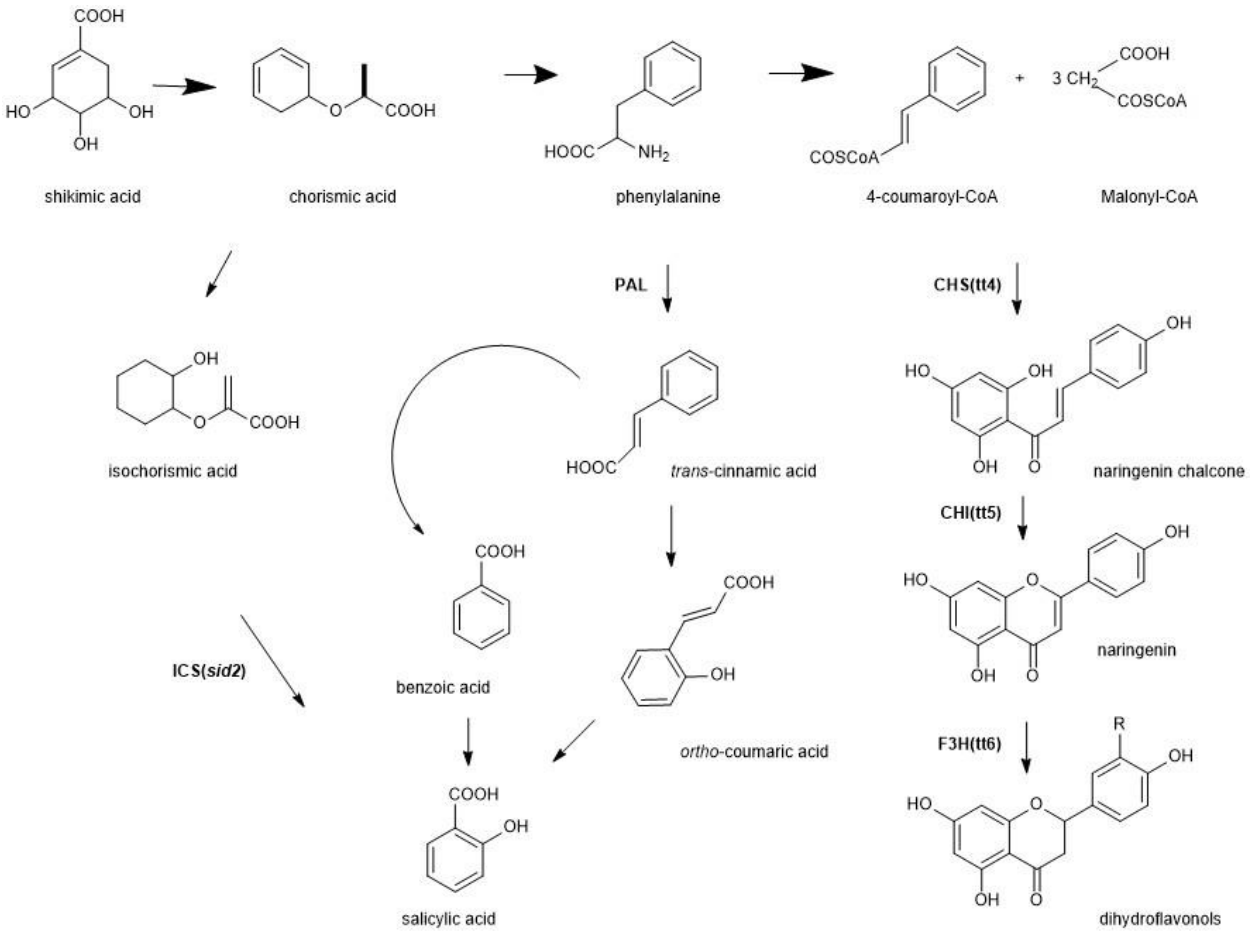

Figure 4.1: Scheme of the salicylic acid and flavonoid biosynthetic pathways.

Enzymes are indicated in bold, with the corresponding genetic loci in parentheses. CHS, chalcone synthase; CHI, chalcone isomerase; flavanone 3-hydroxylase (F3H); PAL, phenylalanine ammonia-lyase; ICS, isochorismate synthase (Burbulis et al, 1999; Wildermuth et al., 2002).

NC is the first product in the flavonoid pathway and can be is converted nonenzymatically to naringenin at very low levels (Dao et al, 2011). Flavonoids such as quercetin, or rutin, can trigger SA-mediated defense also called priming stimulus (Kohler et al., 2002; Ton et al., 2009). Defense priming is classified as an intrinsic part of induced resistance: the plant takes defensive measures against the potential attacker while also preparing its defensive system for a faster and/or stronger reaction in the future. Primed plants display faster, stronger defense responses, and it is usually related to the upregulation of defense-related genes: PAL, PR-1, PR-2, and PR-5 (Kohler et al., 2002; Shah et al., 2014; Ton et al., 2009). These plants may also present cell death lesions followed by callose deposition which is a widely used marker of responsiveness to plant pathogens (Voigt, 2014) and overly presented in *tt5*-LD plants. For example, plants treated with the flavonoid rutin were found to enhance resistance to *Xanthomonas oryzae* pv. oryzae, *Ralstonia solanacearum*, and *Pseudomonas syringae* pv. tomato strain DC3000 in rice, tobacco and Arabidopsis respectively (W. Yang et al., 2016). Rutin-mediated priming resistance was found to be attenuated in *npr1*, *eds1*, *eds5*, *pad4-1*, *ndr1* mutants, and *NahG* transgenic Arabidopsis plants, but not in *snc1-11*, *ein2-5* or *jar1* mutants pointing that rutin affects the SA signaling pathway but not the jasmonate or ethylene pathways (Yang et al., 2016). To confirm this hypothesis, *tt5* was crossed with a transgenic (*NahG*) line that expresses salicylate hydroxylase, a bacterial enzyme that degrades SA. In this case, the *NahG* plants degrade SA as quickly as it is produced and hence do not exhibit SA-mediated defense. If the *tt5* cell death/pathogen resistance phenotype was the result of SA, then the *tt5/NahG* double mutant plants should not produce cell death or pathogen resistance under either LD or SD growth. As expected, the double mutant *tt5/NahG* restored a WT phenotype and the plants lost enhanced disease resistance. Genetic evidence for JA antagonism of SA-signalling pathways has been well documented using jasmonate- signaling mutants (Li et al,

2019). Several JA biosynthesis genes, such as *LOX2*, *AOS*, *AOC2* and *OPR3*, are repressed by SA, and the exogenous application of SA represses the expression of the JA-induced marker gene *PDF1.2*. To verify the exclusively role of SA in *tt5* enhanced defense, *tt5* plants were crossed with plants with *jar1* and *ein2* mutations (Song. T and Wei. Y, data not published) that are disrupted in JA and ET signaling responses, respectively. However, these mutations did not affect the developmental phenotype and disease resistance of the *tt5* mutants grown under LD conditions (Song. T and Wei. Y, data not shown). Pourcel et al. (2013) found that JA regulates the expression of dihydroflavonol reductase (DFR), and thereby regulated anthocyanin accumulation. *tt5* (ler-0) plants treated with naringenin showed jasmonate biosynthetic genes were highly represented among the signaling pathways including jasmonate-zim-domain (JAZ) repressors protein that function in the JA signaling pathway but did not reported any alterations in *PAL* And *ICS1* expression (Pourcel et al., 2013).

Changes in the environment have major influences on the Flavonoid and SA biosynthesis. Both PAL1 and ICS1, are key enzymes of the SA pathway and are transcriptionally upregulated in adverse conditions (Li et al., 2019). Genetic and molecular analyses have indicated that most of SA is synthesized from the isochorismate (ICS1) pathway (approximately 90%) and the remaining is probably produced by phenylalanine (PAL1) from cinnamate via o-coumarate or benzoate (Figure 4.1) (Dempsey and Klessig, 2017; Shakirova et al., 2016; Vlot et al., 2009). When *tt5* plants were crossed with the isochorismate synthase knockout (*sid2*) they restored the LD-grown WT phenotype, *pal1* upregulation, and enhanced resistance. Thus, ICS1 is altering PAL1 activity and the flavonoid pathway in *tt5* plants grown under long days. Lin et al. (2020) found that nWHY1 directly binds to the promoter region of isochorismate synthase (*ics1*) to activate its expression at later stage and indirectly activates S-adenosyl-L-methionine-dependent methyltransferase (*bsmt1*)

gene expression via ethylene response factor (*erf109*). nWHY1 also represses *pal1* expression via R2R3-MYB member 15 (*myb15*) during stress-induced senescence. Earlier, SA-mediated improved thermo-tolerance in *Vitis vinifera* was advocated as a result of SA-induced accumulation of *pal* mRNA, the synthesis of new PAL protein, and significant accumulation of phenolics (Khan et al., 2015). However, PAL can be downregulated by cinnamic acid and other downstream compounds (Chen et al., 2017). For example, the Arabidopsis glycosyltransferase double mutant *ugt78d1/ugt78d2* was characterized by strong inhibition of flavonoid and *PAL* genes due to the accumulation of aglycone compounds. The exogenous application of naringenin on *ugt78d1/ugt78d2* restores *PAL* activity (Yin et al., 2012). This suggests that the *tt5* SA-response might be regulated by several components involving not only PAL but downstream components from the flavonoid pathway.

4.2. Day-length affects the *tt5* SA-mediated defense

It is well known that plant development as well as their resistance to pathogens can be influenced by external stimuli. Light exposure influences all stages of growth and development of plants (Wu and Yang, 2010). Adequate light conditions provide the energy from photosynthesis needed for a robust response to infections caused by pathogens. These responses usually include rapid production of reactive oxygen species (ROS) followed by synthesis of secondary metabolites such as salicylic acid (SA) accumulation of phytoalexins, increased expression of pathogenesis-related (PR) proteins, and hypersensitive cell death (Ballaré, 2014). Accumulation of SA and expression of salicylic acid (SA)-induced pathogenesis-related 1 (PR-1) gene is affected by light in plant-bacteria interactions. Studies also point that Arabidopsis plants grown under low light or in the absence of light have their local and systemic responses compromised to *P. syringae* (Sano et al., 2014). In Arabidopsis, resistance to turnip crinkle virus in dark-treated plants was enhanced

by treatment with exogenous SA. However, SA was only effective when the plants were pretreated in the presence of light. SA treatment carried out in the dark was unable to induce SA mediated signaling leading to resistance or *PR-1* gene expression (Lima et al., 2015). It has been shown that several defense responses are influenced by light and phytochrome (PHY) and cryptochrome (CRY) regulate plant defense responses. In Arabidopsis, SA-induced PR-1 expression was down-regulated in *phyA*, *phyB*, and *phyA/phyB* mutants. Bacterial growth in infected leaves also significantly increased in *phyA/phyB* double mutants compared with WT under LD conditions (Genoud et al., 2002). SAR was also shown to be repressed in *phyA/phyB* double mutants compared with WT (Griebel and Zeier, 2008). Wu and Yang (2010), reported that CRY1 positively regulates inducible resistance to *Pseudomonas syringae* under SD conditions. Arabidopsis *cry1* mutant failed to display effector-triggered local resistance, leading to more pathogen multiplication. On the other hands, plants overexpressing CRY1, exhibited up-regulation local resistance mechanisms (HR, ROS). They also suggested that SAR is positively regulated by CRY1, and that SA-induced PR-1 expression is reduced in the *cry1* mutant, but enhanced in CRY1-overexpressor plants, making *cry1* an important player in plant defense against biotrophic a hemi biotrophic pathogens.

It was found that *tt5* plants grown under short days (SD) exhibited higher susceptibility against *C. higginsianum* and *E. cichoracearum* and did not show cell death lesions, callose depositions, and ROS accumulation. Further experiments revealed that *tt5*-SD lacks the expression of *PAL-1*, *ICS-1*, *PR-1* genes differently from *tt5*-LD. Knocking out *SID2* or degrading SA by *NahG* expression also restores WT phenotype when *tt5* was grown under LD. I hypothesize that a stress factor (day-length in this case) is responsible for triggering the accumulation of NC causing *tt5* response. In situations of light stress, key enzymes from SA production are activated (PAL,

ICS) and flavonoids are accumulated in the epidermis (Su et al., 2013). CHS gene also shows induction upon high light treatment and UV-B treatment being regulated by mostly by blue light (Jenkins et al., 2001). However, CHS can be downregulated by NC accumulation leading the metabolic flux to the lignin pathway since HCT and CHS use the same substrate p-coumaroyl-CoA (Dao et al., 2011b). For example, HPLC profiling showed that flavonoids are accumulated in HCT-downregulated compared to WT. In addition, HCT-silenced plants present the overexpression of several flavonoid biosynthetic pathway genes (Baxter and Stewart-Jr, 2013). When grown under long-days, *tt5* presents high expression of PAL1 and may be rechanneling its normal metabolic flux to the SA pathway leading to enhanced disease resistance and unique phenotype.

4.3. Naringenin Chalcone is accumulated under stress conditions

Although several flavonoids have been listed as important compounds against biotic and abiotic stress, there is no report showing the role of naringenin chalcone (NC) during adverse conditions. Among flavonoids, chalcones are some of the most diverse in terms of structure. They can suffer several modifications such as O-substitution, C-formylation, prenylation, and glycosylation (Veitch and Grayer, 2011). In Arabidopsis, NC (2',4,4',6'-tetrahydroxychalcone) is synthesized from 4-coumaroyl-CoA and malonyl-CoA by chalcone synthase (CHS), a key enzyme in the phenylpropanoid pathway. In animal cells, NC improves adipocyte functions by enhancing adiponectin production and exhibited inhibitory effects on NF-κB-mediated inflammation and cancer (Horiba et al., 2010). Although the downstream compound, Naringenin, shows inhibitory effects on *Pyricularia spore germination* and growth of soybean root, NC does not present any direct relation with disease resistance (Bido et al., 2010). Therefore, the accumulation of NC in the WT and *tt* mutants was analyzed in different growth conditions (2.1).

The aglycone NC is not normally accumulated by WT plants under LD and SD conditions. *tt5* and *tt5/sid2* grown under long days were the only lines that exhibited NC accumulation although *tt5/sid2* presented lower values of NC. Interestingly, plants all plants except *tt4 and tt4/tt5* presented high NC accumulation when expose to stress conditions such as pathogen infection, SD+HL and LD+LT. These results point to clear relationship between NC retention and exogenous stress.

tt5 plants grown under LD showed upregulation of SA responsive genes and NC accumulation. That leads to another question. Is NC is involved in SA-stress signaling? flavonoids also have been implicated in more direct interactions with transport and signal transduction pathways. Nuclear localization of flavonols has been shown in *Arabidopsis thaliana* (Saslowsky et al., 2005) and *Camellia sinensis* (Feucht et al., 2013). It has also been reported that catechin can bind to histone proteins in plants (Falcone Ferreyra et al., 2012), and might modulate nonspecific genes transcription. Transcription of flavonoid biosynthetic enzymes can be altered by NC and apigenin (Pelletier et al., 1999). There is increasing evidence that specific proteins or groups of proteins exhibit more specific interactions with flavonoids in vivo. In Arabidopsis, many targets have been identified such as a microsomal tyrosine aminopeptidase; the tyrosine phosphatase AtPTEN1; a mitogen-activated protein kinase (MAPK); PINOID (PID), a serine/threonine kinase; a phosphatidyl inositol3,4,5-triphosphate kinase (Gupta et al., 2002). In addition, Chalcone synthase (CHS) and chalcone isomerase (CHI) enzymes are encoded in the nucleus and the proteins are localized in the cytoplasm of Arabidopsis where they are associated with the ER. Because, flavonoid regulation of transcription is developmentally regulated at the DNA level (Veitch and Grayer, 2011) it is possible the absence of TT5 might be affecting the normal homeostasis of plants biding to regulatory factors.

As previous mentioned, several secondary metabolites can prime plants to exhibit enhanced resistance. They can trigger a series of mechanisms such as ROS, Ca^{+2} influx, Callose, and HR-like cell death. NC is an intermediate in flavonol biosynthesis and is spontaneously metabolized into naringenin by chalcone isomerase. Although research on the effects of NC has focused on its benefits for human cells, some studies have reported the effect of chalcones on plant cells. Chen et al. (2004) reported phytotoxic symptoms caused by root-applied trans-chalcone (1,3-diphenyl-2-propen-1-one) could represent a loss of 18–68% in fresh weight at 7days after treatment. Trans-chalcone is also thought to affect the biosynthesis of lignin in soybeans by the downregulation of PAL and 4CL and the resultant decrease in cinnamic acid (Chen et al., 2011). (Díaz-Tielas et al. (2012) reported that trans-chalcone caused cells to show signs of programmed cell death, disruption of organelles and chromatin fragmentation in Arabidopsis. They mentioned that plants treated with this compound present reduction of mitochondrial transmembrane potential. Although trans-chalcone has a different structure from NC, these results add to the possible bioactivity of naringenin chalcone on plant cells. To examine this more closely a repeat of the spraying experiment is needed.

Fitness costs associated with defense have been clearly demonstrated (Ayala-Zavala et al., 2004). The results showed in this thesis demonstrate that the accumulation of NC in WT and the other *tt* lines are linked to stress conditions (biotic or abiotic). *tt5* mutants grown under LD, on the other hand, accumulates high levels of NC without any apparent stimulus. I hypothesize that accumulation of NC leads to a trade-off between defenses and growth. Similarly, Hofmann and Jahufer (2011) found that flavonoid accumulation may affect plant productivity attributes. Low levels of quercetin glycoside accumulation and low quercetin:kaempferol ratios would confer

white clover populations with high biomass production, large leaves. In addition, white clover stress-resistant ecotypes would have high quercetin glycoside accumulation.

Other pathways that could be upregulated by NC accumulation or *tt5* mutation may also result in the accumulation of novel metabolites. For example, the aurone pathway is derived from NC in snapdragon. Aurone is a yellow pigment found in ornamental flowers however no antimicrobial effect was reported in Snapdragon. In this system, the chalcone 4'-O glucosyltransferase glycolyzes NC. Subsequently, the product is acted upon by aureusidin 6-O-glucoside in the vacuole to generate aurone as the final product (Wang et al., 2015). In Arapidopsis, glucosyltranferase UDP-GLUCOSYL TRANSFERASE 88A1 (UGT88A1) exhibits 40% of its amino acid sequence similar to snapdragon glucosyltransferase (Figure 4.2) (Ono et al., 2006). Perhaps, the increased levels of NC that accumulate in the LD-grown *tt5* plants leads to the conversion of NC into an aurone-like product that plays a role in plant defense against disease. The HPLC system used to quantify NC did not detect the production of an aurone-like compound, but we may not have looked carefully enough. Similarly, (Lapcik et al., 2006a) identified detectable traces of isoflavonoids from Arabidopsis Col-0 by HPLC-MS and suggested putative chalcone reductase genes that may be related to a new branch in the Arabidopsis genome. According to Lapcik et al. (2006) NC would be converted into isoliquiritigenin (Figure 4.2), by a NADPH-dependent aldo-keto reductase (At2g37760), leading to a different pathway. We evaluated the expression of At2g37760 gene and it showed exclusively expression in *tt5* grown under long days. This may be redirecting the metabolic flux to different branch of the phenylpropanoids and this unknown compound may contributing to *tt5* SA-response. A different quantitative system would be needed to determine if isoflavones were being produced in LD-grown *tt5* plants.

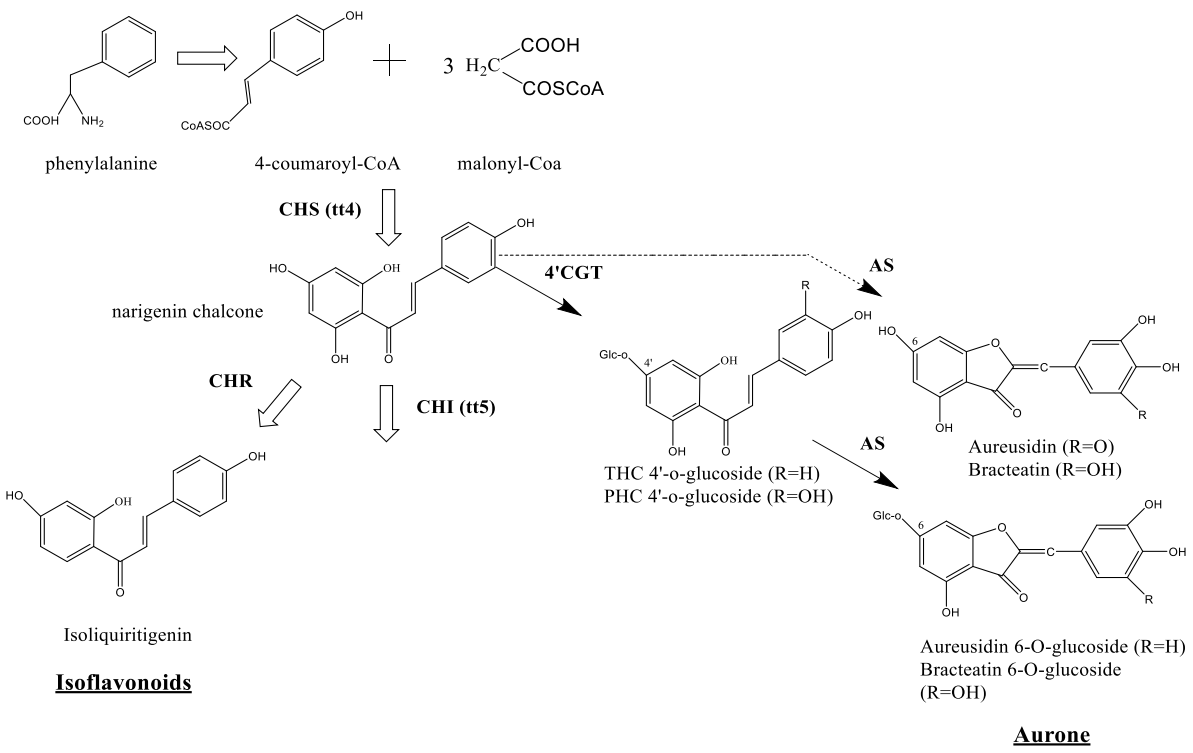

Figure 4.2: Scheme of the hypothetical metabolites derived from naringenin chalcone.

Enzymes are indicated in bold, with the corresponding genetic loci in parentheses. CHS, chalcone synthase; CHI, chalcone isomerase; CHR, chalcone reductase; AS, aureusidin synthase; 4'CGT, chalcone 4'-O-glucosyltransferase (Lapcik et al., 2006; Ono et al., 2006).

4.4. Could the SA response be due to enzymatic structural changes?

Although *tt5*-LD response may be caused by NC accumulation, it could also be caused by the absence of CHI. There is evidence suggesting that CHS, CHI, and DFR interact with one another as part of a large enzymatic complex called a metabolon (Biała and Jasiński, 2018). These complexes are coordinated three dimensional units that act as a flowthrough channel for metabolites. They are thought to work more efficiently, leading to more rapid metabolism via a type of metabolic channel (substrate channeling) (Jørgensen et al., 2005). Metabolons are generally attached on the ER surface by Cytochrome P450 proteins and have been proposed to be part of the metabolism of camalexin, auxin, waxes and phenylpropanoids (Biała and Jasiński, 2018; Kriechbaumer et al., 2016; Lallemand et al., 2013). Key enzymes of the flavonoid pathway such

as CHS, CHI, F_3H, and DFR are all located in the endoplasmic reticulum and thus could be forming metabolons (Lepiniec et al., 2006). Were CHI acting as an anchor in the metabolom, it is possible that the lack of CHI could negatively affect the metabolon organization and blocking or redirecting the metabolic flux of intermediate metabolites in *tt5*. For example, in the absence of CHI, metabolite from PAL might be redirected into the SA pathway, leading to SA biosynthesis and hence the immune response observed in LD-grown *tt5* plants. We know that flavonoid biosynthesis is daylength sensitive, and light intensity sensitive. This would explain why LD-grown or HL-grown tt5 plants exhibit the SA-dependent phenotype. As PAL is activated to generate flavonoids, but the trans-cinnamic acid is redirected into SA biosynthesis, the result is overaccumulation of SA and the *tt5* LD phenotype.

In Arabidopsis, binary interactions between CHS and CHI,F3H, DFR and FLS1 enzyme pairs have been reported (Watkinson et al., 2018; Zhang and Fernie, 2021). So it is possible that in the absence of CHI, CHS will interact with other proteins. Growing evidence suggests the presence of flavonoid enzymes in the nucleus and perhaps other subcellular compartments, as well. Recently, CHS was suggested to interact with the At1g12530 gene product (MOS9), a nuclear-localized protein that has been linked to effector-triggered immunity (ETI) (Watkinson et al., 2018). Overexpression of MOS9 results in a reduction of CHS transcript levels and flavonoid profile. The association of MOS9 with components of the R gene expression network suggests that it could also serve to coordinate multiple cellular processes, including during plant defense (Watkinson et al., 2018). Knocking out TT5 could trigger ETI via CHS-MOS9 interaction, allowing plants to redirect carbon flux into defense-related responses.

4.5. *tt5* also exhibits a wax phenotype

Several factors might be involved in tt5 response. The tt5 mutation is classified as a cuticular wax-deficient phenotype, suggesting a defective external layer. Several studies shown the importance of the cuticle as a natural barrier against biotic and abiotic stress (Martel and Qaderi, 2016; Ziv et al., 2018). Petrov et al. (2015) summarized some environmental factors that can trigger the production of ROS leading to cell death. Mutagenesis approaches identified 31 recessive wax mutant loci (Jenks et al., 2002). Arabidopsis *tt5* mutant was classified as a semi-glaucous wax mutant with a defective cuticle (Shirley et al., 1995b). It is possible that *tt5* exhibits a defective cuticle layer and that might be involved in the *tt5* SA response. Plant cuticular waxes play an important role as a protective barrier against environmental stresses, and their biosynthesis, transport, deposits, and composition, are also affected by various environmental factors (Shepherd and Griffiths, 2006) Among other components, the cuticle is made of wax, which is made of lipids, proteins, and several other compounds including secondary metabolites. Several studies reported that elevated UV-B radiation affects plant cuticular wax formation and gas exchange (Fukuda et al., 2008; Jiang et al., 2009). It was found that cuticular wax content increases by 20–28% in cucumber (*Cucumis sativus* L.), bean (*Phaseolus vulgaris* L.), and barley (*Hordeum vulgare* L.) when plants are exposed to UV-B light (Kakani et al., 2003). In rice, mutations in wilted dwarf and lethal 1 (WDL1) influenced the crystallization and distribution of wax on the surface of leaf. These increase its transpiration rates to 2.3 times higher than those in the WT, leading to increased rates of water loss and lower water use efficiency (Park et al., 2010). The deficient wax accumulation might be leading *tt5* plant to a stress condition in long days or high light triggering ROS, callose deposition, and the SA response genes. Recent work has indicated that the flavonoid pathway might be linked to the leaf cuticle. For example, Virus-induced gene silencing (VIGS) of

tomato (*Solanum lycopersicum*) fruits have been used to down-regulate CHS expression during ripening and analyze the effects at the epidermal and cuticle level (Heredia et al., 2015). Plants affected by SlCHS silencing presented a lower amount of cutin, cuticle, polysaccharides, and phenolics. It was also been reported that the anthocyanin free (*af*) mutant encodes a member (SlCHI1) of the CHI family of enzymes not only for the synthesis of anthocyanins and other flavonoids but also plays a pleiotropic role in promoting the accumulation of terpenoids in glandular trichomes (Heredia et al., 2015; Schaller, 2010). These findings suggest a role for CHI1 in coordinating the developmental plasticity and metabolic activity of an epidermal structure that shields against biotic stress. This may occur via the metabolon that I suggest above is responsible for the flavonoid biosynthetic pathway. If a key cytochrome p450 needed for wax biosynthesis is associated with that complex, one could link the flavonoid and wax production through the protein.

5. Conclusions and future perspectives

In this thesis, the role of the flavonoid pathway in plant immunity system against pathogen attack was investigated. The flavonoid mutant *tt5* presented developmental changes and enhanced resistance to fungal pathogens when grown under specific growth conditions (Figure 3.4). Studying *tt5* plants, we found that they exhibited enhanced resistance against the fungi powdery mildew (*E. cichoracearum*) and anthracnose (*C. higginsianum*). TT5 knockout would also exhibit increased cell death lesion, callose deposition and ROS and NC accumulation but only when grown under LD. To isolate the cause of these phenotypes, *tt5* was crossed with *tt4*, and the double mutant *tt4/tt5* was also examined. *tt4/tt5* plants did not exhibited *tt5*-LD phenotype and showed no resistance against *E. cichoracearum* and *C. higginsianum*. Further observations allowed us to determine that *tt5*-LD constitutively express SA-related genes PR-1, PR-2, ICS1, PAL1. To verify the importance of SA in *tt5* mediated resistance by crossing *tt5* with SA insensitive lines *sid2* and *nahG*. Neither exhibited the pathogen resistance, cell death, or PR expression phenotypes.

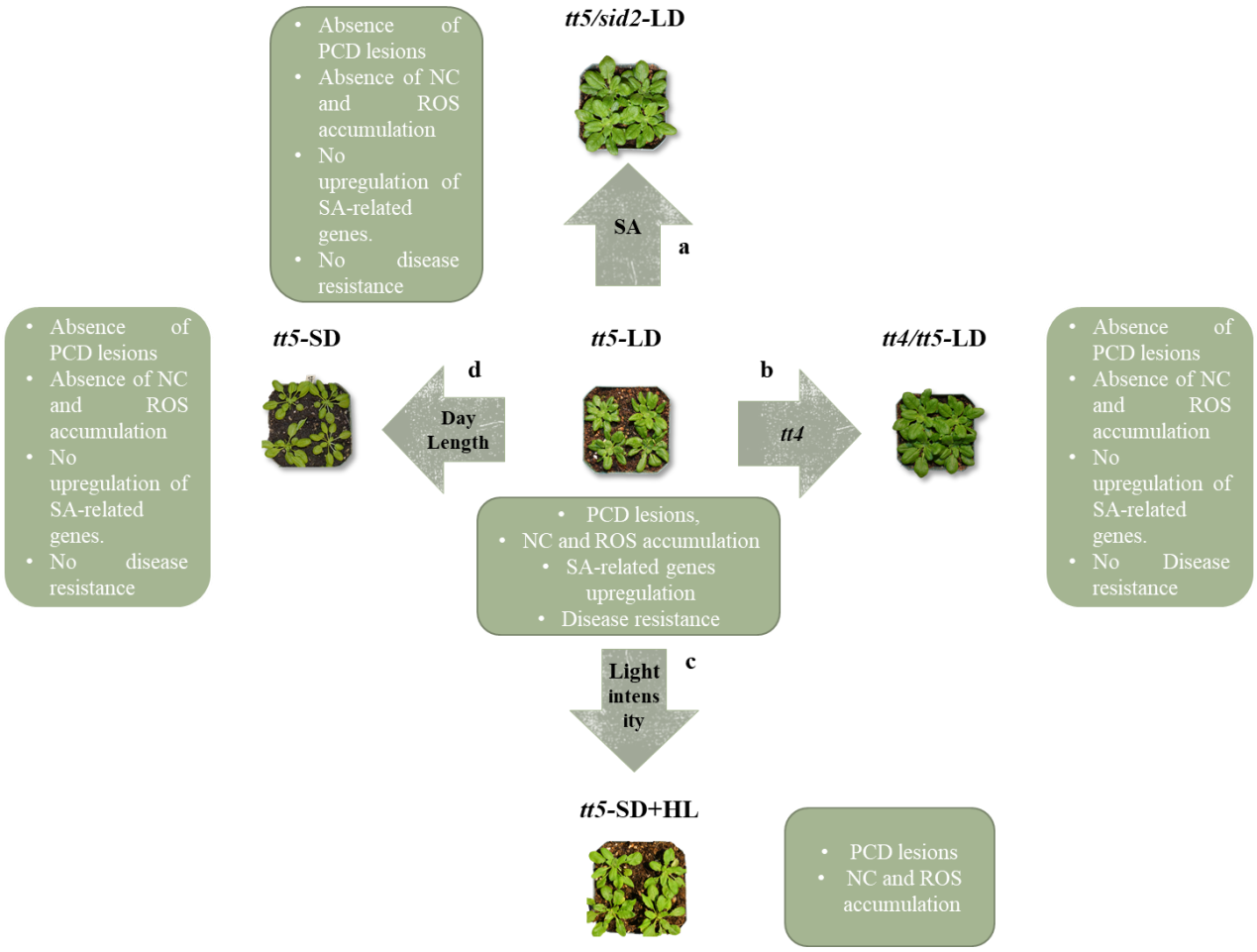

Figure 5.1: Scheme figure of *tt5* response.

Schematic image summarizing the factors affecting *tt5* phenotype and disease resistance. a) *tt5* plants crossed with *sid2*. b) *tt5* plants crossed with tt4. c) *tt5* plants grown under SD+HL (3.8). d) *tt5* plants grown under SD. PCD: Programmed cell death; NC; Naringenin Chalcone; ROS: Reactive oxygen species.

Although I strongly believe that *tt5* response and phenotype is mainly caused by NC accumulation, *tt5* was also classified as a wax mutant, presenting defective wax layer. Based on discussions I had with Dr. David Bird (Department of Biology, Mount Royal University), I found out that *tt5* plants had a general export defect. Not only were they deficient in epicuticular wax, but also in seed mucilage accumulation (D. Bird, Personal Communication). Based on the current literature, I do not expect that export defects are linked to long-day-dependent SA accumulation. In fact, it is not clear if the export defect is impacted by day length in a manner similar to the SA-

dependent growth inhibition. Similarly, it is not clear if the export defect could play a role in the disease resistance observed in long-day-grown *tt5* plants. While working on the main goals of my thesis, I started to investigate the wax defect phenotype of *tt5* and its role in plant defense. My hypothesis is that the *tt5* mutation is pleiotropic. Loss of the *tt5* gene leads to the feedback production of SA when grown under conditions, such as long days, that upregulate the flavonoid biosynthesis pathway (as described in the body of my thesis), it also appears to impact wax deposition, and the general secretory pathway via an unrelated process.

Plant secretion is an essential process which consists of the delivery of substances such as proteins, lipids, carbohydrates, and phenolic metabolites to the cell exterior (Wang et al., 2017). Cuticular waxes are mixtures of very-long-chain fatty acids and their derivatives (Kubitzki, 1987). They protect the aerial tissues, providing plants with a barrier against dehydration, excessive radiation, mechanical damage, and pathogen infection (Serrano et al., 2014). The cuticular wax formation starts with the biosynthesis of C16 and C18 fatty acyl-acyl carrier proteins in epidermal cells (Kunst and Samuels, 2003). After several reactions, very-long-chain fatty acids (VLCFAs) are formed and can either be directly released as cuticular waxes, or converted into other metabolites (e.g. alkanes, aldehydes, secondary alcohols) (Lewandowska et al., 2020). Secondary alcohols and ketones are generated in the ER by the cytochrome P450 enzyme CYP96A15, referred to as midchain alkane hydroxylase MAH1 (Wang et al., 2020). Waxes are then transferred to Golgi and/or plasma membrane by a complex protein-protein interaction.

Cytochrome P450 encompasses a large number of hemeproteins that have important roles in the biosynthesis of defensive compounds, fatty acids, and hormones (Ralston, 2006). These proteins are hypothesized to serve as nucleation points that anchor multi-enzyme complexes, also known as metabolons, to a specific region within the cell (e.g. ER). Metabolons are supramolecular

complexes of sequential metabolic enzymes and cellular structural elements. These complexes are thought to be transient and formed between enzymes of a metabolic pathway that form a metabolic channel (substrate channeling) (Jørgensen et al., 2005). The intermediates generated inside the metabolon are maintained within it to avoid losses to the cytoplasm and to be catalyzed by sequential enzymes. Metabolons are generally attached on the ER surface and have been proposed to be part of the metabolism of camalexin, auxin, wax and phenylpropanoids (Biała and Jasiński, 2018; Kriechbaumer et al., 2016; Lallemand et al., 2013). In addition, key enzymes of the flavonoid pathway such as CHS, CHI, F_3H, and DFR are all located in the endoplasmic reticulum (Lepiniec et al., 2006). There is evidence suggesting that CHS, CHI, and DFR interact with one another in an orientation dependent manner and may participate as part of a metabolon (Watkinson et al., 2018). To avoid sequestration in cellular membranes, chalcones and flavonones must be channeled through the pathway. Flavonoids are then normally trafficked to the cell vacuole (Zhao and Dixon 2010). In addition, Jez et al., (2002) reported that metabolon channeling may protect the chalcone from being completely converted into naringenin by affecting the performance of CHI.

Phenylpropanoids such as coumaric and benzoic acid, naringenin chalcone and naringenin can be found as components of plant cuticle (Ziv et al., 2018). It was found that CHS-silenced tomato plants downregulated the production of cuticle, cutin, polysaccharides and phenolics (Heredia, et al., 2015). This fits with the observations that wax deposition and mucilage export are altered in *tt5* Arabidopsis plants. In transgenic tomatoes, silenced CHI1 plants fail to produce terpenoids in glandular trichomes on the leaves (Kang et al., 2014). Interestingly, the stems of Arabidopsis *tt5* (CHI knock out) plants have a bright green color (semi-glaucous stem surface) as a result of alterations in the epicuticular wax layer, as found in the eceriferum class of

Arabidopsis mutations (Jenks et al., 2002). The eceriferum (*cer*) mutants present deviating epicuticular wax layers. There are currently 27 known *cer* mutants showing different wax accumulation patterns (Cui et al., 2016). Interestingly, Arabidopsis mutants *lacs2*, *lacs3*, and *myb96* exhibit increased cuticle permeability which correlates with enhanced disease resistance against grey mold (*Botrytis cinerea*). In addition, Arabidopsis mutants that show deficient cuticle are often associated with ROS accumulation and induction of innate immunity, suppressing fungal development. (Wang et al., 2020). We hypothesize that CHI knock out negatively affects the transport between ER-GC-PM in plants, causing a dysfunctional allocation of wax component in the leaf cuticle.

To investigate the integrity of *tt5* cuticle layer, and determine if the waxless phenotype is related to the daylength under which the *tt5* plants were grown we treated WT, *tt4* , *tt5 and tt4tt5* leaves with toluidine blue (Tanaka et al., 2004). We verified that *tt5* presents abnormalities in the wax layer in comparison to the WT and *tt4* regardless of the photoperiod. When grown under long-days *tt5* leaves did exhibit higher staining absorption, but this may be due to the necrotic lesions accumulated on the leaves (Figure 5.1). To determine if the waxless phenotype of *tt5* leaves was due to a general downregulation of the wax biosynthesis pathway, the expression of *cer1* and *cer3* were also evaluated in plants grown under LD (Figure 5.2). We did not find difference in *cer1* and *cer3* expression in *tt5* leaves suggesting that *tt5* wax deficiency is generated through a different process involving a different mechanism. To evaluate the relationship between the secretory pathway and Arabidospsis *tt* mutants, *tt4* and *tt5* plants were crossed with *sec1rfp* expressing plants , to generate *tt4sec1rfp* and t*t5sec1rfp*. If the *tt5* mutation disrupts the secretory machinery and thereby wax export, we expect to see a dysfunctional localization of the sec1rfp protein in the *tt5*

secretory pathway. This work is currently underway, F1 plants were obtained, but the Covid-19 shutdown of the lab meant that further work was unable to continue.

The second aspect of this work is understanding if the CHI protein forms part of an ER-localized metabolon, and if its loss in the *tt5* plants leads to the pleiotropic effects on flavonoid biosynthesis, wax export, and SA-mediated plant defense. To this end, I have cloned the CHI and CHS genes into a fluorescent protein reporter construct. I planned to perform transient expression studies on Arabidopsis seedlings defective in CHI (*tt4*) and CHS (*tt5*) to see if the subcellular localization is impacted. The transient expression work will be done in collaboration with Dr. Chris Ambrose (Dept of Biology, University of Saskatchewan).

Looking ahead in this project, to understand how the loss of the *tt5* protein could impact wax biosynthesis it would help to have plants stably expressing CHS and CHI proteins labelled with a fluorescent protein tag. This would be done using cloned constructs that are infiltrated using the floral dip method (Zhang et al 2006). In addition, using the transient expression system, we could examine the subcellular localization of *cer* proteins used in wax biosynthesis in a *tt5* vs WT background. If the lack of *tt5* were to result in the mislocalization of *cer* proteins, it would speak to the role of *tt5* as a metabolon anchor protein. Thus, while it may not be directly involved in wax biosynthesis, its absence could impact wax accumulation by separating the wax biosynthesis enzymes in space. Alternatively, perhaps the carbon-carbon double bond isomerization that is performed by TT5 in the flavonoid pathway is required for wax biosynthesis. This is an intriguing set of questions, that I have most of the tools and technical expertise to examine. Unfortunately, due to the Covid-19 pandemic, I did not have time to finish this work.

WT ***tt4*** ***tt5*** ***tt4/tt5***

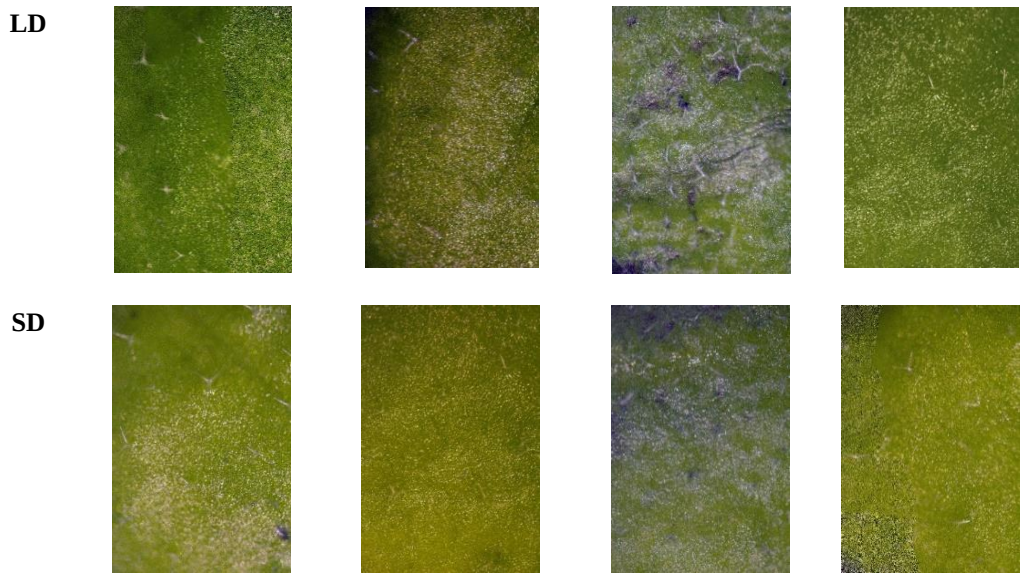

Figure 5.2: Toluidine blue accumulation in plants grown under Long and Short-day conditions.
Non-Inoculated leaves were incubated in toluidine blue solution for 5 min. The blue spots indicate the accumulation of toluidine blue and defective cuticle.

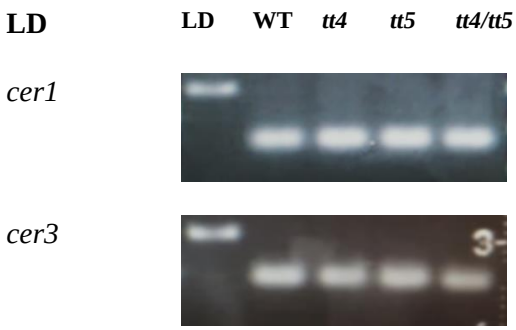

Figure 5.3: Expression of wax biosynthesis related genes in plants grown under Long-day conditions.

Leaf tissue from each of the plant lines was collected for RNA isolation. Expression level of each gene was estimated by RT-PCR. Gene abbreviations: CER1 - eceriferum 1; CER3 – eceriferum 3.

REFERENCES

1. Agrios, G. (2004). Plant pathology: Fifth edition. In *Plant Pathology: Fifth Edition* (Vol. 97).
2. Ahrazem, O., Rubio-Moraga, A., Trapero-Mozos, A., Climent, M. F. L., Gómez-Cadenas, A., and Gómez-Gómez, L. (2015). Ectopic expression of a stress-inducible glycosyltransferase from saffron enhances salt and oxidative stress tolerance in Arabidopsis while alters anchor

root formation. *Plant Science*, *234*, 60–73.

3. An, C., and Mou, Z. (2011). Salicylic Acid and its Function in Plant Immunity. *Journal of Integrative Plant Biology*, *53*(6), 412–428.
4. Andersen, E. J., Ali, S., Byamukama, E., Yen, Y., and Nepal, M. P. (2018). Disease resistance mechanisms in plants. *Genes*, *9*(7).
5. Ayala-Zavala, J. F., Wang, S. Y., Wang, C. Y., and González-Aguilar, G. A. (2004). Effect of storage temperatures on antioxidant capacity and aroma compounds in strawberry fruit. *LWT - Food Science and Technology*, *37*(7), 687–695.
6. Ballaré, C. L. (2014). Light Regulation of Plant Defense. *Annual Review of Plant Biology*, *65*(1), 335–363.
7. Barber, M. S., and Mitchell, H. J. (1997). Regulation of Phenylpropanoid Metabolism in Relation to Lignin Biosynthesis in Plants. *International Review of Cytology*, *172*, 243–293.
8. Bashandy, T., Taconnat, L., Renou, J.-P., Meyer, Y., and Reichheld, J.-P. (2009). Accumulation of Flavonoids in an ntra ntrb Mutant Leads to Tolerance to UV-C. *Molecular Plant*, *2*(2), 249–258.
9. Baxter, H. L., and Stewart-Jr, C. N. (2013). Lignocellulosic feedstocks represent a promising renewable and sustainable alternative to petroleum-based fuels, high production costs associated with con-version proces. *Biofuels*, *4*(6), 635–650.
10. Bent, A. F., and Mackey, D. (2007). Elicitors, effectors, and R genes: the new paradigm and a lifetime supply of questions. *Annual Review of Phytopathology*, *45*, 399–436.
11. Biała, W., and Jasiński, M. (2018). The phenylpropanoid case – It is transport that matters. *Frontiers in Plant Science*, *871*(11), 1–8.
12. Bido, G. de S., Ferrarese, M. de L. L., Marchiosi, R., and Ferrarese-Filho, O. (2010). Naringenin inhibits the growth and stimulates the lignification of soybean root. *Brazilian Archives of Biology and Technology*, *53*(3), 533–542.
13. Blokhina, O., Virolainen, E., and Fagerstedt, K. V. (2003). Antioxidants, oxidative damage and oxygen deprivation stress: A review. *Annals of Botany*, *91*, 179–194.
14. Boyd, L. A., Ridout, C., O'Sullivan, D. M., Leach, J. E., and Leung, H. (2013). Plant-pathogen interactions: Disease resistance in modern agriculture. *Trends in Genetics*, *29*(4), 233–240.
15. Brodersen, P., and Malinovsky, F. (2005). The role of salicylic acid in the induction of cell death in Arabidopsis acd11. *Plant* , *138*(6), 1037–1045.

16. Burbulis, I. E., Winkel-shirley, B., Oct, N., Burbulis, I. E., and Winkel-shirley, B. (1999). Interactions among Enzymes of the Arabidopsis Flavonoid Biosynthetic Pathway 96(22), 12929–12934.
17. Burbulis, I., and Winkel-Shirley, B. (1999). Interactions among enzymes of theArabidopsis flavonoid biosynthetic pathway. *Proceedings of the National Academy of Sciences of the United States of America*, *96*, 12929–12934.
18. Carvalho, I. S., Cavaco, T., Carvalho, L. M., and Duque, P. (2010). Effect of photoperiod on flavonoid pathway activity in sweet potato (Ipomoea batatas (L.) Lam.) leaves. *Food Chemistry*, *118*(2), 384–390.
19. Chen, Y., Li, F., Tian, L., Huang, M., Deng, R., Li, X., and Wu, G. (2017). The phenylalanine ammonia lyase gene ljpal1 is involved in plant defense responses to pathogens and plays diverse roles in lotus japonicus-rhizobium symbioses. *Molecular Plant-Microbe Interactions*, *30*(9), 739–753.
20. Chern, M., Fitzgerald, H. A., Canlas, P. E., Navarre, D. A., and Ronald, P. C. (2005). Overexpression of a rice NPR1 homolog leads to constitutive activation of defense response and hypersensitivity to light. *Molecular Plant-Microbe Interactions*, *18*(6), 511–520.
21. Cui, F., Brosché, M., Lehtonen, M. T. T., Amiryousefi, A., Xu, E., Punkkinen, M., and Overmyer, K. (2016). Dissecting Abscisic Acid Signaling Pathways Involved in Cuticle Formation. *Molecular Plant*, *9*(6), 926–938.
22. Dao, T. T. H., Linthorst, H. J. M., and Verpoorte, R. (2011). Chalcone synthase and its functions in plant resistance. *Phytochemistry Reviews*, *10*(3), 397–412.
23. Delaney, T. P., Uknes, S., Vernooij, B., Friedrich, L., Negrotto, D., Gaffney, T., and Ryalst, J. (1994). *A Central Role of Salicylic Acid in Plant Disease Resistance American Association for the Advancement of Science*. *266*(5188).
24. Dempsey, D. A., and Klessig, D. F. (2017). How does the multifaceted plant hormone salicylic acid combat disease in plants and are similar mechanisms utilized in humans? *BMC Biology*, *15*(1), 1–11.
25. Díaz-Tielas, C., Graña, E., Sotelo, T., Reigosa, M. J., and Sánchez-Moreiras, A. M. (2012). The natural compound trans-chalcone induces programmed cell death in Arabidopsis thaliana roots. *Plant, Cell and Environment*, *35*(8), 1500–1517.
26. Dixon, R. A., and Paiva, N. L. (1995). Stress-induced phenylpropanoid metabolism. *Plant*

Cell, *7*(7), 1085–1097.

27. Dixon, Richard A., Achnine, L., Kota, P., Liu, C. J., Reddy, M. S. S., and Wang, L. (2002). The phenylpropanoid pathway and plant defence - A genomics perspective. *Molecular Plant Pathology*, *3*(5), 371–390.
28. Du, Y., Chu, H., Wang, M., Chu, I. K., and Lo, C. (2010). Identification of flavone phytoalexins and a pathogen-inducible flavone synthase II gene (SbFNSII) in sorghum. *Journal of Experimental Botany*, *61*(4), 983–994.
29. Falcone Ferreyra, M. L., Rius, S. P., and Casati, P. (2012). Flavonoids: Biosynthesis, biological functions, and biotechnological applications. *Frontiers in Plant Science*, *3*(9), 1–15.
30. Ferreira, R. B., Monteiro, S., Freitas, R., Santos, C. N., Chen, Z., Batista, L. M., and Teixeira, A. R. (2006). Fungal Pathogens: The Battle for Plant Infection. *Critical Reviews in Plant Sciences*, *25*(6), 505–524.
31. Feucht, W., Schmid, M., Polster, J., Dithmar, H., and Treutter, D. (2013). Flavanols in the Nuclei of the tea bush (*Camellia sinensis*) - Broadening the perspectives to human health. *Journal of Applied Botany and Food Quality*, *86*(1), 16–23.
32. Fini, A., Guidi, L., Ferrini, F., Brunetti, C., Di Ferdinando, M., Biricolti, S., and Tattini, M. (2012). Drought stress has contrasting effects on antioxidant enzymes activity and phenylpropanoid biosynthesis in Fraxinus ornus leaves: An excess light stress affair? *Journal of Plant Physiology*, *169*(10), 929–939.
33. Fiorani, F., Umbach, A. L., and Siedow, J. N. (2005). The alternative oxidase of plant mitochondria is involved in the acclimation of shoot growth at low temperature. A study of Arabidopsis AOX1a transgenic plants. *Plant Physiology*, *139*(4), 1795–1805.
34. Fraser, C. M., and Chapple, C. (2011). The phenylpropanoid pathway in Arabidopsis. *Arabidopsis Book*, *9*, e0152.
35. Fu, Z. Q., and Dong, X. (2013). *Systemic Acquired Resistance : Turning Local Infection into Global Defense*. *Critical Reviews in Plant Sciences*, *25*(6), 505–524.
36. Fukuda, S., Satoh, A., Kasahara, H., Matsuyama, H., and Takeuchi, Y. (2008). Effects of ultraviolet-B irradiation on the cuticular wax of cucumber (Cucumis sativus) cotyledons. *Journal of Plant Research*, *121*(2), 179–189.
37. Gill, S. S., and Tuteja, N. (2010). Reactive oxygen species and antioxidant machinery in

abiotic stress tolerance in crop plants. *Plant Physiology and Biochemistry*, *48*(12), 909–930.

38. Gill, U. S., Lee, S., and Mysore, K. S. (2015). Host versus nonhost resistance: Distinct wars with similar arsenals. *Phytopathology*, *105*(5), 580–587.
39. Glazebrook, J. (2005). Contrasting mechanisms of defense against biotrophic and necrotrophic pathogens. *Annual Review of Phytopathology*, *43*, 205–227.
40. Guidi, L., Brunetti, C., Fini, A., Agati, G., Ferrini, F., Gori, A., and Tattini, M. (2016). UV radiation promotes flavonoid biosynthesis, while negatively affecting the biosynthesis and the de-epoxidation of xanthophylls: Consequence for photoprotection? *Environmental and Experimental Botany*, *127*, 14–25.
41. Gupta, R., Ting, J. T. L., Sokolov, L. N., Johnson, S. A., and Luan, S. (2002). A tumor suppressor homolog, AtPTEN1, is essential for pollen development in Arabidopsis. *Plant Cell*, *14*(10), 2495–2507.
42. Gururani, M. A., Venkatesh, J., Upadhyaya, C. P., Nookaraju, A., Pandey, S. K., and Park, S. W. (2012). Plant disease resistance genes: Current status and future directions. *Physiological and Molecular Plant Pathology*, *78*, 51–65.
43. Heck, S., Grau, T., Buchala, A., Métraux, J. P., and Nawrath, C. (2003). Genetic evidence that expression of NahG modifies defence pathways independent of salicylic acid biosynthesis in the Arabidopsis-Pseudomonas syringae pv. tomato interaction. *Plant Journal*, *36*(3), 342–352.
44. Heldt, H.-W., and Piechulla, B. (2011). 18 - Phenylpropanoids comprise a multitude of plant secondary metabolites and cell wall components. *Plant Biochemistry*, 431–449.
45. Heldt, H.-W., Piechulla, B., Heldt, H.-W., and Piechulla, B. (2011). 18 – Phenylpropanoids comprise a multitude of plant secondary metabolites and cell wall components. In *Plant Biochemistry* (pp. 431–449).
46. Heredia, A., Heredia-Guerrero, J. A., and Domínguez, E. (2015). CHS silencing suggests a negative cross-talk between wax and flavonoid pathways in tomato fruit cuticle. *Plant Signaling and Behavior*, *10*(5), 1–4.
47. Hofmann, R. W., and Jahufer, M. Z. Z. (2011). Tradeoff between biomass and flavonoid accumulation in white clover reflects contrasting plant strategies. *PLoS ONE*, *6*(4).
48. Horiba, T., Nishimura, I., Nakai, Y., Abe, K., and Sato, R. (2010). Naringenin chalcone improves adipocyte functions by enhancing adiponectin production. *Molecular and Cellular Endocrinology*, *323*(2), 208–214.

49. Howe, G. A., and Jander, G. (2008). Plant immunity to insect herbivores. *Annual Review of Plant Biology*, *59*, 41–66.
50. Hückelhoven, R., Fodor, J., Preis, C., and Kogel, K.-H. (1999). Hypersensitive Cell Death and Papilla Formation in Barley Attacked by the Powdery Mildew Fungus Are Associated with Hydrogen Peroxide but Not with Salicylic Acid Accumulation. *Plant Physiology*, *119*(4), 1251–1260.
51. Hyun, M. W., Yun, Y. H., Kim, J. Y., and Kim, S. H. (2011). Fungal and plant phenylalanine ammonia-lyase. *Mycobiology*, *39*(4), 257–265.
52. Idris, A., Linatoc, A. C., Abu Bakar, M. F., Ibrahim Takai, Z., and Audu, Y. (2018). Effect of Light Quality and Quantity on the Accumulation of Flavonoid in Plant Species. *Journal of Science and Technology*, *10*(3).
53. Inostroza-Blancheteau, C., Reyes-Díaz, M., Arellano, A., Latsague, M., Acevedo, P., Loyola, R., and Alberdi, M. (2014). Effects of UV-B radiation on anatomical characteristics, phenolic compounds and gene expression of the phenylpropanoid pathway in highbush blueberry leaves. *Plant Physiology and Biochemistry*, *85*, 85–95.
54. Ishikawa, A., Kimura, Y., Yasuda, M., Nakashita, H., and Yoshida, S. (2006). Salicylic Acid-Mediated Cell Death in the *Arabidopsis len3* Mutant. *Bioscience, Biotechnology, and Biochemistry*, *70*(6), 1447–1453.
55. Izbiańska, K., Arasimowicz-Jelonek, M., and Deckert, J. (2014). Phenylpropanoid pathway metabolites promote tolerance response of lupine roots to lead stress. *Ecotoxicology and Environmental Safety*, *110*, 61–67.
56. Jenkins, G. I., Long, J. C., Wade, H. K., Shenton, M. R., and Bibikova, T. N. (2001). UV and blue light signalling: Pathways regulating chalcone synthase gene expression in Arabidopsis. *New Phytologist*, *151*(1), 121–131.
57. Jenks, M. a., Eigenbrode, S. D., and Lemieux, B. (2002). Cuticular Waxes of Arabidopsis. *The Arabidopsis Book*, *29*(1), 1.
58. Jez, J. M., Bowman, M. E., and Noel, J. P. (2002). Expanding the biosynthetic repertoire of plant type III polyketide synthases by altering starter molecule specificity. *Proceedings of the National Academy of Sciences of the United States of America*, *99*(8), 5319–5324.
59. Jia, Z., Zou, B., Wang, X., Qiu, J., Ma, H., Gou, Z., and Dong, H. (2010). Quercetin-induced H2O2 mediates the pathogen resistance against Pseudomonas syringae pv. Tomato DC3000

in Arabidopsis thaliana. *Biochemical and Biophysical Research Communications*, *396*(2), 522–527.

60. Jiang, L., Wang, Y., Björn, L. O., and Li, S. (2009). Arabidopsis RADICAL-INDUCED CELL DEATH1 is involved in UV-B signaling. *Photochemical and Photobiological Sciences*, *8*(6), 838–846.
61. Jones, P., Garcia, B. J., Furches, A., Tuskan, G. A., and Jacobson, D. (2019). Plant host-associated mechanisms for microbial selection. *Frontiers in Plant Science*, Vol. 10.
62. Jørgensen, K., Rasmussen, A. V., Morant, M., Nielsen, A. H., Bjarnholt, N., Zagrobelny, M., and Møller, B. L. (2005). Metabolon formation and metabolic channeling in the biosynthesis of plant natural products. *Current Opinion in Plant Biology*, *8*(3), 280–291.
63. Kakani, V. G., Reddy, K. R., Zhao, D., and Sailaja, K. (2003). Field crop responses to ultraviolet-B radiation: A review. *Agricultural and Forest Meteorology*, *120*(1–4), 191–218.
64. Kang, J. H., McRoberts, J., Shi, F., Moreno, J. E., Jones, A. D., and Howe, G. A. (2014). The flavonoid biosynthetic enzyme chalcone isomerase modulates terpenoid production in glandular trichomes of tomato. *Plant Physiology*, *164*(3), 1161–1174.
65. Karnahl, M., Park, M., Krausea, C., Hiller, U., Mayer, U., Stierhof, Y. D., and Jürgens, G. (2018). Functional diversification of Arabidopsis SEC1-related SM proteins in cytokinetic and secretory membrane fusion. *Proceedings of the National Academy of Sciences of the United States of America*, *115*(24), 6309–6314.
66. Karnik, R., Grefen, C., Bayne, R., Honsbein, A., Köhler, T., Kioumourtzoglou, D., and Blatt, M. R. (2013). Arabidopsis Sec1/Munc18 protein SEC11 is a competitive and dynamic modulator of SNARE binding and SYP121-dependent vesicle traffic. *Plant Cell*, *25*(4), 1368–1382.
67. Katagiri, F., Thilmony, R., and He, S. Y. (2002). The Arabidopsis Thaliana-Pseudomonas Syringae Interaction. *The Arabidopsis Book*, *1*(Appendix I), e0039.
68. Khalil, N., Fekry, M., Bishr, M., El-Zalabani, S., and Salama, O. (2018). Foliar spraying of salicylic acid induced accumulation of phenolics, increased radical scavenging activity and modified the composition of the essential oil of water stressed Thymus vulgaris L. *Plant Physiology and Biochemistry*, *123*(9), 65–74.
69. Khan, M. I. R., Fatma, M., Per, T. S., Anjum, N. A, and Khan, N. A. (2015). Salicylic acid-induced abiotic stress tolerance and underlying mechanisms in plants. *Frontiers in Plant*

Science, *6*(June), 462.

70. Kim, S. J., Kwon, D. Y., Kim, Y. S., and Kim, Y. C. (2010). Peroxyl radical scavenging capacity of extracts and isolated components from selected medicinal plants. *Archives of Pharmacal Research*, *33*(6), 867–873.
71. Kohler, A., Schwindling, S., and Conrath, U. (2002). Benzothiadiazole-induced priming for potentiated responses to pathogen infection, wounding, and infiltration of water into leaves requires the NPR1/NIM1 gene in Arabidopsis. *Plant Physiology*, *128*(3), 1046–1056.
72. Kriechbaumer, V., Botchway, S. W., and Hawes, C. (2016). Localization and interactions between Arabidopsis auxin biosynthetic enzymes in the TAA/YUC-dependent pathway. *Journal of Experimental Botany*, *67*(14), 4195–4207.
73. Kubitzki, K. (1987). Phenylpropanoid Metabolism in Relation to Land Plant Origin and Diversification. *Journal of Plant Physiology*, *131*(1), 17–24.
74. Kumar, D. (2014). Salicylic acid signaling in disease resistance. *Plant Science*, *228*, 127–134.
75. Kunst, L., and Samuels, A. L. (2003). Biosynthesis and secretion of plant cuticular wax. *Progress in Lipid Research*, *42*(1), 51–80.
76. Lallemand, B., Erhardt, M., Heitz, T., and Legrand, M. (2013). Sporopollenin biosynthetic enzymes interact and constitute a metabolon localized to the endoplasmic reticulum of tapetum cells. *Plant Physiology*, *162*(2), 616–625.
77. Lapcik, O., Honys, D., Koblovska, R., Mackova, Z., Vitkova, M., and Klejdus, B. (2006). Isoflavonoids are present in Arabidopsis thaliana despite the absence of any homologue to known isoflavonoid synthases. *Plant Physiology and Biochemistry*, *44*(2–3), 106–114.
78. Le Roy, J., Huss, B., Creach, A., Hawkins, S., and Neutelings, G. (2016). Glycosylation Is a Major Regulator of Phenylpropanoid Availability and Biological Activity in Plants. *Frontiers in Plant Science*, *7*(3).
79. Lei, K. J., Zhang, L., Du, X. Y., An, Y., Chang, G. H., and An, G. Y. (2018). A chalcone synthase controls the verticillium disease resistance response in both Arabidopsis thaliana and cotton. *European Journal of Plant Pathology*, *152*(3), 769–781.
80. Lepiniec, L., Debeaujon, I., Routaboul, J. M., Baudry, A., Pourcel, L., Nesi, N., & Caboche, M. (2006). Genetics and biochemistry of seed flavonoids. *Annual Review of Plant Biology*, *57*, 405–430.
81. Lewandowska, M., Keyl, A., and Feussner, I. (2020). Wax biosynthesis in response to danger:

its regulation upon abiotic and biotic stress. *New Phytologist*, *227*(3), 698–713.

82. Li, J., Ou-Lee, T. M., Raba, R., Amundson, R. G., and Last, R. L. (1993). Arabidopsis Flavonoid Mutants Are Hypersensitive to UV-B Irradiation. *The Plant Cell*, *5*(2), 171–179.
83. Li, N., Han, X., Feng, D., Yuan, D., and Huang, L. J. (2019). Signaling crosstalk between salicylic acid and ethylene/Jasmonate in plant defense: Do we understand what they are whispering? *International Journal of Molecular Sciences*, *20*(3).
84. Li, X., Zhang, L. P., Zhang, L., Yan, P., Ahammed, G. J., and Han, W. Y. (2019). Methyl salicylate enhances flavonoid biosynthesis in tea leaves by stimulating the phenylpropanoid pathway. *Molecules*, *24*(2).
85. Lima, M. P. R., Soares, A. M. V. M., and Loureiro, S. (2015). Responses of wheat (Triticum aestivum) and turnip (Brassica rapa) to the combined exposure of carbaryl and ultraviolet radiation. *Environmental Toxicology and Chemistry*, *34*(7), 1665–1674.
86. Lin, W., Zhang, H., Huang, D., Schenke, D., Cai, D., Wu, B., and Miao, Y. (2020). Dual-localized WHIRLY1 affects salicylic acid biosynthesis via coordination of isochorismate synthase1, phenylalanine ammonia lyase1, and S-adenosyl-L-methionine-dependent methyltransferase1. *Plant Physiology*, *184*(4), 1884–1899.
87. Lipka, U., Fuchs, R., and Lipka, V. (2008). Arabidopsis non-host resistance to powdery mildews. *Current Opinion in Plant Biology*, *11*(4), 404–411.
88. Mackey, D., Belkhadir, Y., Alonso, J. M., Ecker, J. R., and Dangl, J. L. (2003). Arabidopsis RIN4 is a target of the type III virulence effector AvrRpt2 and modulates RPS2-mediated resistance. *Cell*, *112*(3), 379–389.
89. Martel, A. B., and Qaderi, M. M. (2016). Does salicylic acid mitigate the adverse effects of temperature and ultraviolet-B radiation on pea (Pisum sativum) plants? *Environmental and Experimental Botany*, *122*, 39–48.
90. Martínez, C., Pons, E., Prats, G., and León, J. (2004). Salicylic acid regulates flowering time and links defence responses and reproductive development. *Plant Journal*, *37*(2), 209–217.
91. Mierziak, J., Kostyn, K., and Kulma, A. (2014). Flavonoids as important molecules of plant interactions with the environment. *Molecules*, *19*(10), 16240–16265.
92. Mir, R., Jallu, S., and Singh, T. P. (2015). The shikimate pathway: Review of amino acid sequence, function and three-dimensional structures of the enzymes. *Critical Reviews in Microbiology*, *41*(2), 172–189.

93. Mosher, S., Moeder, W., Nishimura, N., Jikumaru, Y., Joo, S. H., Urquhart, W., and Yoshioka, K. (2010). The lesion-mimic mutant cpr22 shows alterations in abscisic acid signaling and abscisic acid insensitivity in a salicylic acid-dependent manner. *Plant Physiology*, *152*(4), 1901–1913.
94. Mur, L. A. J., Kenton, P., Lloyd, A. J., Ougham, H., and Prats, E. (2008). The hypersensitive response; The centenary is upon us but how much do we know? *Journal of Experimental Botany*, *59*(3), 501–520.
95. Mysore, K. S., and Ryu, C. M. (2004). Nonhost resistance: How much do we know? *Trends in Plant Science*, *9*(2), 97–104.
96. Nourimand, M., and Todd, C. D. (2016). Allantoin increases cadmium tolerance in Arabidopsis via activation of antioxidant mechanisms. *Plant and Cell Physiology*, *57*(12), 2485–2496.
97. Ono, E., Fukuchi-Mizutani, M., Nakamura, N., Fukui, Y., Yonekura-Sakakibara, K., Yamaguchi, M., and Tanaka, Y. (2006). Yellow flowers generated by expression of the aurone biosynthetic pathway. *Proceedings of the National Academy of Sciences of the United States of America*, *103*(29), 11075–11080.
98. Park, J. J., Jin, P., Yoon, J., Yang, J. Il, Jeong, H. J., Ranathunge, K., and An, G. (2010). Mutation in Wilted Dwarf and Lethal 1 (WDL1) causes abnormal cuticle formation and rapid water loss in rice. *Plant Molecular Biology*, *74*(1), 91–103.
99. Parkhi, V., Kumar, V., Campbell, L. A. M., Bell, A. A., Shah, J., and Rathore, K. S. (2010). Resistance against various fungal pathogens and reniform nematode in transgenic cotton plants expressing Arabidopsis NPR1. *Transgenic Research*, *19*(6), 959–975.
100. Peer, W. A., Brown, D. E., Tague, B. W., Muday, G. K., Taiz, L., and Murphy, A. S. (2001). Flavonoid accumulation patterns of transparent testa mutants of arabidopsis. *Plant Physiology*, *126*(2), 536–548.
101. Peer, Wendy Ann, and Murphy, A. S. (2007). Flavonoids and auxin transport: modulators or regulators? *Trends in Plant Science*, *12*(12), 556–563.
102. Pelletier, M. K., Burbulis, I. E., and Winkel-shirley, B. (1999). Disruption of specific flavonoid genes enhances the accumulation of flavonoid enzymes and end-products in Arabidopsis seedlings. *Plant Molecular Biology ,40*, 45–54.
103. Petrov, V., Hille, J., Mueller-Roeber, B., and Gechev, T. S. (2015). ROS-mediated abiotic

stress-induced programmed cell death in plants. *Frontiers in Plant Science*, *6*(2), 1–16.

104. Pourcel, L., Irani, N. G., Koo, A. J. K., Bohorquez-Restrepo, A., Howe, G. A., and Grotewold, E. (2013). A chemical complementation approach reveals genes and interactions of flavonoids with other pathways. *Plant Journal*, *74*(3), 383–397.
105. Pourcel, L., Routaboul, J. M., Cheynier, V., Lepiniec, L., and Debeaujon, I. (2007). Flavonoid oxidation in plants: from biochemical properties to physiological functions. *Trends in Plant Science*, *12*(1), 29–36.
106. Ralston, L., and Yu, O. (2006). Metabolons involving plant cytochrome P450s. *Phytochemistry Reviews*, *5*(2–3), 459–472.
107. Ribera, A. E., and Zuñiga, G. (2012). Induced plant secondary metabolites for phytopatogenic fungi control : a review. *Plant Nutrition*, *12*(4), 893–911.
108. Robert-Seilaniantz, A., Grant, M., and Jones, J. D. G. (2011). Hormone Crosstalk in Plant Disease and Defense: More Than Just JASMONATE-SALICYLATE Antagonism. *Annual Review of Phytopathology*, *49*(1), 317–343.
109. Sanchez-Vallet, A., Ramos, B., Bednarek, P., López, G., Piślewska-Bednarek, M., Schulze-Lefert, P., and Molina, A. (2010). Tryptophan-derived secondary metabolites in Arabidopsis thaliana confer non-host resistance to necrotrophic Plectosphaerella cucumerina fungi. *Plant Journal*, *63*(1), 115–127.
110. Sano, S., Aoyama, M., Nakai, K., Shimotani, K., Yamasaki, K., Sato, M. H., and Shiina, T. (2014). Light-dependent expression of flg22-induced defense genes in Arabidopsis. *Frontiers in Plant Science*, *5*(10), 1–12.
111. Saslowsky, D. E., Warek, U., and Winkel, B. S. J. (2005). Nuclear localization of flavonoid enzymes in Arabidopsis. *Journal of Biological Chemistry*, *280*(25), 23735–23740.
112. Schaller, H. (2010). Sterol and Steroid Biosynthesis and Metabolism in Plants and Microorganisms. *Comprehensive Natural Products II*, 755–787.
113. Schenk, S. T., and Schikora, A. (2015). *http://www.bio-protocol.org/e1412*. *5*(3), 1–7.
114. Serrano, M., Coluccia, F., Torres, M.. (2014). The cuticle and plant defense to pathogens. *Frontiers in Plant Science*, *5*(6), 1–8.
115. Shah, J., Chaturvedi, R., Chowdhury, Z., Venables, B., and Petros, R. A. (2014). Signaling by small metabolites in systemic acquired resistance. *Plant Journal*, *79*(4), 645–658.
116. Shakirova, F. M., Allagulova, C. R., Maslennikova, D. R., Klyuchnikova, E. O., Avalbaev, A.

M., and Bezrukova, M. V. (2016). Salicylic acid-induced protection against cadmium toxicity in wheat plants. *Environmental and Experimental Botany*, *122*, 19–28.

117. Shepherd, T., and Griffiths, D. W. (2006). The effects of stress on plant cuticular waxes. *New Phytologist*, *171*, 469–499.
118. Shigenaga, A. M., and Argueso, C. T. (2016). No hormone to rule them all: Interactions of plant hormones during the responses of plants to pathogens. *Seminars in Cell and Developmental Biology*, *56*, 174–189.
119. Shirley, B W, Kubasek, W. L., Storz, G., Bruggemann, E., Koornneef, M., Ausubel, F. M., and Goodman, H. M. (1995). Analysis of Arabidopsis mutants deficient in flavonoid biosynthesis. *The Plant Journal* , *8*, 659–671.
120. Shirley, Brenda W. (1996). Flavonoid biosynthesis: "New" functions for an "old" pathway. *Trends in Plant Science*, *1*(11), 377–382.
121. Silva-Navas, J., Moreno-Risueno, M. A., Manzano, C., Téllez-Robledo, B., Navarro-Neila, S., Carrasco, V., Del Pozo, J. C. (2016). Flavonols mediate root phototropism and growth through regulation of proliferation-to-differentiation transition. *Plant Cell*, *28*(6), 1372–1387.
122. Slaughter, A., Daniel, X., Flors, V., Luna, E., Hohn, B., and Mauch-Mani, B. (2012). Descendants of Primed Arabidopsis Plants Exhibit Resistance to Biotic Stress. *Plant Physiology*, *158*(2), 835–843.
123. Snyder, B. A., and Nicholson, R. L. (1990). Synthesis of Phytoalexins in Sorghum as a Site-Specific Response to Fungal Ingress. *Science*, *248*(4963), 1637–1639.
124. Spoel, S. H., Koornneef, A., Claessens, S. M. C., Jerôme, P., Pelt, J. A. Van, Mueller, M. J., and Métraux, J. (2003). NPR1 Modulates Cross-Talk between Salicylate- and Jasmonate-Dependent Defense Pathways through a Novel Function in the Cytosol. *The Plant Cell*, *15*(3), 760–770.
125. Stangarlin, J. R., Kuhn, O. J., Toledo, M. V., Portz, R. L., Schwan-Estrada, K. R. F., and Pascholati, S. F. (2011). A defesa vegetal contra fitopatógenos. *Scientia Agraria Paranaenis*, *10*(1), 18–46.
126. Stewart, E. L., Lucas, G. B., Campbell, C. L., and Lucas, L. T. (1991). Introduction to Plant Diseases: Identification and Management. *Mycologia*, *83*.
127. Stout, J., and Chapple, C. (2004). Chapter three The phenylpropanoid pathway in arabidopsis: Lessons learned from mutants in sinapate ester biosynthesis. *Recent Advances in*

Phytochemistry, *38*, 39–67.

128. Su, H., Jiang, H., and Li, Y. (2013). Effects of PAL and ICS on the production of total flavonoids, daidzein and puerarin in Pueraria thomsonii Benth. suspension cultures under low light stress. *Journal of Plant Biochemistry and Biotechnology*, *24*(1), 34–41.
129. Sumanta, N., Haque, C. I., Nishika, J., and Suprakash, R. (2014). Spectrophotometric Analysis of Chlorophylls and Carotenoids from Commonly Grown Fern Species by Using Various Extracting Solvents. *Research Journal of Chemical Sciences*, *4*(9), 2231–2606.
130. Takshak, S., and Agrawal, S. B. (2014). Secondary metabolites and phenylpropanoid pathway enzymes as influenced under supplemental ultraviolet-B radiation in Withania somnifera Dunal, an indigenous medicinal plant. *Journal of Photochemistry and Photobiology*, *140*, 332–343.
131. Tanaka, T., Tanaka, H., Machida, C., Watanabe, M., and Machida, Y. (2004). A new method for rapid visualization of defects in leaf cuticle reveals five intrinsic patterns of surface defects in Arabidopsis. *Plant Journal*, *37*(1), 139–146.
132. Tattini, M., Guidi, L., Morassi-Bonzi, L., Pinelli, P., Remorini, D., Degl'Innocenti, E., and Agati, G. (2005). On the role of flavonoids in the integrated mechanisms of response of Ligustrum vulgare and Phillyrea latifolia to high solar radiation. *New Phytologist*, *167*(2), 457–470.
133. Ton, J., Ent, S. Van Der, Hulten, M. Van, Pozo, M., van Oosten, V., van Loon, L. C., and Pieterse, C. M. J. (2009). Priming as a mechanism behind induced resistance against pathogens, insects and abiotic stress. *IOBC/Wprs Bulletin*, *44*, 3–13.
134. Treutter, D. (2005). Significance of flavonoids in plant resistance and enhancement of their biosynthesis. *Plant Biology*, *7*(6), 581–591.
135. Tzin, V., and Galili, G. (2010). New Insights into the shikimate and aromatic amino acids biosynthesis pathways in plants. *Molecular Plant*, *3*(6), 956–972.
136. Uleberg, E., Rohloff, J., Jaakola, L., Trôst, K., Junttila, O., Häggman, H., and Martinussen, I. (2012). Effects of temperature and photoperiod on yield and chemical composition of northern and southern clones of bilberry (*Vaccinium myrtillus* l.). *Journal of Agricultural and Food Chemistry*, *60*(42), 10406–10414.
137. Veitch, N. C., and Grayer, R. J. (2011). Flavonoids and their glycosides, including anthocyanins. *Natural Product Reports*, *28*(10), 1626–1695.

138. Ververidis, F., Trantas, E., Douglas, C., Vollmer, G., Kretzschmar, G., and Panopoulos, N. (2007). Biotechnology of flavonoids and other phenylpropanoid-derived natural products. Part I: Chemical diversity, impacts on plant biology and human health. *Biotechnology Journal*, *2*(10), 1214–1234.

139. Vlot, A. C., Dempsey, D. A., and Klessig, D. F. (2009). Salicylic Acid, a Multifaceted Hormone to Combat Disease. *Annual Review of Phytopathology*, *47*(1), 177–206.

140. Vogt, T. (2010). Phenylpropanoid biosynthesis. *Molecular Plant*, *3*(1), 2–20.

141. Voigt, C. A. (2014). Callose-mediated resistance to pathogenic intruders in plant defense-related papillae. *Frontiers in Plant Science*, *5*(4), 1–6. https://doi.org/10.3389/fpls.2014.00168

142. Wang, C., Chin, Y., Lin, C., Chen, P., and To, K. (2015). *Transforming the Snapdragon Aurone Biosynthetic Genes into Petunia Alters Coloration Patterns in Transgenic Flowers*. *12*, 702–722.

143. Wang, W., Wen, Y., Berkey, R., and Xiao, S. (2009). Specific Targeting of the Arabidopsis Resistance Protein RPW8.2 to the Interfacial Membrane Encasing the Fungal Haustorium Renders Broad-Spectrum Resistance to Powdery Mildew. *Plant Cell*, *21*(9), 2898–2913.

144. Wang, Xiangfeng, Chung, K. P., Lin, W., and Jiang, L. (2017). Protein secretion in plants: Conventional and unconventional pathways and new techniques. *Journal of Experimental Botany*, *69*(1), 21–37.

145. Wang, Xiaoyu, Kong, L., Zhi, P., and Chang, C. (2020). Update on cuticular wax biosynthesis and its roles in plant disease resistance. *International Journal of Molecular Sciences*, *21*(15), 1–15.

146. Waqas, M. A., Kaya, C., Riaz, A., Farooq, M., Nawaz, I., Wilkes, A., and Li, Y. (2019). Potential Mechanisms of Abiotic Stress Tolerance in Crop Plants Induced by Thiourea. *Frontiers in Plant Science*, *10*(10), 1–14.

147. Wasson, A. P., Pellerone, F. I., and Mathesius, U. (2006). Silencing the flavonoid pathway in Medicago truncatula inhibits root nodule formation and prevents auxin transport regulation by rhizobia. *The Plant Cell*, *18*(7), 1617–1629.

148. Watkinson, J. I., Bowerman, P. A., Crosby, K. C., Hildreth, S. B., Helm, R. F., and Winkel, B. S. J. (2018). Identification of MOS9 as an interaction partner for chalcone synthase in the nucleus. *PeerJ*, *2018*(9), 1–20.

149. Way, H. M., Kazan, K., Mitter, N., Goulter, K. C., Birch, R. G., and Manners, J. M. (2002). Constitutive expression of a phenylalanine ammonia-lyase gene from Stylosanthes humilis in transgenic tobacco leads to enhanced disease resistance but impaired plant growth. *Physiological and Molecular Plant Pathology*, *60*(6), 275–282.

150. Wildermuth, M. C., Dewdney, J., Wu, G., and Ausubel, F. M. (2002). corrigendum: Isochorismate synthase is required to synthesize salicylic acid for plant defence. *Nature*, *417*(6888), 571–571.

151. Williams, R. J., Spencer, J. P. E., and Rice-Evans, C. (2004). Flavonoids: Antioxidants or signalling molecules? *Free Radical Biology and Medicine*, *36*(7), 838–849.

152. Wilson, K. E., Wilson, M., and Greenbergt, B. M. (1998). *Identification of the Flavonoid Glycosides that Accumulate in*. *67*(5), 547–553.

153. Wu, L., and Yang, H. Q. (2010). CRYPTOCHROME 1 is implicated in promoting R protein-mediated plant resistance to pseudomonas syringae in arabidopsis. *Molecular Plant*, *3*(3), 539–548.

154. Xiao, J., Muzashvili, T. S., and Georgiev, M. I. (2014). Advances in the biotechnological glycosylation of valuable flavonoids. *Biotechnology Advances*, *32*(6), 1145–1156.

155. Xu, C., Natarajan, S., and Sullivan, J. H. (2008). Impact of solar ultraviolet-B radiation on the antioxidant defense system in soybean lines differing in flavonoid contents. *Environmental and Experimental Botany*, *63*(1), 39–48.

156. Yan, C., and Xie, D. (2015). Jasmonate in plant defence: Sentinel or double agent? *Plant Biotechnology Journal*, *13*(9), 1233–1240.

157. Yang, L., Qin, L., Liu, G., Peremyslov, V. V, Dolja, V. V, and Wei, Y. (2014a). Myosins XI modulate host cellular responses and penetration resistance to fungal pathogens. *Proceedings of the National Academy of Sciences of the United States of America*, *111*(38), 13996–14001.

158. Yang, W., Xu, X., Li, Y., Wang, Y., Li, M., Wang, Y., and Chu, Z. (2016). Rutin-mediated priming of plant resistance to three bacterial pathogens initiating the early SA signal pathway. *PLoS ONE*, *11*(1), 1–15.

159. Yi, S. Y., Shirasu, K., Moon, J. S., Lee, S. G., and Kwon, S. Y. (2014). The activated SA and JA signaling pathways have an influence on flg22-triggered oxidative burst and callose deposition. *PLoS ONE*, *9*(2).

160. Yin, R., Messner, B., Faus-Kessler, T., Hoffmann, T., Schwab, W., Hajirezaei, M. R., and

Schäffner, A. R. (2012). Feedback inhibition of the general phenylpropanoid and flavonol biosynthetic pathways upon a compromised flavonol-3-O-glycosylation. *Journal of Experimental Botany*, *63*(7), 2465–2478.

161. Yu, O., Jung, W., Shi, J., Croes, R. a, Fader, G. M., McGonigle, B., and Odell, J. T. (2000). Production of the isoflavones genistein and daidzein in non-legume dicot and monocot tissues. *Plant Physiology*, *124*(2), 781–794.
162. Zhang, H., Sun, Y., Xie, X., Kim, M. S., Dowd, S. E., and Paré, P. W. (2009). A soil bacterium regulates plant acquisition of iron via deficiency-inducible mechanisms. *Plant Journal*, *58*(4), 568–577.
163. Zhang, W. J., and Björn, L. O. (2009). The effect of ultraviolet radiation on the accumulation of medicinal compounds in plants. *Fitoterapia*, *80*(4), 207–218.
164. Zhang, Y., and Fernie, A. R. (2021). Metabolons, enzyme–enzyme assemblies that mediate substrate channeling, and their roles in plant metabolism. *Plant Communications*, *2*(1), 100081.
165. Ziv, C., Zhao, Z., Gao, Y. G., and Xia, Y. (2018). Multifunctional Roles of Plant Cuticle During Plant-Pathogen Interactions. *Frontiers in Plant Science*, *9*(7), 1–8.

APPENDIX

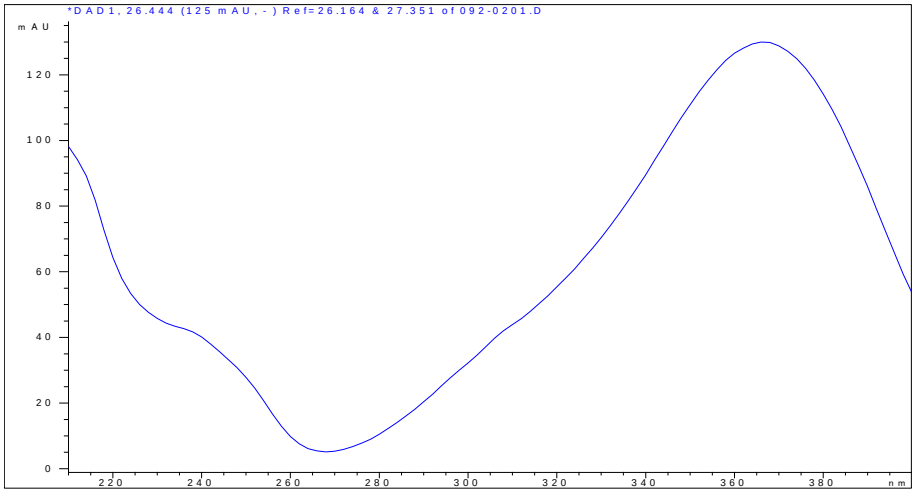

Figure A.1: Naringenin chalcone UV-spectrum

Absorbance spectra of the flavonoid NC. The UV absorbance spectra, from 200 to 400 nm, was collected using the photodiode-array detector.

Table A.1: HPLC data for flavonoids isolated from *Arabidopsis thaliana*

Peak number	Possible ID	Retention Time (min)
1	Quercetin	16-17 min
2	Kaempferol	18-19 min
3	Hydroxycinnamic acid derivatives	22-22.8 min
4	Naringenin chalcone	23-25min

Genotypes

Chromatograms (LD)

WT

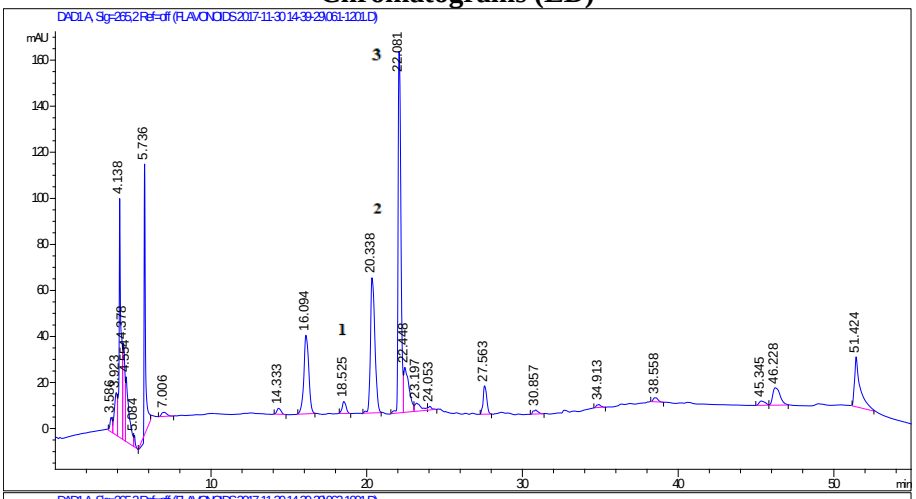

tt4

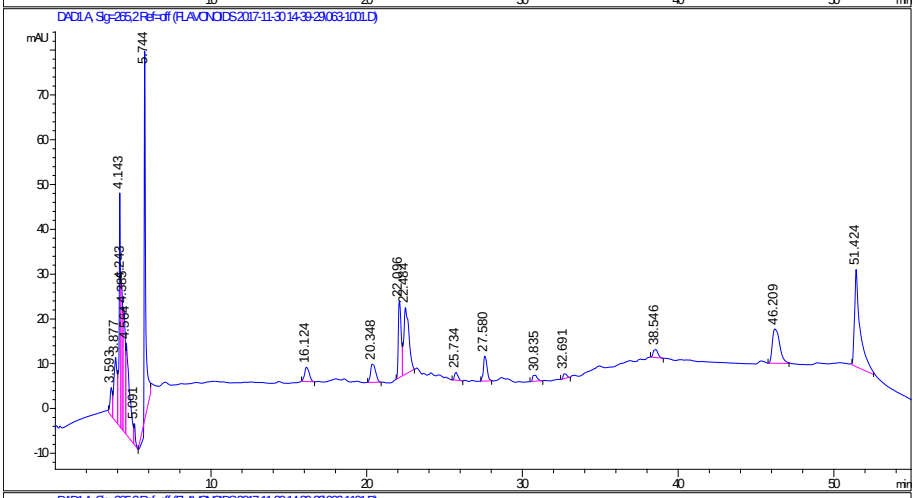

tt5

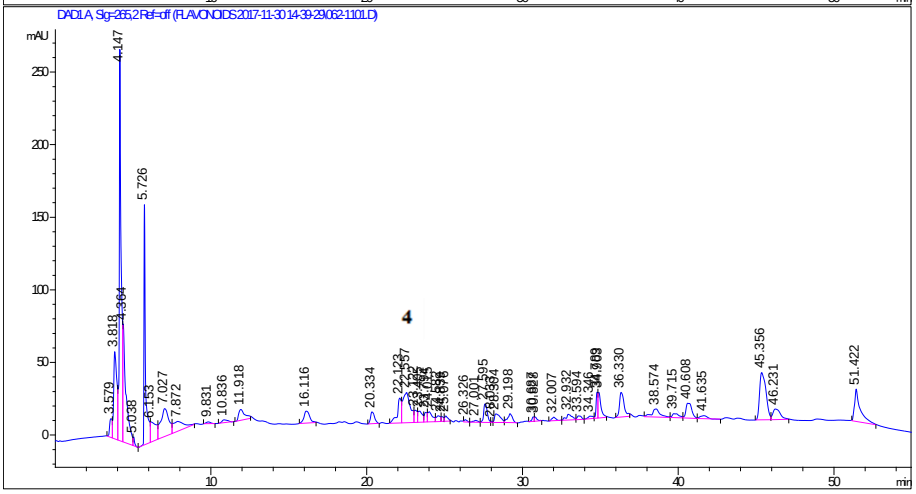

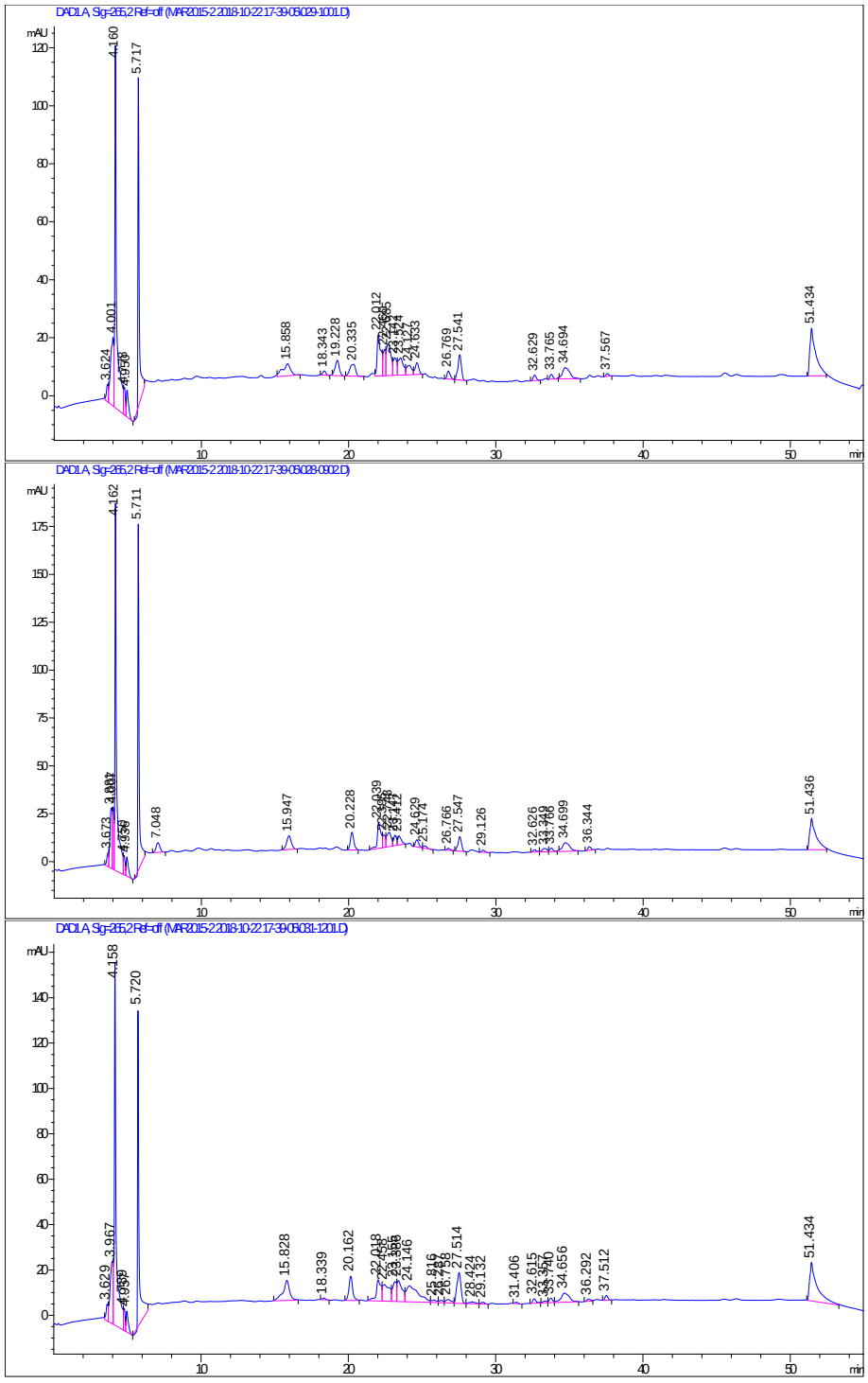

Figure A.2: Chromatograms of plants grown under LD.

Extracts were subjected to reverse-phase HPLC using a nonlinear acetonitrile/water gradient. The compounds were detected with a photodiode-array detector (chromatogram shown is absorbance at 265 nm).

Genotype	Chromatogram (SD)
WT	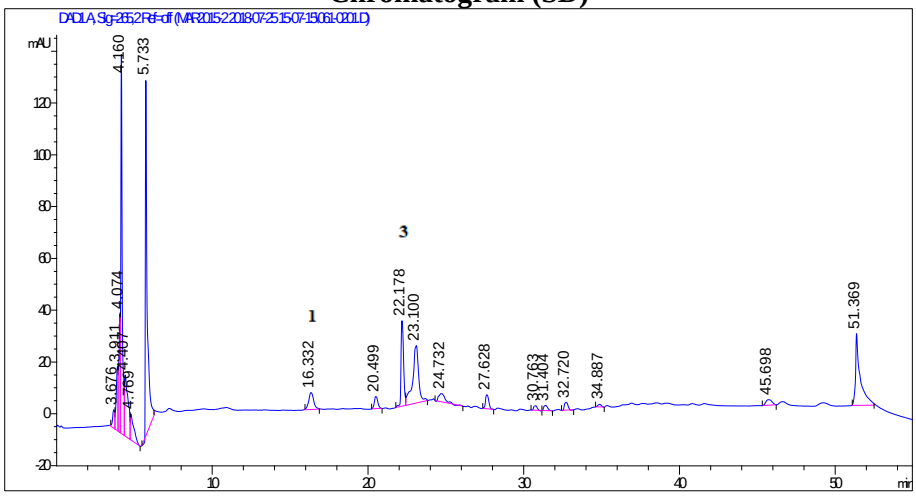
tt4	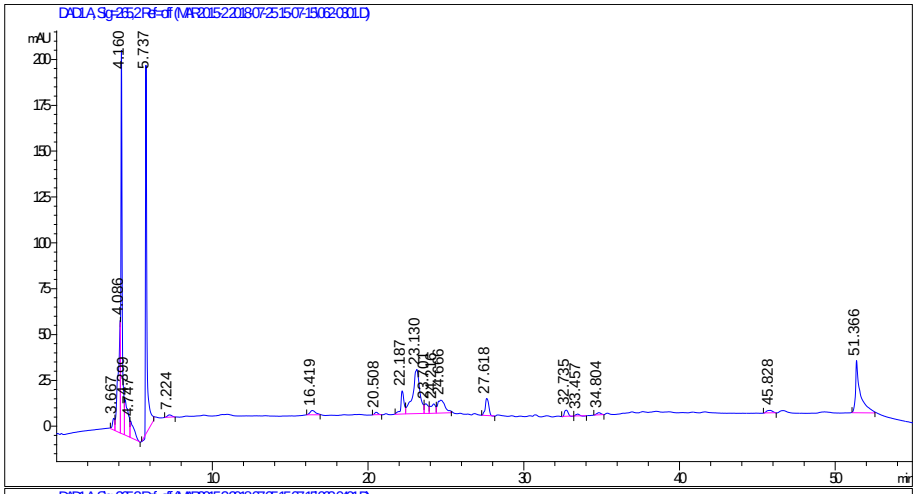
tt5	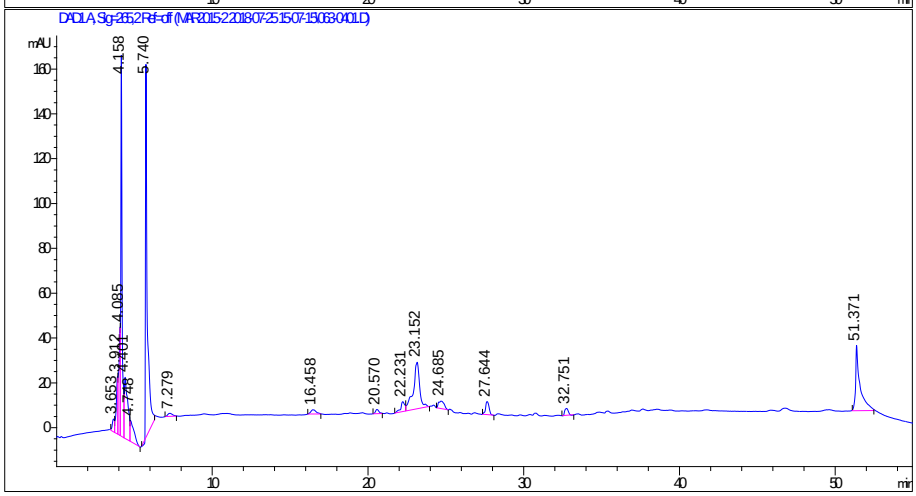

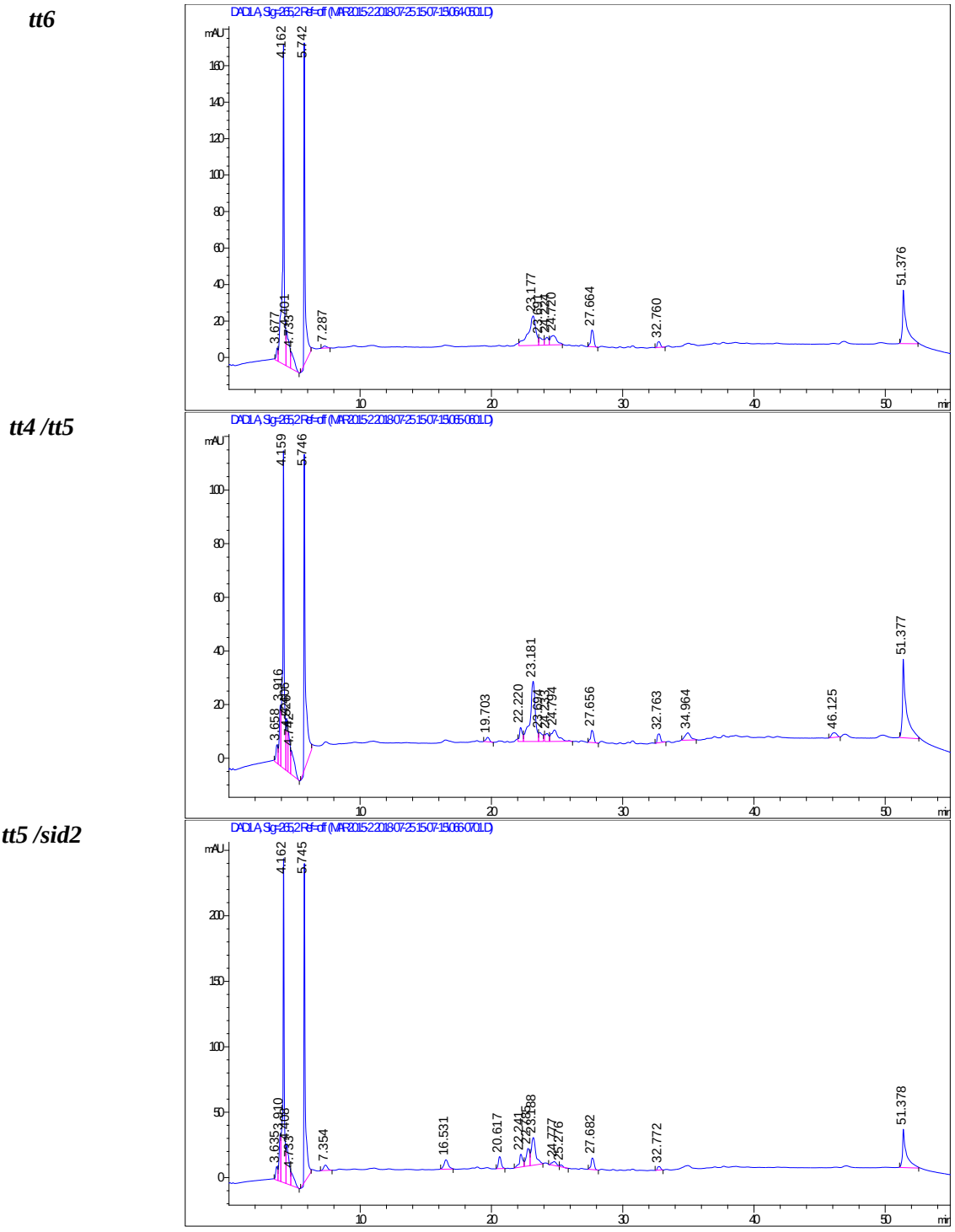

Figure A.3: Chromatograms of plants grown under SD.

Extracts were subjected to reverse-phase HPLC using a nonlinear acetonitrile/water gradient. The compounds were detected with a photodiode-array detector (chromatogram shown is absorbance at 265 nm).

Genotype	Chromatogram (LD+LT)
WT	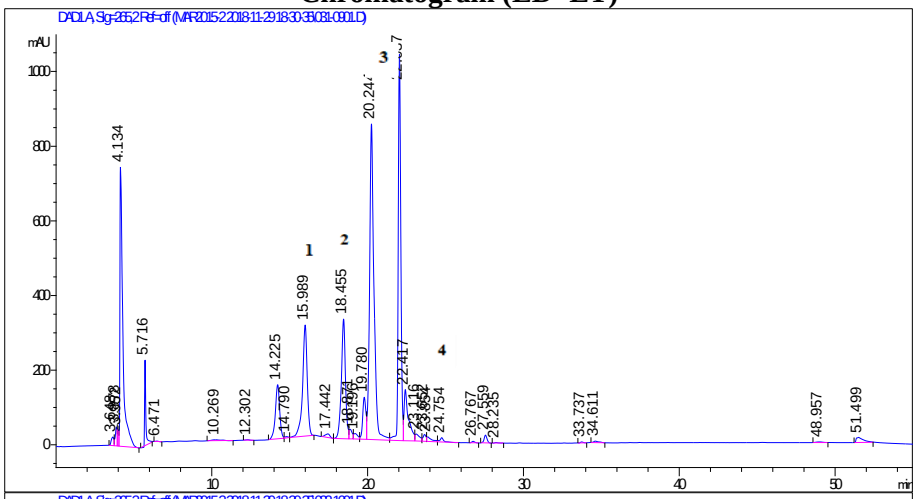
tt4	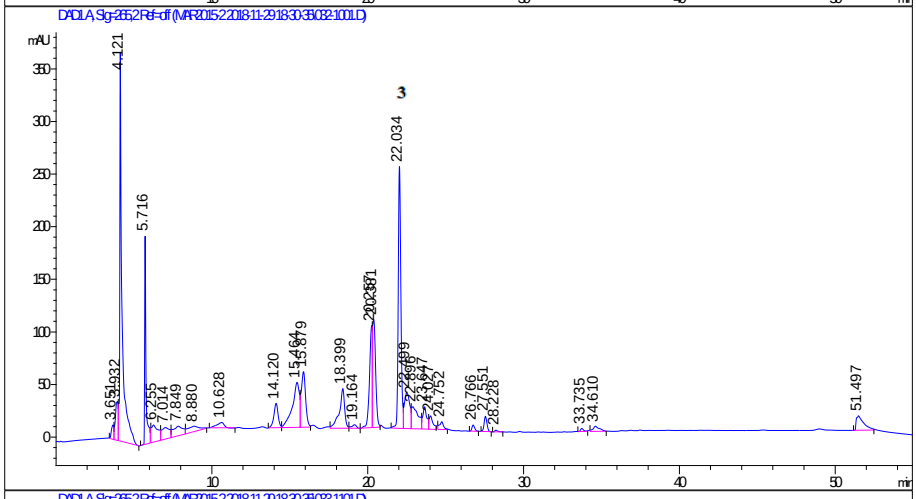
tt5	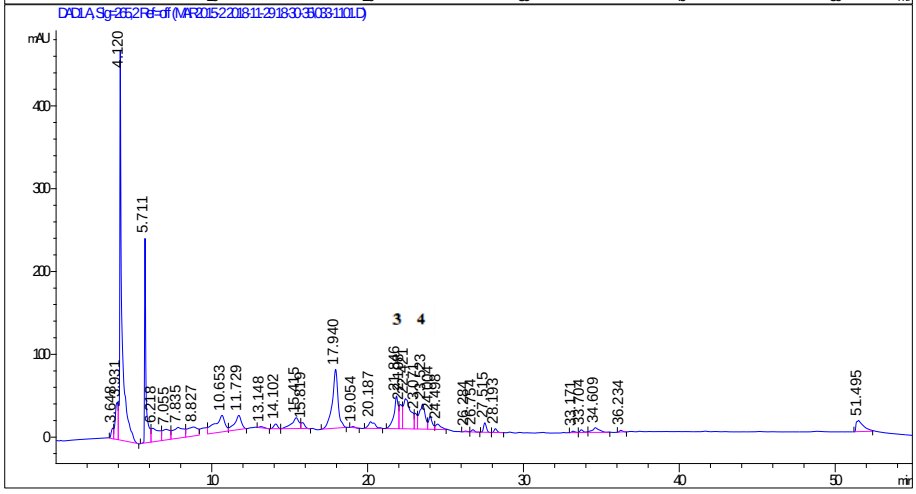

tt4/tt5

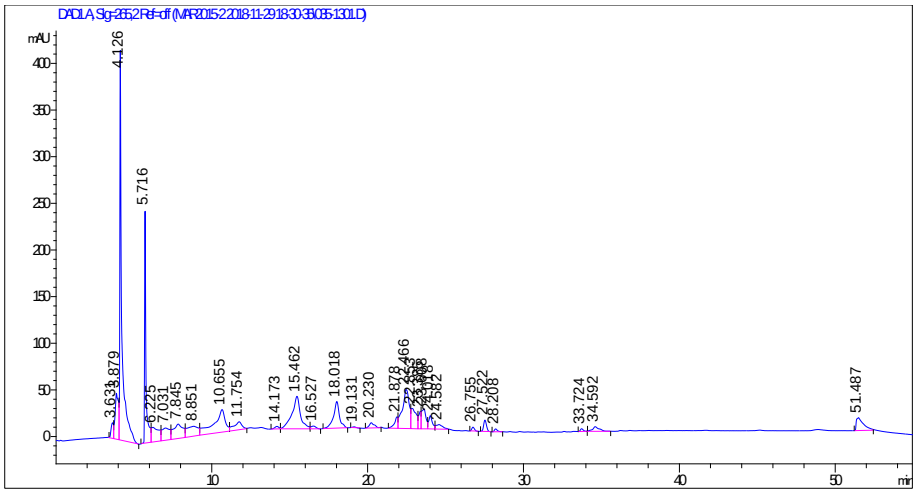

Figure A.4: Chromatograms of plants grown under LD + LT.

Extracts were subjected to reverse-phase HPLC using a nonlinear acetonitrile/water gradient. The compounds were detected with a photodiode-array detector (chromatogram shown is absorbance at 265 nm).

Genotypes

WT

Chromatogram (SD+HL)

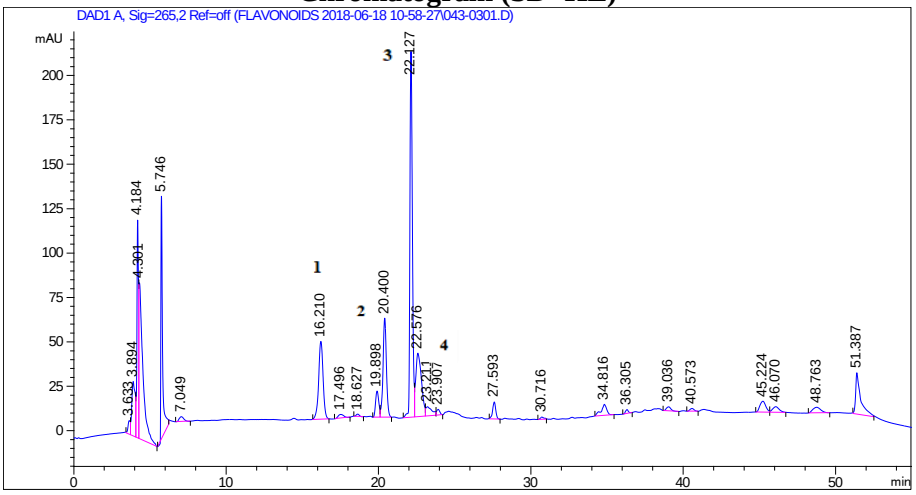

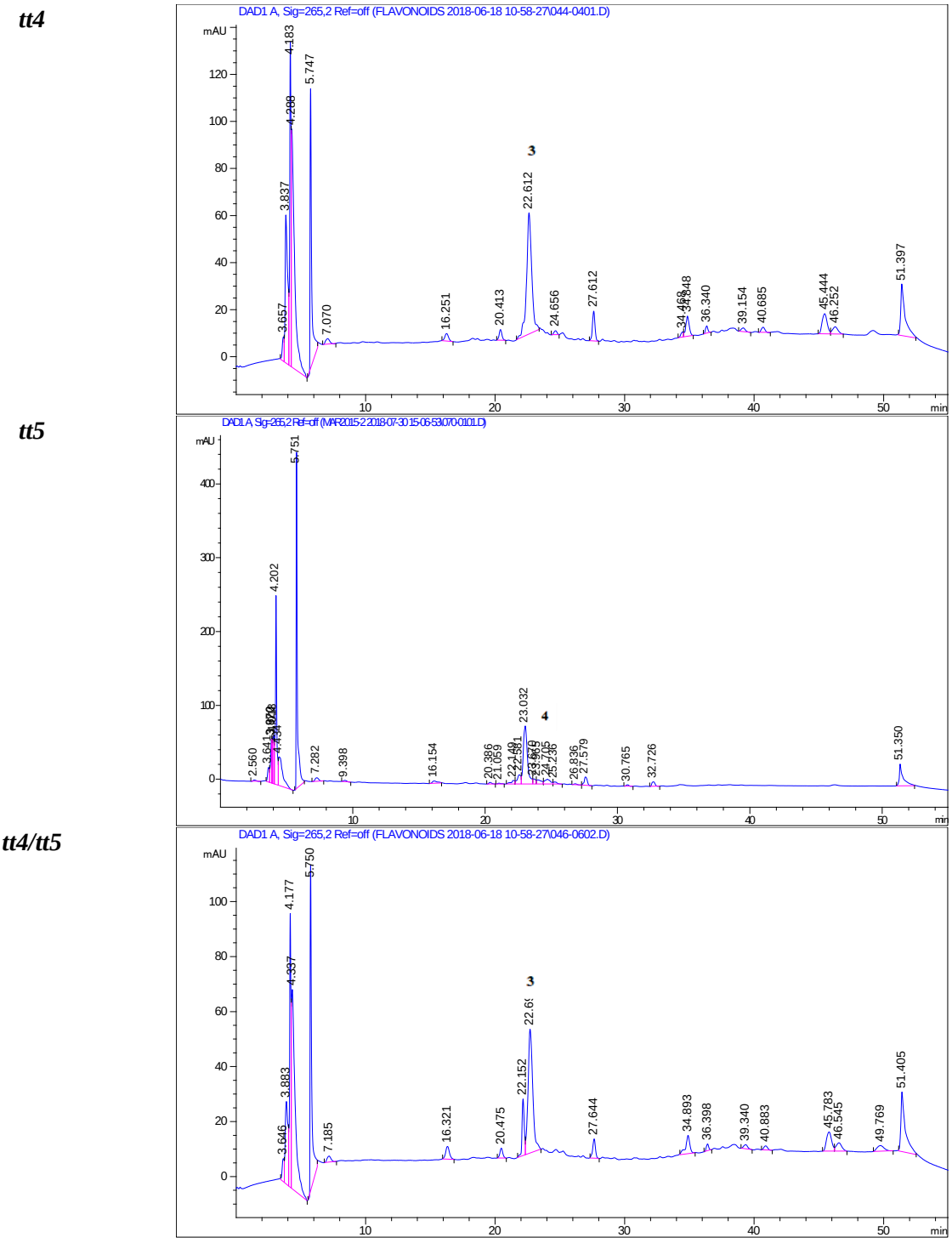

Figure A.5: Chromatograms of plants grown under SD + HL.

Extracts were subjected to reverse-phase HPLC using a nonlinear acetonitrile/water gradient. The compounds were detected with a photodiode-array detector (chromatogram shown is absorbance at 265 nm).

Genotypes **Chromatogram (LD + Colletotrichum higinssianum)**

WT

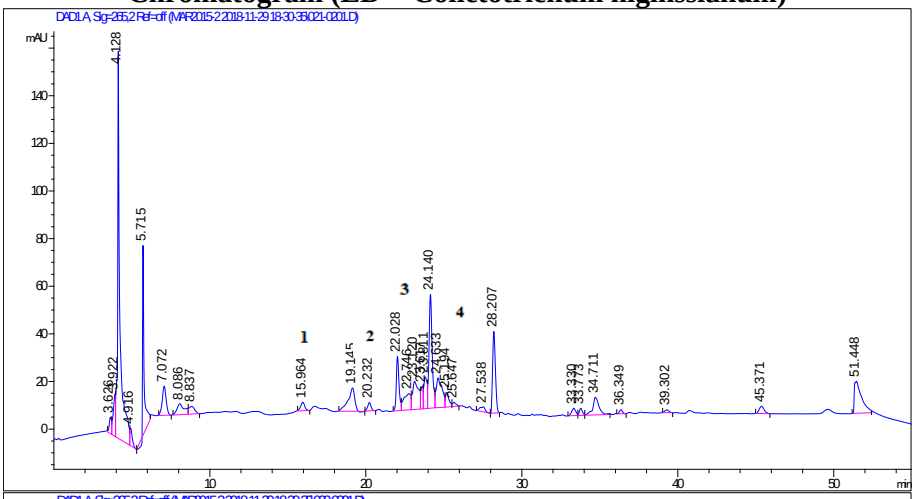

tt4

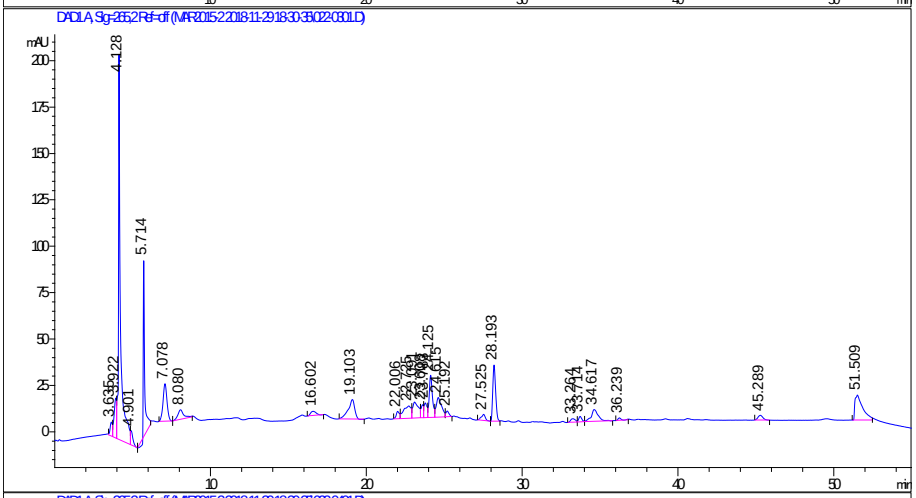

tt5

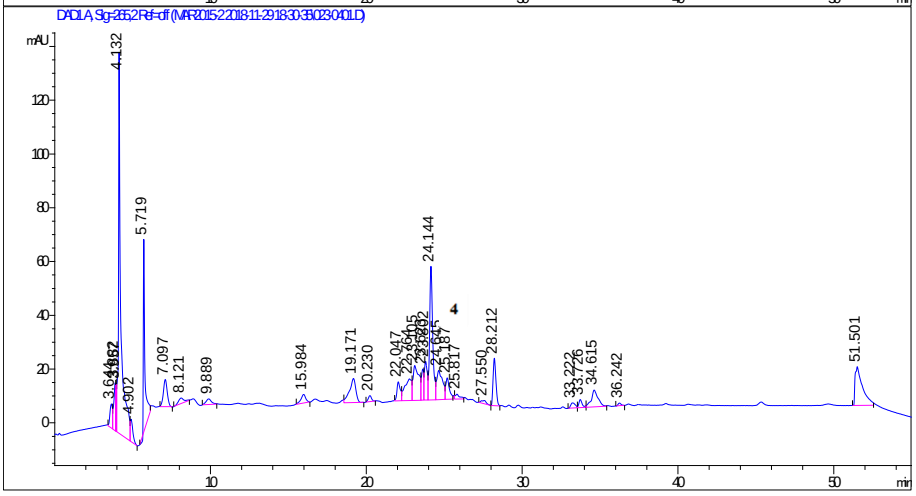

tt6

tt4/tt5

tt5/sid2

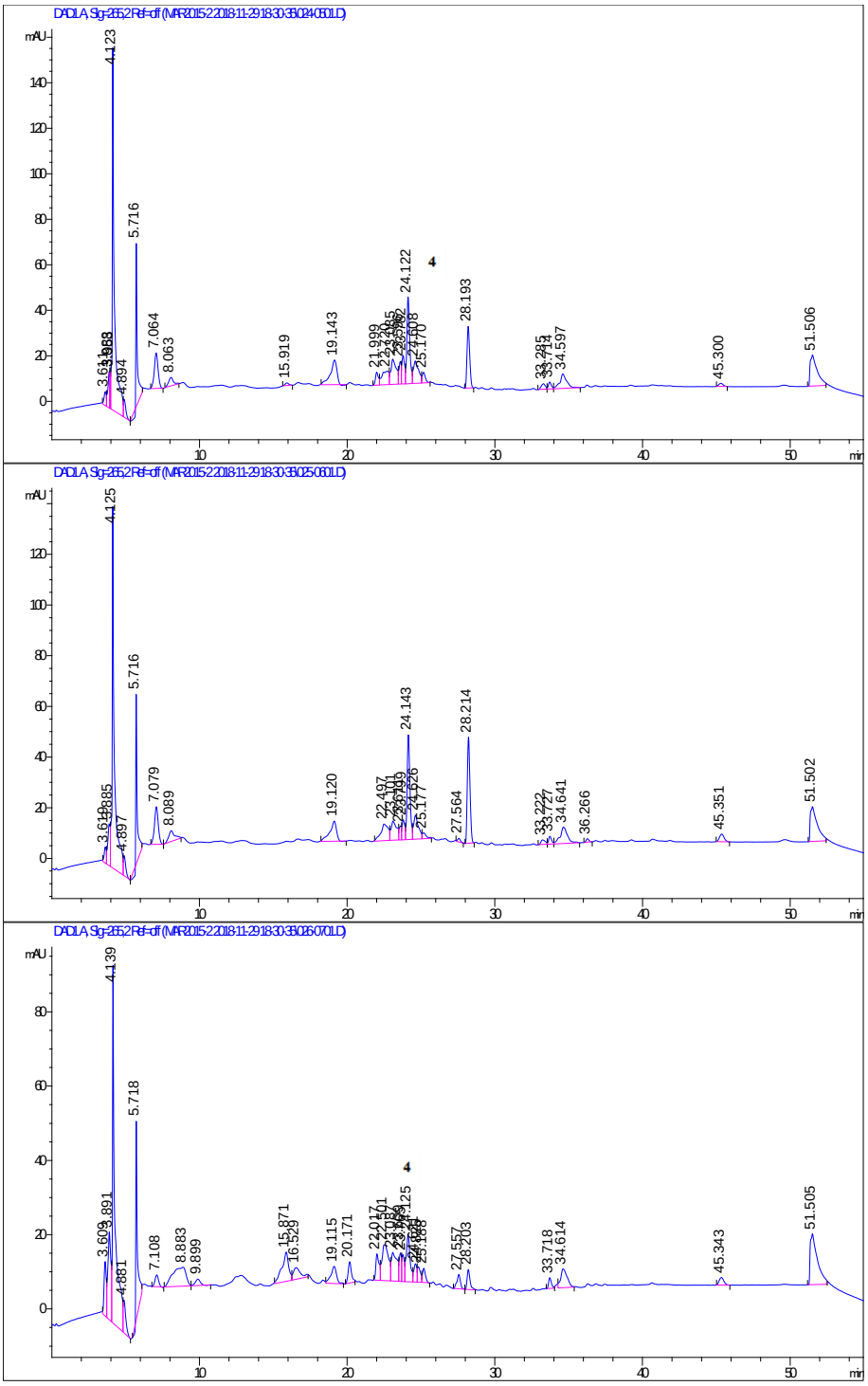

Figure A.6: Chromatograms of plants grown under LD and infected with *Colletotrichum higinssianum.*

Extracts were subjected to reverse-phase HPLC using a nonlinear acetonitrile/water gradient. The compounds were detected with a photodiode-array detector (chromatogram shown is absorbance at 265 nm).

Genotypes	Chromatogram (LD + *Erysiphe cichoracearum*)
WT	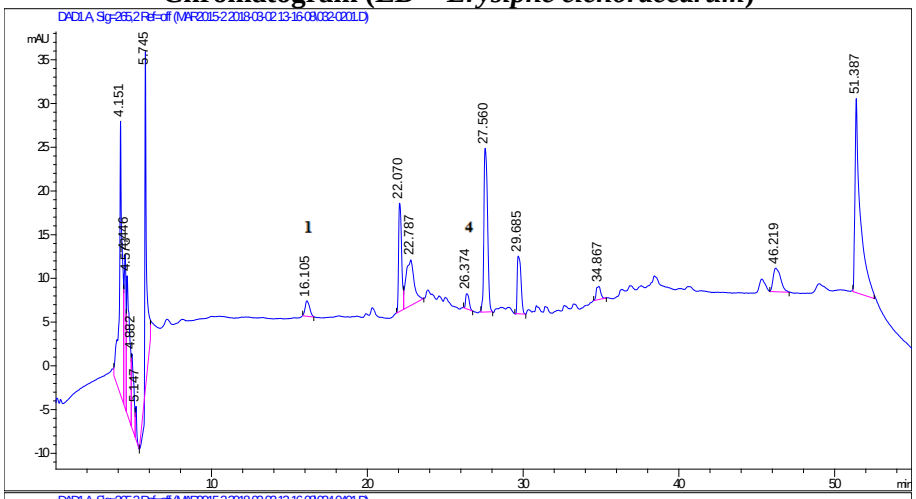
tt4	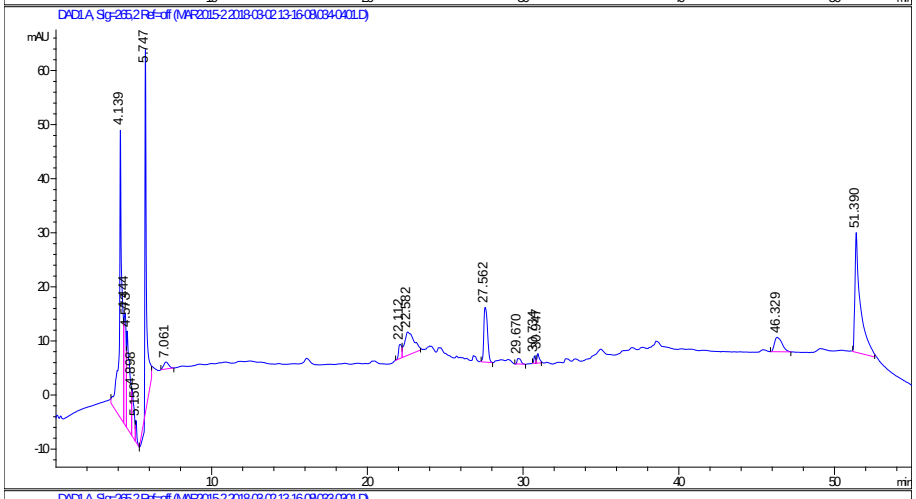
tt5	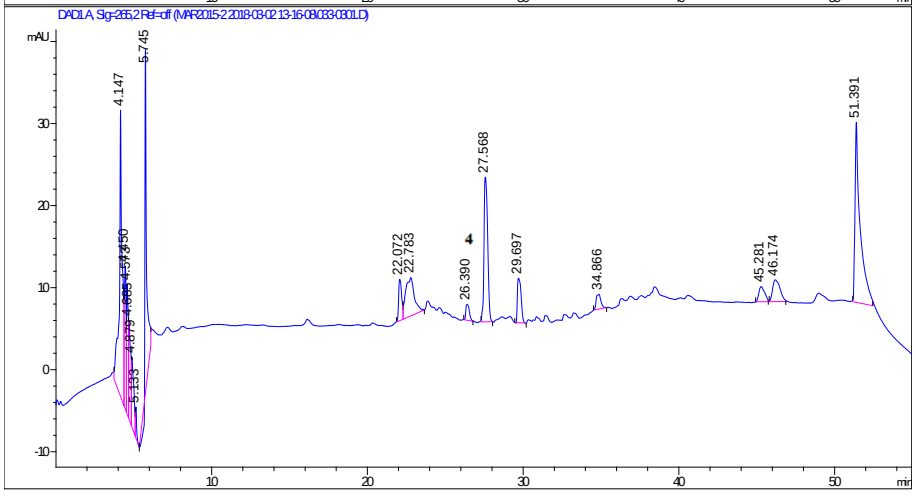

tt6

tt4/tt5

tt5/sid2

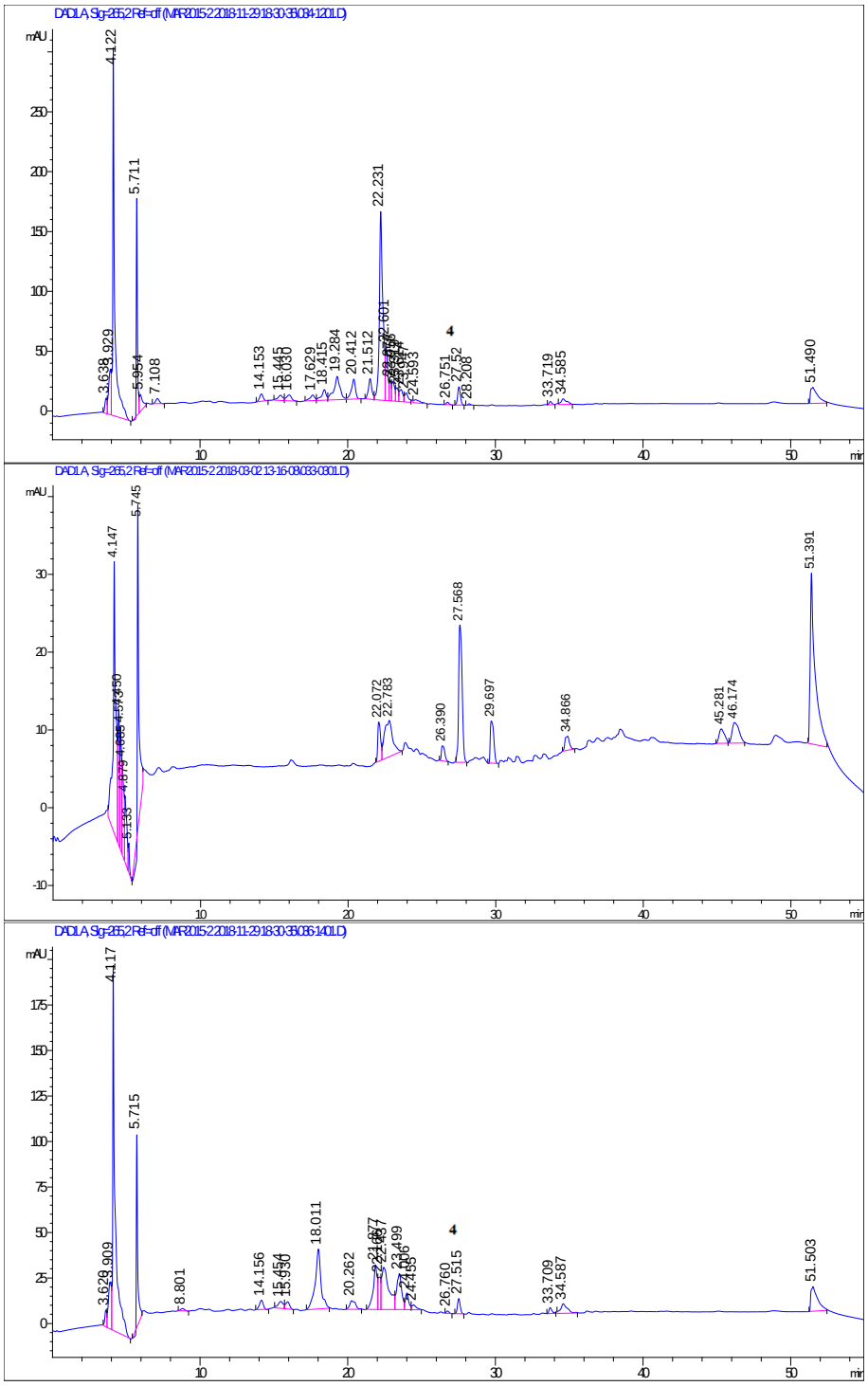

Figure A.7: Chromatograms of plants grown under LD and infected with *Erysiphe cichoracearum.*

Extracts were subjected to reverse-phase HPLC using a nonlinear acetonitrile/water gradient. The compounds were detected with a photodiode-array detector (chromatogram shown is absorbance at 265 nm).

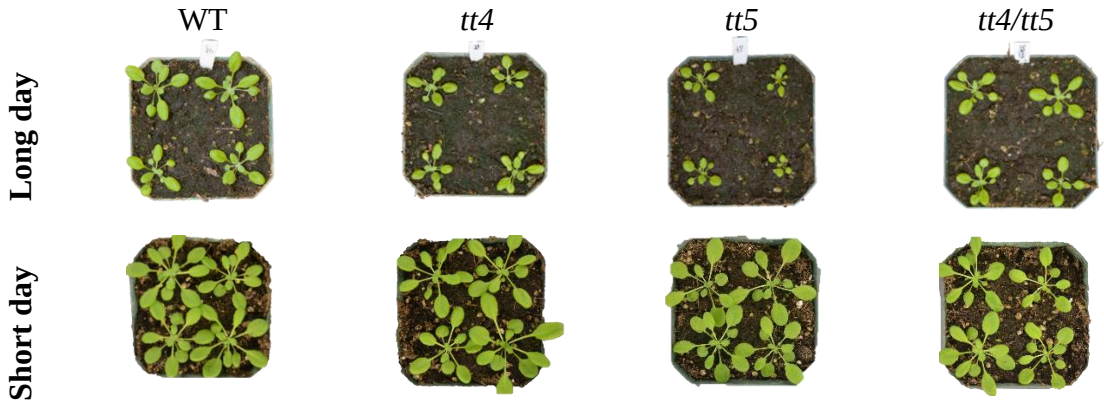

Figure A.8: Controls samples of the experiment 3.6.

Plants were grown in an environmental growth chamber under two different conditions: Long Day (LD) 22˚C, 16hr light/8 hr dark photoperiod and a light intensity at 200 µmol $m^{-2}s^{-1}$; Short Day (SD) 22˚C, 8 hr light/16 hr dark photoperiod and a light intensity at 200 µmol $m^{-2}s^{-1}$. Control samples were sprayed with a water to evaluate the naringenin chalcone solution (200 µg/mL) response and kept under control conditions.

Figure A.9: ANOVA statistical analysis

Figure A.9.1 – ANOVA of chlorophyll retention on *transparent testa* lines grown under long and short-days infected with Anthracnose (*Colletotrichum higginsianum*) disease at 0 and 5 (dpi).

The GLM Procedure

Class Level Information

Class	Levels	Values
genotype	6	tt4 tt4tt5 tt5 tt5sid2 tt6 wt
condition	2	Id sd

Number of observations 36

11:45 Saturday, April 29, 2000 2

The GLM Procedure

Dependent Variable: chl_total chl total Odpi

Source	DF	Sum of Squares	Mean Square	F Value	Pr > F
Model	6	22.6588513	3.7764752	0.98	0.4539
Error	29	111.2858467	3.8374430		
Corrected Total	35	133.9446980			

R-Square	Coeff Var	Root MSE	chl_total Mean
0.169166	30.58949	1.958939	6.403963

Source	DF	Type III SS	Mean Square	F Value	Pr > F
genotype	5	4.95722560	0.99144512	0.26	0.9321
condition	1	17.70162573	17.70162573	4.61	0.0402

11:45 Saturday, April 29, 2000 3

The GLM Procedure

Tukey's Studentized Range (HSD) Test for chl_total

NOTE: This test controls the Type I experimentwise error rate, but it generally has a higher
Type II error rate than REGWQ.

Alpha	0.05
Error Degrees of Freedom	29
Error Mean Square	3.837443
Critical Value of Studentized Range	4.31121
Minimum Significant Difference	3.4478

Means with the same letter are not significantly different.

Tukey Grouping	Mean	N	genotype
A	6.847	6	wt
A			
A	6.666	6	tt4
A			
A	6.548	6	tt6
A			
A	6.415	6	tt5sid2
A			
A	6.266	6	tt5
A			
A	5.682	6	tt4tt5

The GLM Procedure

Tukey's Studentized Range (HSD) Test for chl_total

NOTE: This test controls the Type I experimentwise error rate, but it generally has a higher
Type II error rate than REGWQ.

Alpha	0.05
Error Degrees of Freedom	29
Error Mean Square	3.837443

Critical Value of Studentized Range 2.89240
Minimum Significant Difference 1.3355

Means with the same letter are not significantly different.

Tukey Grouping	Mean	N	condition
A	7.1052	18	sd
B	5.7027	18	ld

11:45 Saturday, April 29, 2000 5

The MEANS Procedure

Analysis Variable : chl_total

genotype	N Obs	Mean	Std Dev	Std Error	Variance	N	Minimum
tt4	9	6.6661200	2.1891480	0.8937159	4.7923690	6	4.2653100
tt4tt5	9	5.6817950	2.3274284	0.9501686	5.4169227	6	3.5161000
tt5	9	6.2661467	1.2364133	0.5047636	1.5287179	6	4.9150200
tt5sid2	9	6.4148300	1.8712797	0.7639467	3.5016876	6	3.9886000
tt6	9	6.5481450	2.7662378	1.1293119	7.6520718	6	4.1503100
wt	9	6.8467400	1.7046188	0.6959077	2.9057254	6	3.7713600

Analysis Variable : chl_total

N

genotype	Obs	Maximum	Median	Range	Sum
tt4	9	10.0883000	6.7358800	5.8229900	39.9967200
tt4tt5	9	8.7169100	4.7498000	5.2008100	34.0907700
tt5	9	7.7776000	6.1435400	2.8625800	37.5968800
tt5sid2	9	9.2955900	6.1218800	5.3069900	38.4889800
tt6	9	11.6248700	5.7309800	7.4745600	39.2888700
wt	9	8.6684000	7.1242500	4.8970400	41.0804400

The MEANS Procedure

Analysis Variable : chl_total

condition	N Obs	Mean	Std Dev	Std Error	Variance	N	Minimum
ld	18	5.7027411	1.1676624	0.2752207	1.3634354	18	3.5161000
sd	18	7.1051844	2.3397419	0.5514825	5.4743924	18	3.7713600

Analysis Variable : chl_total

condition	N Obs	Maximum	Median	Range	Sum
ld	18	7.9375100	5.9316750	4.4214100	102.6493400
sd	18	11.6248700	7.5853850	7.8535100	127.8933200

The GLM Procedure

Class Level Information

Class	Levels	Values
genotype	6	tt4 tt4tt5 tt5 tt5sid2 tt6 wt
condition	2	Id sd

Number of observations 36

11:45 Saturday, April 29, 2000 2

The GLM Procedure

Dependent Variable: chl_total chl total 5dpi

Source	DF	Sum of Squares	Mean Square	F Value	Pr > F
Model	6	12.39207455	2.06534576	2.83	0.0270
Error	29	21.13082499	0.72864914		
Corrected Total	35	33.52289954			

R-Square	Coeff Var	Root MSE	chl_total Mean
0.369660	20.83742	0.853609	4.096522

Source	DF	Type III SS	Mean Square	F Value	Pr > F
genotype	5	12.36063743	2.47212749	3.39	0.0156
condition	1	0.03143712	0.03143712	0.04	0.8369

11:45 Saturday, April 29, 2000 3

The GLM Procedure

Tukey's Studentized Range (HSD) Test for chl_total

Alpha	0.05
Error Degrees of Freedom	29
Error Mean Square	0.728649
Critical Value of Studentized Range	4.31121
Minimum Significant Difference	1.5024

Means with the same letter are not significantly different.

Tukey Grouping		Mean	N	genotype
	A	5.1852	6	tt5
	A			
B	A	4.3600	6	tt4
B	A			
B	A	4.0696	6	wt
B	A			
B	A	4.0336	6	tt6
B				
B		3.5091	6	tt4tt5
B				
B		3.4216	6	tt5sid2

The GLM Procedure

Tukey's Studentized Range (HSD) Test for chl_total

NOTE: This test controls the Type I experimentwise error rate, but it generally has a higher Type II error rate than REGWQ.

Alpha	0.05
Error Degrees of Freedom	29
Error Mean Square	0.728649
Critical Value of Studentized Range	2.89240
Minimum Significant Difference	0.5819

Means with the same letter are not significantly different.

Tukey Grouping	Mean	N	condition
A	4.1261	18	ld
A			
A	4.0670	18	sd

The MEANS Procedure

Analysis Variable : chl_total

genotype	N Obs	Mean	Std Dev	Std Error	Variance	N Minimum
tt4	9	4.3600467	0.9575170	0.3909047	0.9168388	6 2.9500000
tt4tt5	9	3.5090502	0.8272886	0.3377392	0.6844065	6 2.1814710
tt5	9	5.1852383	1.2296802	0.5020148	1.5121133	6 3.4200000
tt5sid2	9	3.4215767	0.7470523	0.3049828	0.5580871	6 2.1000000
tt6	9	4.0335933	0.4343736	0.1773323	0.1886804	6 3.5480400
wt	9	4.0696267	0.6101855	0.2491072	0.3723264	6 3.2000000

Analysis Variable : chl_total

genotype	N Obs	Maximum	Median	Range	Sum
tt4	9	5.9539600	4.3050500	3.0039600	26.1602800

tt4tt5	9	4.5140200	3.5294050	2.3325490	21.0543010
tt5	9	6.2200500	5.6706250	2.8000500	31.1114300
tt5sid2	9	4.2939100	3.4677750	2.1939100	20.5294600
tt6	9	4.8520000	3.9503800	1.3039600	24.2015600
wt	9	4.7775000	4.1956500	1.5775000	24.4177600

The MEANS Procedure

Analysis Variable : chl_total

condition	N Obs	Mean	Std Dev	Std Error	Variance	N	Minimum
ld	18	4.1260728	1.0976198	0.2587115	1.2047692	18	2.1814710
sd	18	4.0669711	0.8748239	0.2061980	0.7653168	18	2.1000000

Analysis Variable : chl_total

condition	N Obs	Maximum	Median	Range	Sum
ld	18	6.2200500	4.0007600	4.0385790	74.2693110
sd	18	5.9539600	4.0050400	3.8539600	73.2054800

Figure A.9.2 – ANOVA of the penetration frequency on infected plants leaves at 3 days post inoculation (dpi) with *Colletotrichum higginsianum.*

The GLM Procedure

Class Level Information

Class	Levels	Values
genotype	6	tt4 tt4tt5 tt5 tt5sid2 tt6 wt
condition	2	Id sd

Number of observations 36

11:45 Saturday, April 29, 2000 2

The GLM Procedure

Dependent Variable: penetration penetration

Source	DF	Sum of Squares	Mean Square	F Value	Pr > F
Model	6	1409.944444	234.990741	4.42	0.0027
Error	29	1542.805556	53.200192		
Corrected Total	35	2952.750000			

R-Square	Coeff Var	Root MSE	penetration Mean
0.477502	16.54559	7.293846	44.08333

Source	DF	Type III SS	Mean Square	F Value	Pr > F
genotype	5	888.5833333	177.7166667	3.34	0.0167
condition	1	521.3611111	521.3611111	9.80	0.0040

11:45 Saturday, April 29, 2000 3

Tukey's Studentized Range (HSD) Test for penetration

NOTE: This test controls the Type I experimentwise error rate, but it generally has a higher
Type II error rate than REGWQ.

Alpha	0.05
Error Degrees of Freedom	29
Error Mean Square	53.20019
Critical Value of Studentized Range	4.31121
Minimum Significant Difference	12.837

Means with the same letter are not significantly different.

Tukey Grouping	Mean	N	genotype
A	50.167	6	tt5sid2
A			
B A	46.833	6	tt6
B A			
B A	46.167	6	wt
B A			
B A	45.500	6	tt4
B A			
B A	41.167	6	tt4tt5
B			
B	34.667	6	tt5

The GLM Procedure

Tukey's Studentized Range (HSD) Test for penetration

NOTE: This test controls the Type I experimentwise error rate, but it generally has a higher
Type II error rate than REGWQ.

Alpha	0.05
Error Degrees of Freedom	29
Error Mean Square	53.20019
Critical Value of Studentized Range	2.89240

Minimum Significant Difference 4.9726

Means with the same letter are not significantly different.

Tukey Grouping	Mean	N	condition
A	47.889	18	sd
B	40.278	18	ld

11:45 Saturday, April 29, 2000 5

The MEANS Procedure

Analysis Variable : penetration

genotype	N Obs	Mean	Std Dev	Std Error	Variance	N	Minimum
tt4	9	45.5000000	5.7532599	2.3487585	33.1000000	6	38.0000000
tt4tt5	9	41.1666667	2.4832774	1.0137938	6.1666667	6	38.0000000
tt5	9	34.6666667	16.2316563	6.6265459	263.4666667	6	15.0000000
tt5sid2	9	50.1666667	5.6361926	2.3009660	31.7666667	6	44.0000000
tt6	9	46.8333333	5.4924190	2.2422707	30.1666667	6	40.0000000
wt	9	46.1666667	6.9402209	2.8333333	48.1666667	6	39.0000000

Analysis Variable : penetration

genotype	N Obs	Maximum	Median	Range	Sum

tt4	9	55.0000000	44.5000000	17.0000000	273.0000000
tt4tt5	9	45.0000000	40.5000000	7.0000000	247.0000000
tt5	9	60.0000000	35.5000000	45.0000000	208.0000000
tt5sid2	9	59.0000000	49.5000000	15.0000000	301.0000000
tt6	9	54.0000000	47.5000000	14.0000000	281.0000000
wt	9	55.0000000	46.0000000	16.0000000	277.0000000

The MEANS Procedure

Analysis Variable : penetration

condition	N Obs	Mean	Std Dev	Std Error	Variance	N	Minimum
ld	18	40.2777778	10.2314714	2.4115809	104.6830065	18	15.0000000
sd	18	47.8888889	6.1919197	1.4594495	38.3398693	18	38.0000000

Analysis Variable : penetration

condition	N Obs	Maximum	Median	Range	Sum
ld	18	59.0000000	40.5000000	44.0000000	725.0000000
sd	18	60.0000000	47.5000000	22.0000000	862.0000000

Figure A.9.3: ANOVA of hyphae progression on plants infected with *Erysiphe cichoracearum*.

The GLM Procedure

Class Level Information

Class	Levels	Values
genotype	6	tt4 tt4tt5 tt5 tt5sid2 tt6 wt
condition	2	ld sd

Number of observations 48

11:45 Saturday, April 29, 2000 2

The GLM Procedure

Dependent Variable: _dpi 2dpi

Source	DF	Sum of Squares	Mean Square	F Value	Pr > F
Model	6	66815.1250	11135.8542	0.73	0.6295
Error	41	626963.8542	15291.8013		
Corrected Total	47	693778.9792			

R-Square	Coeff Var	Root MSE	_dpi Mean
0.096306	28.23422	123.6600	437.9792

Source	DF	Type III SS	Mean Square	F Value	Pr > F
genotype	5	66642.60417	13328.52083	0.87	0.5085
condition	1	172.52083	172.52083	0.01	0.9159

11:45 Saturday, April 29, 2000 3

The GLM Procedure

Tukey's Studentized Range (HSD) Test for _dpi

NOTE: This test controls the Type I experimentwise error rate, but it generally has a higher Type II error rate than REGWQ.

Alpha	0.05
Error Degrees of Freedom	41
Error Mean Square	15291.8
Critical Value of Studentized Range	4.22659
Minimum Significant Difference	184.79

Means with the same letter are not significantly different.

Tukey Grouping	Mean	N	genotype
A	475.00	8	tt4
A			
A	464.00	8	tt5sid2
A			

A	463.00	8	tt4tt5
A			
A	445.00	8	tt5
A			
A	413.75	8	wt
A			
A	367.13	8	tt6

The GLM Procedure

Tukey's Studentized Range (HSD) Test for _dpi

NOTE: This test controls the Type I experimentwise error rate, but it generally has a higher Type II error rate than REGWQ.

Alpha	0.05
Error Degrees of Freedom	41
Error Mean Square	15291.8
Critical Value of Studentized Range	2.85610
Minimum Significant Difference	72.094

Means with the same letter are not significantly different.

Tukey Grouping	Mean	N	condition
A	439.88	24	sd
A			
A	436.08	24	ld

The MEANS Procedure

Analysis Variable : _dpi

genotype	N Obs	Mean	Std Dev	Std Error	Variance	N	Minimum
tt4	8	475.0000000	111.3065266	39.3527999	12389.14	8	314.0000000
tt4tt5	8	463.0000000	138.2905843	48.8931050	19124.29	8	236.0000000
tt5	8	445.0000000	110.6964963	39.1371216	12253.71	8	258.0000000
tt5sid2	8	464.0000000	132.6886797	46.9125326	17606.29	8	284.0000000
tt6	8	367.1250000	107.6654043	38.0654687	11591.84	8	271.0000000
wt	8	413.7500000	128.9404625	45.5873377	16625.64	8	249.0000000

Analysis Variable : _dpi

genotype	N Obs	Maximum	Median	Range	Sum
tt4	8	597.0000000	515.5000000	283.0000000	3800.00
tt4tt5	8	592.0000000	485.5000000	356.0000000	3704.00

tt5	8	591.0000000	465.5000000	333.0000000	3560.00	
tt5sid2	8	724.0000000	444.0000000	440.0000000	3712.00	
tt6	8	580.0000000	336.5000000	309.0000000	2937.00	
wt	8	564.0000000	446.5000000	315.0000000	3310.00	

The MEANS Procedure

Analysis Variable : _dpi

condition	N Obs	Mean	Std Dev	Std Error	Variance	N	Minimum
ld	24	436.0833333	136.4678388	27.8563809	18623.47	24	236.0000000
sd	24	439.8750000	107.3933495	21.9215757	11533.33	24	249.0000000

Analysis Variable : _dpi

condition	N Obs	Maximum	Median	Range	Sum
ld	24	724.0000000	460.5000000	488.0000000	10466.00
sd	24	592.0000000	454.0000000	343.0000000	10557.00

11:45 Saturday, April 29, 2000 1

The GLM Procedure

Class Level Information

Class	Levels	Values
genotype	6	tt4 tt4tt5 tt5 tt5sid2 tt6 wt
condition	2	ld sd

Number of observations 48

The GLM Procedure

Dependent Variable: _dpi 5dpi

Source	DF	Sum of Squares	Mean Square	F Value	Pr > F
Model	6	4520721.83	753453.64	2.23	0.0595
Error	41	13863447.42	338132.86		
Corrected Total	47	18384169.25			

R-Square	Coeff Var	Root MSE	_dpi Mean

0.245903 13.32895 581.4919 4362.625

Source	DF	Type III SS	Mean Square	F Value	Pr > F
genotype	5	3624188.500	724837.700	2.14	0.0793
condition	1	896533.333	896533.333	2.65	0.1111

The GLM Procedure

Tukey's Studentized Range (HSD) Test for _dpi

NOTE: This test controls the Type I experimentwise error rate, but it generally has a higher Type II error rate than REGWQ.

Alpha	0.05
Error Degrees of Freedom	41
Error Mean Square	338132.9
Critical Value of Studentized Range	4.22659
Minimum Significant Difference	868.94

Means with the same letter are not significantly different.

Tukey Grouping	Mean	N	genotype
A	4747.1	8	tt5sid2
A			
B A	4476.8	8	tt4tt5

B	A			
B	A	4476.5	8	tt6
B	A			
B	A	4412.5	8	tt4
B	A			
B	A	4200.8	8	wt
B				
B		3862.1	8	tt5

The GLM Procedure

Tukey's Studentized Range (HSD) Test for _dpi

NOTE: This test controls the Type I experimentwise error rate, but it generally has a higher Type II error rate than REGWQ.

Alpha	0.05
Error Degrees of Freedom	41
Error Mean Square	338132.9
Critical Value of Studentized Range	2.85610
Minimum Significant Difference	339.01

Means with the same letter are not significantly different.

Tukey Grouping	Mean	N	condition
A	4499.3	24	sd
A			

A 4226.0 24 ld

The MEANS Procedure

Analysis Variable : _dpi

genotype	N Obs	Mean	Std Dev	Std Error	Variance	N	Minimum
tt4	8	4412.50	361.7106184	127.8840155	130834.57	8	3753.00
tt4tt5	8	4476.75	729.1620925	257.7977301	531677.36	8	3637.00
tt5	8	3862.13	881.4947431	311.6554552	777032.98	8	2600.00
tt5sid2	8	4747.13	248.4853761	87.8528472	61744.98	8	4339.00
tt6	8	4476.50	251.5733349	88.9446056	63289.14	8	4120.00
wt	8	4200.75	737.5565354	260.7656138	543989.64	8	2862.00

Analysis Variable : _dpi

genotype	N Obs	Maximum	Median	Range	Sum
tt4	8	4808.00	4418.50	1055.00	35300.00
tt4tt5	8	5756.00	4410.50	2119.00	35814.00
tt5	8	4967.00	3914.00	2367.00	

30897.00

tt5sid2 8 5000.00 4871.00 661.0000000
37977.00

tt6 8 4926.00 4521.00 806.0000000
35812.00

wt 8 4972.00 4478.50 2110.00
33606.00

The MEANS Procedure

Analysis Variable : _dpi

N

condition Obs Mean Std Dev Std Error Variance N
Minimum

ld 24 4225.96 781.2742924 159.4769471 610389.52 24
2600.00

sd 24 4499.29 387.2240649 79.0417813 149942.48 24
3567.00

Analysis Variable : _dpi

N

condition Obs Maximum Median Range
Sum

ld 24 5756.00 4328.50 3156.00
101423.00

sd 24 4991.00 4555.50 1424.00
107983.00

11:45 Saturday, April 29, 2000 1

The GLM Procedure

Class Level Information

Class	Levels	Values
condition	2	ld sd
genotype	6	tt4 tt4tt5 tt5 tt5sid2 tt6 wt

Number of observations 48

The GLM Procedure

Dependent Variable: _dpi 7dpi

Source	DF	Sum of Squares	Mean Square	F Value	Pr > F
Model	6	2703362.50	450560.42	0.85	0.5365
Error	41	21633081.42	527636.13		
Corrected Total	47	24336443.92			

R-Square	Coeff Var	Root MSE	_dpi Mean

0.111083 10.94772 726.3857 6635.042

Source	DF	Type III SS	Mean Square	F Value	Pr > F
condition	1	125052.083	125052.083	0.24	0.6290
genotype	5	2578310.417	515662.083	0.98	0.4431

The GLM Procedure

Tukey's Studentized Range (HSD) Test for _dpi

NOTE: This test controls the Type I experimentwise error rate, but it generally has a higher Type II error rate than REGWQ.

Alpha	0.05
Error Degrees of Freedom	41
Error Mean Square	527636.1
Critical Value of Studentized Range	4.22659
Minimum Significant Difference	1085.5

Means with the same letter are not significantly different.

Tukey Grouping	Mean	N	genotype
A	6999.6	8	tt5sid2
A			
A	6736.1	8	tt4tt5

A			
A	6687.0	8	tt6
A			
A	6611.9	8	tt4
A			
A	6551.6	8	tt5
A			
A	6224.0	8	wt

The GLM Procedure

Tukey's Studentized Range (HSD) Test for _dpi

NOTE: This test controls the Type I experimentwise error rate, but it generally has a higher Type II error rate than REGWQ.

Alpha	0.05
Error Degrees of Freedom	41
Error Mean Square	527636.1
Critical Value of Studentized Range	2.85610
Minimum Significant Difference	423.48

Means with the same letter are not significantly different.

Tukey Grouping	Mean	N	condition
A	6686.1	24	ld
A			

A 6584.0 24 sd

The MEANS Procedure

Analysis Variable : _dpi

genotype	N Obs	Mean	Std Dev	Std Error	Variance	N	Minimum
tt4	8	6611.88	652.0897041	230.5485258	425220.98	8	5548.00
tt4tt5	8	6736.13	721.8540489	255.2139465	521073.27	8	5796.00
tt5	8	6551.63	995.8680259	352.0925171	991753.13	8	4731.00
tt5sid2	8	6999.63	775.9020442	274.3227985	602023.98	8	5725.00
tt6	8	6687.00	709.5251934	250.8550378	503426.00	8	5719.00
wt	8	6224.00	254.5730319	90.0051586	64807.43	8	5881.00

Analysis Variable : _dpi

genotype	N Obs	Maximum	Median	Range	Sum
tt4	8	7631.00	6528.00	2083.00	52895.00
tt4tt5	8	7737.00	6487.00	1941.00	53889.00

tt5	8	7655.00	6665.00	2924.00	52413.00
tt5sid2	8	8106.00	7160.00	2381.00	55997.00
tt6	8	7500.00	6671.50	1781.00	53496.00
wt	8	6687.00	6121.50	806.0000000	49792.00

The MEANS Procedure

Analysis Variable : _dpi

condition	N Obs	Mean	Std Dev	Std Error	Variance	N	Minimum
ld	24	6686.08	832.1630754	169.8645765	692495.38	24	4731.00
sd	24	6584.00	600.1448376	122.5040520	360173.83	24	5548.00

Analysis Variable : _dpi

condition	N Obs	Maximum	Median	Range	Sum
ld	24	8106.00	6503.00	3375.00	160466.00
sd	24	7500.00	6556.00	1952.00	158016.00

Figure A.9.4: ANOVA of HR-like cell death lesions in plants grown under Long and Short-day conditions.

The GLM Procedure

Class Level Information

Class	Levels	Values
genotype	6	tt4 tt4tt5 tt5 tt5sid2 tt6 wt
condition	2	ld sd

Number of observations 36

16:46 Monday, May 1, 2000 2

The GLM Procedure

Dependent Variable: fluorescence fluorescence

Source	DF	Sum of Squares	Mean Square	F Value	Pr > F
Model	6	118533601.2	19755600.2	5.84	0.0004
Error	29	98072853.6	3381822.5		
Corrected Total	35	216606454.8			

R-Square	Coeff Var	Root MSE	fluorescence Mean
0.547230	82.03259	1838.973	2241.759

Source	DF	Type III SS	Mean Square	F Value	Pr > F
genotype	5	101726334.5	20345266.9	6.02	0.0006
condition	1	16807266.8	16807266.8	4.97	0.0337

16:46 Monday, May 1, 2000 3

The GLM Procedure

Tukey's Studentized Range (HSD) Test for fluorescence

NOTE: This test controls the Type I experimentwise error rate, but it generally has a higher
Type II error rate than REGWQ.

Alpha	0.05
Error Degrees of Freedom	29
Error Mean Square	3381823
Critical Value of Studentized Range	4.31121
Minimum Significant Difference	3236.7

Means with the same letter are not significantly different.

Tukey Grouping	Mean	N	genotype
A	5996	6	tt5
B	1607	6	tt4tt5
B			
B	1565	6	tt5sid2
B			
B	1501	6	tt6
B			
B	1395	6	tt4
B			
B	1386	6	wt

16:46 Monday, May 1, 2000 4

The GLM Procedure

Tukey's Studentized Range (HSD) Test for fluorescence

NOTE: This test controls the Type I experimentwise error rate, but it generally has a higher
Type II error rate than REGWQ.

Alpha	0.05
Error Degrees of Freedom	29
Error Mean Square	3381823
Critical Value of Studentized Range	2.89240

Minimum Significant Difference 1253.7

Means with the same letter are not significantly different.

Tukey Grouping	Mean	N	condition
A	2925.0	18	ld
B	1558.5	18	sd

16:46 Monday, May 1, 2000 5

The MEANS Procedure

Analysis Variable : fluorescence

genotype	N Obs	Mean	Std Dev	Std Error	Variance	N	Minimum
tt4	9	1395.17	266.2043284	108.6774620	70864.74	6	1090.00
tt4tt5	9	1607.11	136.3618824	55.6695054	18594.56	6	1404.00
tt5	9	5996.22	4770.54	1947.57	22758093.10	6	1542.00
tt5sid2	9	1565.06	188.8964933	77.1166705	35681.89	6	1324.00
tt6	9	1500.67	255.8552542	104.4524701	65461.91	6	1145.00
wt	9	1386.33	165.3114233	67.4881059	27327.87	6	1200.00

Analysis Variable : fluorescence

genotype	N Obs	Maximum	Median	Range	Sum

tt4	9	1876.00	1354.00	786.0000000	8371.00
tt4tt5	9	1789.00	1591.33	385.0000000	9642.67
tt5	9	11210.00	5623.00	9668.00	35977.33
tt5sid2	9	1872.00	1568.67	548.0000000	9390.33
tt6	9	1839.00	1481.33	694.0000000	9004.00
wt	9	1578.00	1382.00	378.0000000	8318.00

The MEANS Procedure

Analysis Variable : fluorescence

condition	N Obs	Mean	Std Dev	Std Error	Variance	N	Minimum
ld	18	2925.04	3423.09	806.8304912	11717557.95	18	1090.00
sd	18	1558.48	187.9773044	44.3066755	35335.47	18	1209.00

Analysis Variable : fluorescence

condition	N Obs	Maximum	Median	Range	Sum
ld	18	11210.00	1494.67	10120.00	52650.67
sd	18	1876.00	1579.17	667.0000000	28052.67

Figure A.9.5: ANOVA of Hydrogen peroxide (H_2O_2) accumulation in plants grown under Long and Short-day conditions.

The GLM Procedure

Class Level Information

Class	Levels	Values
genotype	6	tt4 tt4tt5 tt5 tt5sid2 tt6 wt
condition	2	ld sd

Number of observations 36

16:46 Monday, May 1, 2000 2

The GLM Procedure

Dependent Variable: fluorescence fluorescence

Source	DF	Sum of Squares	Mean Square	F Value	Pr > F
Model	6	1339259.415	223209.903	5.72	0.0005
Error	29	1132227.712	39042.335		
Corrected Total	35	2471487.127			

R-Square	Coeff Var	Root MSE	fluorescence Mean
0.541884	165.8891	197.5913	119.1105

Source	DF	Type III SS	Mean Square	F Value	Pr > F
genotype	5	1148212.233	229642.447	5.88	0.0007
condition	1	191047.182	191047.182	4.89	0.0350

16:46 Monday, May 1, 2000 3

The GLM Procedure

Tukey's Studentized Range (HSD) Test for fluorescence

NOTE: This test controls the Type I experimentwise error rate, but it generally has a higher
Type II error rate than REGWQ.

Alpha	0.05
Error Degrees of Freedom	29
Error Mean Square	39042.33
Critical Value of Studentized Range	4.31121
Minimum Significant Difference	347.77

Means with the same letter are not significantly different.

Tukey Grouping	Mean	N	genotype
A	518.4	6	tt5
B	43.9	6	tt6
B			
B	39.3	6	tt5sid2
B			
B	38.9	6	tt4
B			
B	37.6	6	tt4tt5
B			
B	36.6	6	wt

16:46 Monday, May 1, 2000 4

The GLM Procedure

Tukey's Studentized Range (HSD) Test for fluorescence

NOTE: This test controls the Type I experimentwise error rate, but it generally has a higher
Type II error rate than REGWQ.

Alpha	0.05
Error Degrees of Freedom	29
Error Mean Square	39042.33
Critical Value of Studentized Range	2.89240

Minimum Significant Difference 134.71

Means with the same letter are not significantly different.

Tukey Grouping	Mean	N	condition
A	191.96	18	ld
B	46.26	18	sd

16:46 Monday, May 1, 2000 5

The MEANS Procedure

Analysis Variable : fluorescence

genotype	N Obs	Mean	Std Dev	Std Error	Variance	N	Minimum
tt4	9	38.8627778	12.2252145	4.9909229	149.4558685	6	26.0100000
tt4tt5	9	37.5666667	4.2136814	1.7202282	17.7551111	6	31.6666667
tt5	9	518.4188889	514.0681449	209.8674413	264266.06	6	44.0000000
tt5sid2	9	39.3000000	8.8814663	3.6258435	78.8804444	6	29.1000000
tt6	9	43.9333333	11.2497309	4.5926834	126.5564444	6	31.1000000
wt	9	36.5811111	4.0340339	1.6468874	16.2734296	6	31.2000000

Analysis Variable : fluorescence

genotype	N Obs	Maximum	Median	Range	Sum

tt4	9	53.5000000	37.5000000	27.4900000	233.1766667
tt4tt5	9	41.3333333	39.2000000	9.6666667	225.4000000
tt5	9	1054.33	482.0400000	1010.33	3110.51
tt5sid2	9	51.7000000	38.0000000	22.6000000	235.8000000
tt6	9	61.1000000	44.3166667	30.0000000	263.6000000
wt	9	41.4000000	36.6100000	10.2000000	219.4866667

The MEANS Procedure

Analysis Variable : fluorescence

condition	N Obs	Mean	Std Dev	Std Error	Variance	N	Minimum
ld	18	191.9587037	366.1846453	86.3105486	134091.19	18	26.0100000
sd	18	46.2622222	7.2340654	1.7050856	52.3317020	18	38.1200000

Analysis Variable : fluorescence

condition	N Obs	Maximum	Median	Range	Sum
ld	18	1054.33	32.7833333	1028.32	3455.26
sd	18	63.0000000	44.6500000	24.8800000	832.7200000

Figure A.9.6: ANOVA of super oxide (O^{-}_{2}) accumulation in plants grown under Long and Short-day conditions.

The GLM Procedure

Class Level Information

Class	Levels	Values
genotype	6	tt4 tt4tt5 tt5 tt5sid2 tt6 wt
condition	2	ld sd

Number of observations 36

16:46 Monday, May 1, 2000 2

The GLM Procedure

Dependent Variable: fluorescence fluorescence

Source	DF	Sum of Squares	Mean Square	F Value	Pr > F
Model	6	291676.2736	48612.7123	5.49	0.0007
Error	29	256858.1019	8857.1759		
Corrected Total	35	548534.3755			

R-Square	Coeff Var	Root MSE	fluorescence Mean
0.531737	159.2574	94.11257	59.09464

Source	DF	Type III SS	Mean Square	F Value	Pr > F
genotype	5	255297.8510	51059.5702	5.76	0.0008
condition	1	36378.4225	36378.4225	4.11	0.0520

16:46 Monday, May 1, 2000 3

The GLM Procedure

Tukey's Studentized Range (HSD) Test for fluorescence

NOTE: This test controls the Type I experimentwise error rate, but it generally has a higher
Type II error rate than REGWQ.

Alpha	0.05
Error Degrees of Freedom	29
Error Mean Square	8857.176
Critical Value of Studentized Range	4.31121
Minimum Significant Difference	165.64

Means with the same letter are not significantly different.

Tukey Grouping	Mean	N	genotype
A	247.36	6	tt5
B	24.01	6	tt4
B			
B	22.48	6	wt
B			
B	21.46	6	tt5sid2
B			
B	20.31	6	tt4tt5
B			
B	18.96	6	tt6

16:46 Monday, May 1, 2000 4

The GLM Procedure

Tukey's Studentized Range (HSD) Test for fluorescence

NOTE: This test controls the Type I experimentwise error rate, but it generally has a higher
Type II error rate than REGWQ.

Alpha	0.05
Error Degrees of Freedom	29
Error Mean Square	8857.176
Critical Value of Studentized Range	2.89240

Minimum Significant Difference 64.161

Means with the same letter are not significantly different.

Tukey Grouping	Mean	N	condition
A	90.88	18	ld
A			
A	27.31	18	sd

16:46 Monday, May 1, 2000 5

The MEANS Procedure

Analysis Variable : fluorescence

genotype	N Obs	Mean	Std Dev	Std Error	Variance	N	Minimum
tt4	9	24.0070681	7.1556157	2.9212679	51.2028367	6	17.0000000
tt4tt5	9	20.3087447	6.8090232	2.7797721	46.3627967	6	11.8700000
tt5	9	247.3642211	241.5158757	98.5984434	58329.92	6	26.0000000
tt5sid2	9	21.4553011	8.8433392	3.6102781	78.2046474	6	7.8456319
tt6	9	18.9555216	11.7084406	4.7799509	137.0875822	6	2.1000000
wt	9	22.4769579	2.1281044	0.8687950	4.5288283	6	20.0000000

Analysis Variable : fluorescence

genotype	N Obs	Maximum	Median	Range	Sum

tt4	9	33.0000000	22.0000000	16.0000000	144.0424088
tt4tt5	9	28.9800000	20.1450000	17.1100000	121.8524682
tt5	9	500.0000000	229.7500000	474.0000000	1484.19
tt5sid2	9	31.8000000	21.7500000	23.9543681	128.7318066
tt6	9	30.2200000	20.8194996	28.1200000	113.7331298
wt	9	25.6573367	22.1022053	5.6573367	134.8617472

The MEANS Procedure

Analysis Variable : fluorescence

condition	N Obs	Mean	Std Dev	Std Error	Variance	N	Minimum
ld	18	90.8831830	173.5333685	40.9022072	30113.83	18	2.1000000
sd	18	27.3060885	3.6042716	0.8495350	12.9907741	18	21.0000000

Analysis Variable : fluorescence

condition	N Obs	Maximum	Median	Range	Sum
ld	18	500.0000000	17.7218745	497.9000000	1635.90
sd	18	33.0000000	27.6049109	12.0000000	491.5095929

Figure A.9.7: ANOVA of callose deposition in plants grown under Long and Short-day conditions.

The GLM Procedure

Class Level Information

Class	Levels	Values
genotype	6	tt4 tt4tt5 tt5 tt5sid2 tt6 wt
condition	2	ld sd

Number of observations 36

16:46 Monday, May 1, 2000 2

The GLM Procedure

Dependent Variable: Fluorescence Fluorescence

Source	DF	Sum of Squares	Mean Square	F Value	Pr > F
Model	6	30007.36663	5001.22777	5.48	0.0007
Error	29	26459.69429	912.40325		
Corrected Total	35	56467.06092			

R-Square	Coeff Var	Root MSE	Fluorescence Mean
0.531414	121.5268	30.20601	24.85544

Source	DF	Type III SS	Mean Square	F Value	Pr > F
genotype	5	22451.65238	4490.33048	4.92	0.0022
condition	1	7555.71426	7555.71426	8.28	0.0074

16:46 Monday, May 1, 2000 3

The GLM Procedure

Tukey's Studentized Range (HSD) Test for Fluorescence

NOTE: This test controls the Type I experimentwise error rate, but it generally has a higher
Type II error rate than REGWQ.

Alpha	0.05
Error Degrees of Freedom	29
Error Mean Square	912.4033
Critical Value of Studentized Range	4.31121
Minimum Significant Difference	53.164

Means with the same letter are not significantly different.

Tukey Grouping	Mean	N	genotype
A	79.71	6	tt5
B	22.38	6	tt4
B			
B	14.92	6	tt6
B			
B	14.08	6	wt
B			
B	11.27	6	tt5sid2
B			
B	6.76	6	tt4tt5

The GLM Procedure

Tukey's Studentized Range (HSD) Test for Fluorescence

NOTE: This test controls the Type I experimentwise error rate, but it generally has a higher
Type II error rate than REGWQ.

Alpha	0.05
Error Degrees of Freedom	29

Error Mean Square	912.4033
Critical Value of Studentized Range	2.89240
Minimum Significant Difference	20.593

Means with the same letter are not significantly different.

Tukey Grouping	Mean	N	condition
A	39.34	18	ld
B	10.37	18	sd

The MEANS Procedure

Analysis Variable : Fluorescence

genotype	N Obs	Mean	Std Dev	Std Error	Variance	N	Minimum
tt4	9	22.3809367	15.5080926	6.3311523	240.5009371	6	5.9827012
tt4tt5	9	6.7628550	5.3907580	2.2007677	29.0602715	6	1.6606205
tt5	9	79.7121349	77.3766503	31.5888852	5987.15	6	3.7672246
tt5sid2	9	11.2740912	6.6590648	2.7185518	44.3431443	6	4.4916340
tt6	9	14.9203227	5.5267292	2.2562777	30.5447353	6	10.9506898
wt	9	14.0822928	21.7137426	8.8645983	471.4866168	6	4.3521734

Analysis Variable : Fluorescence

genotype	N Obs	Maximum	Median	Range	Sum
tt4	9	47.0890204	19.7082667	41.1063191	134.2856200
tt4tt5	9	14.6883560	5.2371517	13.0277355	40.5771301
tt5	9	155.4715059	79.8066339	151.7042813	478.2728094
tt5sid2	9	23.6536842	9.8883924	19.1620502	67.6445473
tt6	9	25.6117312	13.0280523	14.6610414	89.5219364
wt	9	58.3127560	4.6255499	53.9605826	84.4937569

The MEANS Procedure

Analysis Variable : Fluorescence

condition	N Obs	Mean	Std Dev	Std Error	Variance	N	Minimum
ld	18	39.3427075	53.0175134	12.4963477	2810.86	18	3.6020464
sd	18	10.3681703	8.1413338	1.9189308	66.2813167	18	1.6606205

Analysis Variable : Fluorescence

condition	N Obs	Maximum	Median	Range	Sum
ld	18	155.4715059	14.0347035	151.8694595	708.1687349
sd	18	33.1627105	9.2615234	31.5020900	186.6270652

Figure A.9.8: ANOVA of NC accumulation in Arabidopsis lines grown under LD.

The ANOVA Procedure

Class Level Information

Class	Levels	Values
genotype	6	tt4 tt4tt5 tt5 tt5sid2 tt6 wt

Number of observations 18

15:54
Friday, April 28, 2000 2

The ANOVA Procedure

Dependent Variable: conc conc

Source	DF	Sum of Squares	Mean Square	F Value	Pr > F
Model	5	24.43281489	4.88656298	482.71	<.0001
Error	12	0.12147907	0.01012326		
Corrected Total	17	24.55429397			

R-Square	Coeff Var	Root MSE	conc Mean
0.995053	17.66559	0.100614	0.569550

Source	DF	Anova SS	Mean Square	F Value	Pr > F
genotype	5	24.43281489	4.88656298	482.71	<.0001

15:54
Friday, April 28, 2000 3

The ANOVA Procedure

Tukey's Studentized Range (HSD) Test for conc

NOTE: This test controls the Type I experimentwise error rate, but it generally has a higher Type II error rate than REGWQ.

Alpha	0.05
Error Degrees of Freedom	12
Error Mean Square	0.010123

Critical Value of Studentized Range 4.75015
Minimum Significant Difference 0.2759

Means with the same letter are not significantly different.

Tukey Grouping	Mean	N	genotype
A	3.16667	3	tt5
B	0.25063	3	tt5sid2
C			
C	0.00000	3	tt4
C			
C	0.00000	3	tt4tt5
C			
C	0.00000	3	tt6
C			
C	0.00000	3	wt

The MEANS Procedure

Analysis Variable : conc

genotype	N Obs	Mean	Std Dev	Std Error	Variance	Maximum
tt4	9	0	0	0	0	0
tt4tt5	9	0	0	0	0	0
tt5	9	3.1666667	0.2081666	0.1201850	0.0433333	3.4000000
tt5sid2	9	0.2506333	0.1319326	0.0761713	0.0174062	0.4000000
tt6	9	0	0	0	0	0
wt	9	0	0	0	0	0

Analysis Variable : conc

genotype	N Obs	Median	Range	Sum
tt4	9	0	0	0
tt4tt5	9	0	0	0
tt5	9	3.1000000	0.4000000	9.5000000
tt5sid2	9	0.2019000	0.2500000	0.7519000
tt6	9	0	0	0
wt	9	0	0	0

Figure A.9.9: ANOVA of NC accumulation in plants infected with *Colletotrichum higginssianum* grown under Long-day conditions.

The ANOVA Procedure

Class Level Information

Class	Levels	Values
genotype	6	tt4 tt4tt5 tt5 tt5sid2 tt6 wt

Number of observations 18

11:45
Saturday, April 29, 2000 2

The ANOVA Procedure

Dependent Variable: conc conc

Source	DF	Sum of Squares	Mean Square	F Value	Pr > F
Model	5	104.0325167	20.8065033	14.91	<.0001
Error	12	16.7425333	1.3952111		
Corrected Total	17	120.7750500			

R-Square	Coeff Var	Root MSE	conc Mean
0.861374	38.49616	1.181191	3.068333

Source	DF	Anova SS	Mean Square	F Value	Pr > F
genotype	5	104.0325167	20.8065033	14.91	<.0001

11:45
Saturday, April 29, 2000 3

The ANOVA Procedure

Tukey's Studentized Range (HSD) Test for conc

NOTE: This test controls the Type I experimentwise error rate, but it generally has a higher Type II error rate than REGWQ.

Alpha 0.05

Error Degrees of Freedom	12
Error Mean Square	1.395211
Critical Value of Studentized Range	4.75015
Minimum Significant Difference	3.2394

Means with the same letter are not significantly different.

Tukey Grouping			Mean	N	genotype
		A	5.3700	3	tt5
		A			
		A	5.3533	3	tt6
		A			
		A	5.2800	3	wt
		A			
	B	A	2.4067	3	tt5sid2
	B				
	B		0.0000	3	tt4
	B				
	B		0.0000	3	tt4tt5

The MEANS Procedure

Analysis Variable : conc

genotype	N Obs	Mean	Std Dev	Std Error	Variance	N	Minimum
tt4	9	0	0	0	0	3	0
tt4tt5	9	0	0	0	0	3	0
tt5	9	5.3700000	2.0000000	1.1547005	4.0000000	3	3.3700000
tt5sid2	9	2.4066667	0.5810622	0.3354764	0.3376333	3	1.9200000
tt6	9	5.3533333	1.7417329	1.0055899	3.0336333	3	3.5300000
wt	9	5.2800000	1.0000000	0.5773503	1.0000000	3	4.2800000

Analysis Variable : conc

genotype	N Obs	Maximum	Median	Range	Sum
tt4	9	0	0	0	0
tt4tt5	9	0	0	0	0
tt5	9	7.3700000	5.3700000	4.0000000	16.1100000
tt5sid2	9	3.0500000	2.2500000	1.1300000	7.2200000
tt6	9	7.0000000	5.5300000	3.4700000	16.0600000
wt	9	6.2800000	5.2800000	2.0000000	15.8400000

Figure A.9.10: ANOVA of NC accumulation in plants infected with *Erysiphe cichoracearum* grown under Long-day conditions.

```
The ANOVA Procedure

                              Class Level Information

                Class         Levels    Values

                genotype           6    tt4 tt4tt5 tt5 tt5sid2 tt6 wt


                             Number of observations    18
                                                         11:45
Saturday, April 29, 2000   2

                                  The ANOVA Procedure

Dependent Variable: conc   conc

                                          Sum of
      Source                     DF         Squares     Mean Square    F
Value    Pr > F

      Model                       5     24.43271111      4.88654222
39.81    <.0001

      Error                      12      1.47306667      0.12275556

      Corrected Total            17     25.90577778


                    R-Square     Coeff Var      Root MSE     conc Mean

                    0.943138      22.02014      0.350365      1.591111


      Source                     DF        Anova SS     Mean Square    F
Value    Pr > F

      genotype                    5     24.43271111      4.88654222
39.81    <.0001
                                                            11:45
Saturday, April 29, 2000   3

                                  The ANOVA Procedure

                      Tukey's Studentized Range (HSD) Test for conc

 NOTE: This test controls the Type I experimentwise error rate, but it
generally has a higher
                             Type II error rate than REGWQ.


                      Alpha                                     0.05
                      Error Degrees of Freedom                    12
                      Error Mean Square                     0.122756
```

Critical Value of Studentized Range 4.75015
Minimum Significant Difference 0.9609

Means with the same letter are not significantly different.

Tukey Grouping	Mean	N	genotype
A	2.8267	3	wt
A			
A	2.6800	3	tt5
A			
A	2.0400	3	tt6
A			
A	2.0000	3	tt5sid2
B	0.0000	3	tt4
B			
B	0.0000	3	tt4tt5

11:45 Saturday, April 29, 2000 4

The MEANS Procedure

Analysis Variable : conc

genotype	N Obs	Mean	Std Dev	Std Error	Variance	N	Minimum
tt4	9	0	0	0	0	3	0
tt4tt5	9	0	0	0	0	3	0
tt5	9	2.6800000	0.2389561	0.1379613	0.0571000	3	2.4700000
tt5sid2	9	2.0000000	0.3000000	0.1732051	0.0900000	3	1.7000000
tt6	9	2.0400000	0.3119295	0.1800926	0.0973000	3	1.7500000
wt	9	2.8266667	0.7015222	0.4050240	0.4921333	3	2.1000000

Analysis Variable : conc

genotype	N Obs	Maximum	Median	Range	Sum
tt4	9	0	0	0	0
tt4tt5	9	0	0	0	0
tt5	9	2.9400000	2.6300000	0.4700000	8.0400000
tt5sid2	9	2.3000000	2.0000000	0.6000000	6.0000000
tt6	9	2.3700000	2.0000000	0.6200000	6.1200000
wt	9	3.5000000	2.8800000	1.4000000	8.4800000

Figure A.9.11: ANOVA of NC accumulation of plants grown under Short-day + High light conditions.

The ANOVA Procedure

Class Level Information

Class	Levels	Values
genotype	4	tt4 tt4tt5 tt5 wt

Number of observations 12

11:45
Saturday, April 29, 2000 2

The ANOVA Procedure

Dependent Variable: conc conc

Source	DF	Sum of Squares	Mean Square	F Value	Pr > F
Model	3	48.61422500	16.20474167	49.84	<.0001
Error	8	2.60086667	0.32510833		
Corrected Total	11	51.21509167			

R-Square	Coeff Var	Root MSE	conc Mean
0.949217	28.56865	0.570183	1.995833

Source	DF	Anova SS	Mean Square	F Value	Pr > F
genotype	3	48.61422500	16.20474167	49.84	<.0001

11:45
Saturday, April 29, 2000 3

The ANOVA Procedure

Tukey's Studentized Range (HSD) Test for conc

NOTE: This test controls the Type I experimentwise error rate, but it generally has a higher Type II error rate than REGWQ.

Alpha	0.05
Error Degrees of Freedom	8
Error Mean Square	0.325108

Critical Value of Studentized Range 4.52880
Minimum Significant Difference 1.4909

Means with the same letter are not significantly different.

Tukey Grouping	Mean	N	genotype
A	4.3600	3	tt5
A			
A	3.6233	3	wt
B	0.0000	3	tt4
B			
B	0.0000	3	tt4tt5

The MEANS Procedure

Analysis Variable : conc

genotype	N Obs	Mean	Std Dev	Std Error	Variance	N	Minimum
tt4	9	0	0	0	0	3	0
tt4tt5	9	0	0	0	0	3	0
tt5	9	4.3600000	0.9689169	0.5594044	0.9388000	3	3.3000000
wt	9	3.6233333	0.6013596	0.3471951	0.3616333	3	3.0000000

Analysis Variable : conc

genotype	N Obs	Maximum	Median	Range	Sum
tt4	9	0	0	0	0
tt4tt5	9	0	0	0	0

```
        tt5          9      5.2000000       4.5800000       1.9000000
13.0800000

        wt           9      4.2000000       3.6700000       1.2000000
10.8700000

ƒƒƒƒƒƒƒƒƒƒƒƒƒƒƒƒƒƒƒƒƒƒƒƒƒƒƒƒƒƒƒƒƒƒƒƒƒƒƒƒƒƒƒƒƒƒƒƒƒƒƒƒƒƒƒƒƒƒƒƒƒƒƒƒƒƒƒƒƒƒƒƒƒƒƒƒ
ƒƒƒƒ
```

Figure A.9.12: ANOVA of NC accumulation and phenotype of plants grown under Long-day + Low temperature conditions.

The ANOVA Procedure

Class Level Information

Class	Levels	Values
genotype	4	tt4 tt4tt5 tt5 wt

Number of observations 12

11:45

Saturday, April 29, 2000 2

The ANOVA Procedure

Dependent Variable: conc conc

Source	DF	Sum of Squares	Mean Square	F Value	Pr > F
Model	3	984.911225	328.303742	155.38	<.0001
Error	8	16.902867	2.112858		
Corrected Total	11	1001.814092			

R-Square	Coeff Var	Root MSE	conc Mean
0.983128	19.50007	1.453567	7.454167

Source	DF	Anova SS	Mean Square	F Value	Pr > F
genotype	3	984.9112250	328.3037417	155.38	<.0001

11:45

Saturday, April 29, 2000 3

The ANOVA Procedure

Tukey's Studentized Range (HSD) Test for conc

NOTE: This test controls the Type I experimentwise error rate, but it generally has a higher Type II error rate than REGWQ.

Alpha 0.05

Error Degrees of Freedom	8
Error Mean Square	2.112858
Critical Value of Studentized Range	4.52880
Minimum Significant Difference	3.8006

Means with the same letter are not significantly different.

Tukey Grouping	Mean	N	genotype
A	22.190	3	tt5
B	7.627	3	wt
C	0.000	3	tt4
C			
C	0.000	3	tt4tt5

11:45
Saturday, April 29, 2000 4

The MEANS Procedure

Analysis Variable : conc

genotype	N Obs	Mean	Std Dev	Std Error	Variance	N	Minimum
tt4	9	0	0	0	0	3	0
tt4tt5	9	0	0	0	0	3	0
tt5	9	22.1900000	2.7639284	1.5957548	7.6393000	3	19.6000000
wt	9	7.6266667	0.9011844	0.5202991	0.8121333	3	6.7000000

Analysis Variable : conc

genotype	N Obs	Maximum	Median	Range	Sum

```
          tt4           9              0               0               0
0

          tt4tt5        9              0               0               0
0

          tt5           9     25.1000000      21.8700000       5.5000000
66.5700000

          wt            9      8.5000000       7.6800000       1.8000000
22.8800000

ƒƒƒƒƒƒƒƒƒƒƒƒƒƒƒƒƒƒƒƒƒƒƒƒƒƒƒƒƒƒƒƒƒƒƒƒƒƒƒƒƒƒƒƒƒƒƒƒƒƒƒƒƒƒƒƒƒƒƒƒƒƒƒƒƒƒƒƒƒƒƒ
ƒƒƒƒ
```